Myeloid Cells and Beyond: Previously Unidentified Roles of Colony Stimulating Factor 1 in Neuroinflammation and 5-Lipoxygenase in Myelination

By

MARILYN WANG

DISSERTATION

Submitted in partial satisfaction of the requirements for the degree of

DOCTOR OF PHILOSOPHY

in

Immunology

in the

OFFICE OF GRADUATE STUDIES

of the

UNIVERSITY OF CALIFORNIA

DAVIS

Approved:

_____

Athena Soulika, Chair

_____

David Pleasure

_____

Nicholas Marsh-Armstrong

_____

Fuzheng Guo

Committee in Charge

2024

Abstract

Multiple sclerosis (MS) is an autoimmune, demyelinating disease of the central nervous system. Importantly, it is an illness with unmet medical need. Although current therapeutics mitigate relapses, there is no treatment that halts the progression of MS. In order to develop improved medicines, we must better understand the disease and factors that drive it. Hence, the mouse model of MS, experimental autoimmune encephalomyelitis (EAE) has been employed in the field of neuroimmunology. In my thesis, I elucidate the roles of two myeloid cell-associated proteins in affecting EAE pathogenesis.

In chapter 1, I review the current understanding of the role of myeloid cells in MS. In the healthy CNS, dendritic cells, granulocytes, tissue resident macrophages are present in small quantities. Importantly, microglia reside in the healthy CNS and continuously monitor the milieu. During inflammatory conditions, microglia become activated, and a host of other myeloid cells and lymphocytes infiltrate into the CNS and cause demyelination. Although lymphocytes are important, myeloid cells are an underappreciated component of MS disease which initiate and perpetuate the disease. Additionally, I review a few of the current MS therapeutics on the market, their targets, and their impact on myeloid cells.

One target that has been studied for its therapeutic potential in MS treatment is CSF1R. PLX5622, a CSF1R antagonist, is known to deplete microglia. Microglial depletion has been previously proposed to be the cause of reduced EAE clinical symptoms that are detected in CSF1R-antagonized mice. In chapter 2, I show that PLX5622 formulated into rodent chow (PLX5622 diet; PD), in addition to ameliorating EAE clinical score, also increases infiltration into the CNS of PD mice. I determined that this was not due to changes in peripheral priming. Furthermore, although spinal cords were largely devoid of infiltration, cerebella showed increased infiltration in PD compared to CD mice. I propose that decreased incidence

of ascending paralysis, a symptom associated with spinal cord demyelinating damage, is due to immune cell relocation to the cerebellum. Lastly, I explore possible mechanisms causing the observed relocation.

An area of unmet therapeutic need is in developmental and adult myelination. In chapter 3, I explore the function of 5 lipoxygenase (5LO) in the healthy central nervous system (CNS). First, I show that 5LO, 5LO pathway, and 5LO's enzymatic products, leukotrienes (LTs), are detected in development and adulthood in the CNS; this suggests that the 5LO pathway is present and active in healthy conditions. Due to the detection of the highest levels of 5LO pathway components being detected during developmental myelination, we investigate the connection between 5LO and the most dynamic cell type in the CNS, oligodendrocyte lineage cells (OLCs). Addition of leukotrienes onto differentiating oligodendrocyte progenitor cells *in vitro* promotes oligodendrocyte differentiation in my experiments, providing initial evidence of the link between LTs and OLCs. Next, *in vivo* experiments involving fate mapping of cells in the corpus callosum of 5LO global knockout mice and their littermate controls confirms that 5LO and LTs promote OLC differentiation. Lastly, pharmacological and genetic methods reveal that microglia are the primary expressors of 5LO and ostensibly, LTs.

Acknowledgements

I would like to thank my advisor, Dr. Athena Soulika, for her mentorship throughout my PhD. I have learned countless skills, including all the techniques, how to be a better presenter, how to write scientifically, and how to better design and plan experiments. These skills, as well as independent thinking will be indispensable for my future career moving forward.

I would like to thank Dr. Pleasure for his mentorship as my advisor during the first two years of my PhD, when I was just figuring out how to be a graduate student. His mentorship laid a foundation for my time in grad school. I would also like to thank Fuzheng Guo for his help with my work in Chapter 3, including providing me with neonatal rats for my *in vitro* experiments. His expertise on glia was valuable for my work.

I would like to thank Dr. Nicholas Marsh-Armstrong, Dr. Guo, Dr. Pleasure, and Dr. Soulika for serving as my dissertation committee and providing critical feedback all of these years. I would like to thank my lab mates, past and present, for their help and comradery. I would like to thank Dr. Nicole Baumgarth for her support and guidance as my graduate advisor all of these years, and particularly at the end.

Additionally, I'd like to thank my husband Chris for his endless patience, encouragement, and support during my long days, and long years of grad school. I look forward to starting the next chapter of our lives as I finally begin my career. Lastly, I'd like to thank all of the lifelong friends that I've met during grad school for their continued support, and for lifting me up when I was down.

Chapter 1:

Myeloid Cells in Multiple Sclerosis

Marilyn Wang, Athena Soulika

Published in Intech Open

Abstract

In steady state, the central nervous system (CNS) houses a variety of myeloid cells, such as microglia, non-parenchymal macrophages and dendritic cells, and granulocytes. Most of these cells enter the CNS during embryogenesis and are crucial for proper CNS development. In adulthood, these resident myeloid cells exert both sentinel and crucial homeostatic functions. In neuroinflammatory conditions, like multiple sclerosis (MS), both lymphoid and myeloid cells from the periphery infiltrate the tissue and cause local damage. Although lymphocytes are undeniably important players in MS, CNS-resident and infiltrating myeloid cells have recently gained much-deserved attention for their roles in disease progression.

Here we will review significant advances made in recent years delineating myeloid cell functions within the CNS both in homeostasis and MS. We will also discuss how these cells are affected by currently employed therapeutics for MS patients.

1.1 Introduction

Myeloid cells are crucial for the central nervous system (CNS) tissue function both in development and adulthood. Other than microglia, which are found in the parenchyma, meningeal and perivascular spaces along with the choroid plexus are populated by special subsets of macrophages, and dendritic cells. Additionally, granulocyte cells are also present in the homeostatic CNS. Studies in rodents have elucidated mechanisms by which these cells promote tissue physiology.

In multiple sclerosis (MS), myeloid cells play a dominant role. Studies in mice and human samples show that myeloid cells from the periphery enter the tissue through a compromised blood brain barrier (BBB) and together with CNS resident cells perpetuate the inflammatory environment through secretion of inflammatory cytokines, and reactivation of primed T cells. However, myeloid cells may also exhibit anti-

inflammatory and pro-reparative functions. The exact contribution of each myeloid subset to disease progression is currently the focus of thorough investigation.

Here, we will provide an overview of myeloid cell types and functions in homeostasis and how these populations evolve in neuroinflammation. In addition, we will review the effects of therapeutics currently employed for MS patients on myeloid cell populations and functions.

1.2. CNS -resident myeloid cells in homeostasis

The CNS houses a variety of myeloid cell subsets that exert multiple functions crucial to homeostasis such as BBB maintenance, sampling of the local milieu, synaptic pruning and maintenance of neuronal populations in development and adulthood. In this section, we will elaborate on their developmental origin and known functions of these subsets in CNS physiology.

Microglia

Microglia are the resident immune cells within the CNS parenchyma proper. They derive from Runx1+ erythromyeloid precursors in the extra-embryonic yolk sac, and enter the brain early in embryonic development [1-3]. Before migrating out of the yolk sac, these progenitors acquire CD45 and CX3CR1 expression [4] and seed the brain parenchyma around embryonic day 9.5 [3, 5, 6], through a process that is mediated largely by the metalloproteinases MMP8 and MMP9[4].

Microglia development relies on transcription factors PU.1, IRF8, and colony stimulating factor 1 receptor (CSF1R) signaling [7], whereas transcription factors such as MYB, BATF3 and ID2 are not necessary, suggesting that microglia are transcriptionally distinct than myeloid cells found in peripheral tissues [2, 6]. Moreover, the microglial transcriptional profile changes at each developmental stage, are roughly divided into early microglia (microglia that seed the brain from E10.5- E12.5), pre-microglia (microglia found in the CNS from E12.5 up to P9) and adult microglia [6, 8]. Early microglia are highly proliferative, pre-

microglia exert functions on synapse pruning [6] and excess neuron elimination [9], and adult microglia perform immune surveillance but also synaptic refinement [7, 10-12]. During development, microglia control the numbers of neural progenitors via phagocytosis. This was shown by clodronate-mediated microglia deletion in organotypic brain cultures [9] or in CSF1R knockout mice, which lack microglia [13]. However, CSF1R is also expressed in other cells including peripheral myeloid subsets and neurons. Specific deletion of CSF1R on nestin+ cells recapitulated some of the observed effects in the global CSF1R knockout [13].

Complement components C1q and C3, tag extra synapses which are then removed by microglia via CR3 receptor mediated phagocytosis [11, 12]. This process is known as synaptic pruning [11]. Neuronally derived CX3CL1 acting on microglial CX3CR1 is one of the cues that guides microglia to the synapses [11]. Mice deficient in microglia or CX3CR1 exhibit neuronal connectivity and behavioral deficits similar to those observed in autism spectrum disorder [6, 14-16]. Developing microglia also control neural cells in the cerebellum and were shown to induce Purkinje cell death via NADPH activity [1, 17]. On the other hand, developing microglia also secrete trophic factors that promote neuronal circuits formation and neuronal survival. Microglial-derived insulin-like growth factor 1 (IGF-1) promotes survival of cortical layer V neurons in postnatal development. In addition it induces the fate of many cell lineages, such as oligodendrocytes and also protects them from glutamate-mediated apoptosis [1]. Basic fibroblast growth factor, hepatocyte growth factor, epidermal growth factor, platelet-derived growth factor, nerve growth factor, and brain-derived neurotrophic factor are all also secreted by microglia and contribute to neuronal development, maintenance, and function throughout life [18-20].

As microglia mature, they adopt a ramified morphology characterized by a small body and thin, long processes. Interestingly, recent studies suggest that adult microglia are not a homogeneous population, and their activation state is the result of region-specific cues [21-27]. They are self -renewing via a local progenitor [28, 29] but in certain instances, and when microglia are depleted for prolonged periods of

time via genetic or pharmacologic methods, peripheral myeloid cells can enter and engraft in the CNS for long periods but remain functionally distinct [30]. Microglia in steady state CNS depend on CSF1R signaling for survival. Both CSF1R ligands, CSF1 and IL-34, are found in the normal CNS and their expression is regionally controlled [31]. Interestingly, in the absence of CSF1, microglia numbers decrease by 30%, while in the absence of IL-34 microglial numbers decrease by 70%. IL-34 in particular controls the migration of microglial precursor cells in the CNS via CSF1R signaling in development [32]. TGF-β signaling is also necessary for homeostatic microglial functions and in its absence, they assume a transcriptome that is similar to that of peripheral macrophages [33].

Defining microglial markers that are distinct from those of peripheral monocytes has been the focus of investigation for many years. New RNAseq techniques yielded a number of genes that are preferentially expressed by microglia but not peripheral myeloid cells in homeostasis [6, 14, 34-36]. Lately, the most commonly employed markers are the purinergic receptor P2Y, G coupled protein 12 (P2RY12), the transmembrane protein TMEM119, and the transcriptional regulator Sal-like 1 (SALL1) [6, 14, 34-36]. Both P2RY12 and TMEM119 are expressed by the vast majority of microglia within the healthy CNS. The function of TMEM119 has not been yet elucidated. P2RY12 serves as a chemotactic receptor that guides microglia to sites of injury [23]. SALL1 is a microglia fate-determining factor, vital for expression of essential microglial genes and normal microglial morphology [23, 33]. Whether these markers are still able to differentiate between microglia and infiltrating myeloid cells in neuroinflammation, when all these cells undergo major transcriptional changes is still under investigation. However, SALL1 and TMEM119 are emerging as the most reliable microglial markers.

Adult microglia exert multiple roles in tissue maintenance: they phagocytose debris or dead cells, clear toxic amyloid-β, shape neural circuits via phagocytosing inappropriate or inactive connections [12], provide trophic support to neurons by producing growth factors, and regulate neurogenesis in the hippocampus and the subventricular zone (SVZ). Interestingly, microglia-derived CX3CL1 increases with

exercise and confers a protective effect on neuronal cells, while CX3CR1 deletion results in activated microglia with an inflammatory phenotype, leading to decreased rates of adult neurogenesis in the hippocampus [37-39]. In addition, microglia phagocytose neuronal progenitors in the adult SVZ, thus controlling the local pool of neurons [14, 38, 40]. Microglia also influence oligodendrocyte development and myelinogenesis both during development and in adulthood. In the adult CNS, microglia are necessary for myelin homeostasis and maintenance of adult oligodendrocyte progenitor cells [41, 42]. Microglia promote BBB function [43, 44] and in case of injury, they migrate to the affected site to promote repair [45].

Microglial malfunction is associated with neurodegenerative diseases such as Alzheimer's disease, Parkinson's disease, and neurodevelopmental and psychological defects such as Rett syndrome and obsessive compulsive disorder [6]. Furthermore, lack of phagocytosis by microglia results in excess synapses which is associated with impaired memory formation [12].

Tissue-resident macrophages

In addition to microglia, the healthy CNS houses three types of non-parenchymal tissue resident macrophages. They are named based on their location and are currently categorized as perivascular macrophages, meningeal macrophages and macrophages in the choroid plexus [46]. These macrophage populations are optimally placed to regulate and interrogate peripheral cell entry, act as sentinels by sampling their environment, and quickly respond in the event of an insult. Previously thought to be derived from bone marrow (BM) monocytic progenitor cells, it is now established that the majority of CNS-resident macrophages are long-lived and transcriptionally more similar to microglia than macrophages found in non-CNS tissues. Similarly to microglia, most of these cells are derived from erythromyeloid progenitors found in the extraembryonic yolk sac or fetal liver and their generation is PU.1 dependent, and independent of MYB and BATF3 [3, 34]. Choroid plexus macrophages are the most

distinct among these types of CNS non-parenchymal macrophages and originate from either embryonic precursors or BM.

Perivascular macrophages are located between the blood vessel endothelium (of BBB) and the glia limitans, which form the barrier to the CNS parenchyma. They are wrapped around endothelial walls with their elongated cell bodies and monitor the perivascular space [47]. Perivascular macrophages provide nutrients to endothelial cells, regulate vascular permeability, maintain BBB integrity, clear toxic amyloid-□ from the CNS, sample debris to assess the local milieu, and communicate with surrounding cells [46]. Their location is ideal to simultaneously sample both the CNS interstitial fluid and blood [46]. Perivascular macrophages infiltrate the CNS at the same time as microglia (E 9.5) and populate the abluminal spaces of the newly developed vasculature. Together with microglia, these macrophages play significant roles on the refinements of the developing vasculature [48]. In adulthood and in response to injury, perivascular macrophages promote anastomoses and the repair of vasculature [49].

Meningeal macrophages have a very similar origin and transcriptional control as perivascular macrophages. They are located in between meningeal vasculature and ER-TR7+ fibroblast-like cells that line the meninges. They also express similar markers to those of perivascular macrophages and are also long lived with negligible contribution from the periphery [34, 47].

The choroid plexus macrophages reside on the apical side of the epithelium facing the cerebrospinal fluid (CSF) in the stroma. The stroma of the choroid plexus is highly vascularized and surrounded by a monolayer of cuboidal epithelial cells, which are joined together by tight junctions forming the blood-CSF barrier. The choroid plexus is located in all four ventricles in the brain and is responsible for producing CSF [46]. It allows trafficking of a variety of immune cell types and is an area with an anti-inflammatory environment [50, 51]. In addition, the choroid plexus is the gateway to the CNS and is an area through which pioneering T cells gain access into the CNS in preclinical stages of the MS murine model

experimental autoimmune encephalomyelitis (EAE) [52]. Unlike the other types of CNS macrophages, these macrophages are partially replenished from the bone marrow [34].

All of these brain resident macrophages express the mannose receptor CD206, scavenger receptor CD163, along with CD11b, CXC3R1 and MHC-II. Perivascular and meningeal macrophages also express the lymphatic vessel endothelial hyaluronan receptor LYVE1, which is not expressed in choroid plexus associated macrophages [34, 47, 53].

Dendritic Cells

At steady state, dendritic cells (DCs) are sparsely distributed within the nonparenchymal CNS spaces. They are more numerous in the leptomeninges and dura mater, less prominent in the choroid plexus and mostly absent from perivascular spaces [54].

DCs develop from committed DC or monocyte progenitors in the BM and are dependent upon FLT3 signaling [55]. They are relatively short-lived and are replenished roughly every 1-2 weeks [56]. Mature DCs are divided into conventional DCs (cDCs), plasmacytoid DCs (pDCs) and monocyte-derived DCs (moDCs). cDCs are further subdivided into cDC1 and cDC2. cDC1s are associated with Th1 responses [57, 58] while cDC2 with Th2 and Th17 [59]. cDC1s are also able to cross present antigens and activate CD8+ T cells. cDCs leave the BM in the form of a committed precursor, while pDCs mature in the BM before entering the circulation. In addition, moDCs are not usually found in steady state but are crucial mediators on inflammatory responses [60].

IRF4 and IRF8 are transcription markers differentially expressed in the various DC subsets. cDC1s are IRF8+IRF4lo/-, cDC2s are IRF8loIRF4+, pDCs are IRF8+IRF4+ and moDCs are IRF4loIRF8lo [61]. cDC1s do not express CD11b. Within the mouse CNS the majority of DCs are cDC2 and are mostly located in the leptomeninges and dura mater. Within the choroid plexus the majority of DCs are cDC1s [54].

Granulocytes

Although their presence is commonly ignored within the CNS at steady state, various types of granulocytes such as neutrophils, mast cells, basophils and eosinophils are found within perivascular and meningeal spaces and the choroid plexus [15]. Mast cells in particular are also found within the parenchyma [62, 63]. Neutrophils exit the bone marrow in a mature state and are thought to be short-lived. However, studies have shown that subsets of neutrophils live much longer than previously thought and more importantly, some have been found in various organs likely as a local reservoir [64]. It is now acknowledged that neutrophils or neutrophil subsets may have different functions. Other than the well-documented inflammatory functions, pro-reparative CD206+ neutrophils, VEGF-responding angiogenic neutrophils, and CD11c+Ly6G+ "hybrid" cell type have been identified [65-68]. Interestingly neutrophils were recently detected in the normal murine CNS localized within the subdural meningeal spaces but their contribution to tissue homeostasis is still not known [69].

Mast cells (MCs) are derived from CD34+ bone marrow progenitor cells, enter the circulation in an immature state, and mature once they reach the tissue in response to local cues. They are mostly known for their effects during allergic/atopic responses mediated IgE crosslinking of their Fc□RI receptor. MCs are a heterogeneous population and depending on the types of proteases they carry within their granules, they are broadly categorized into at least three subtypes: MCs that contain only tryptase (MCT), MCs that contain only chymase (MCC) and MCs that contain tryptase, chymase, carboxypeptidase, and cathepsin G (MCCT) [70, 71]. MCs cells are loaded with granules containing preformed mediators and can synthesize mediators de novo. They are found in many tissues and usually associated with vascular epithelial cells and nerves. CNS mast cells are constitutively active and degranulate in response to homeostatic or inflammatory stimuli [63, 72-74]. Their preformed granules are released immediately upon activation and contain various mediators such as histamine, serotonin, and TNF□ in addition to proteases. They can quickly synthesize lipid mediators such as prostaglandins and leukotrienes, and growth factors. A late

phase activation of mast cells results in de novo production of inflammatory cytokines such as IL-6 and TNF-□ [70, 75].

Within the healthy CNS, MCs are found within the thalamus, hypothalamus, entorhinal cortex, hippocampus, the meninges, perivascular spaces and within the brain in proximity to BBB. They interact with neurons and microglia and their granules contain a plethora of mediators including neurotransmitters. Their location allows them to modulate BBB permeability and genetically modified mice that lack MCs display decreased BBB permeability both in homeostasis and neuroinflammation [63, 73, 74].

MC activity in stress has been associated with migraines [74, 76]. Moreover, histamine released from MC was shown to promote wakefulness in adult mice [77], and microglial synaptic pruning in the developing CNS, which then regulates of sexual behavior in adulthood [78].

1.3. Myeloid cells in multiple sclerosis

Pathologically MS is characterized by focal demyelinating lesions disseminated in space and time and neuronal and axonal damage. MS lesions are rich in myeloid cells (microglia, infiltrating monocyte-derived macrophages and DCs), and outnumber lymphoid cells [79]. Below we will discuss current knowledge on myeloid cells in MS, which are now emerging as crucial players in disease pathogenesis and progression. Some of this knowledge is derived from studies on the animal model of MS, experimental autoimmune encephalomyelitis (EAE). Although this model has been criticized [80], it mimics most of the CNS pathology observed in MS such as tissue infiltration by immune cells, formation of lesion, local inflammation and progressive axonal loss [81, 82].

Monocytes are not found in the healthy CNS but are regularly found in the CNS and CSF of the MS patients. Once they enter the CNS, monocytes mature into macrophages and participate in disease progression. There are three well characterized monocyte subsets categorized based on expression patterns of the LPS receptor CD14 and the Fc□RIII, CD16: the classical CD14++CD16- (similar to the inflammatory monocyte

in mice Ly6ChiCCR2+), the non-classical CD14+CD16++ (similar to the anti-inflammatory CX3CR1+Ly6Clo in mice) and the intermediate CD14++CD16+. CD16+ monocytes have been associated with inflammation and promoting the generation of Th17 cells. MS patients with active disease show increased CD14+ cells both in the blood and the CSF. These cells also contribute to breaking down the blood-brain barrier [83, 84].

Both conventional and plasmacytoid DCs are increased in the blood and CSF of MS patients. cDCs are usually found early in disease and pDCs numbers are highly increased in the CSF during relapses. Circulating cDCs in MS patients upregulate CCR5 which is a receptor for CCL3 and CCL5, both of which are upregulated in MS lesions. However, cDCs in primary progressive MS display an immature phenotype [85]. Interestingly, although pDC numbers increase in MS, these cells are found to be phenotypically similar to that of healthy controls. Although the data on circulating pDCs are still conflicting, imbalances in DC populations may result in significant changes in T cell functionally in MS [86].

Myeloid cells in MS lesions

MS lesions are found both within the brain and spinal cord and can be formed within the white and the grey matter [87, 88]. The most commonly employed classification is the four types of lesions described by Lucchinetti and colleagues [89]. Type I is characterized by macrophage products, type II by antibody and complement deposition while type III lacks complement and antibody deposition. Types I and II have clearly demarcated borders, while type III is characterized by diffuse demyelination and lack clear demarcation. Type IV is characterized by dystrophic apoptotic oligodendrocytes. In most of these lesions the major cell types are myeloid cells [79].

Although more pronounced during relapses, infiltrating myeloid cells and activated microglia are found within the CNS of MS patients throughout the disease and are associated with demyelination, oligodendrocytic loss and axonal damage [88, 90, 91]. With the exception of rapid progressive MS. in

which the CNS is intensely infiltrated [90], in progressive forms of the disease, the tissue is not massively infiltrated, however, myeloid cells (microglia and/or infiltrating myeloid) remain activated [88, 92]. During progressive stages of the disease, axonal loss is prominent leading to tissue atrophy in both MS and EAE [82, 88]. These processes are likely mediated via the production of oxygen radicals produced by either microglia or infiltrating myeloid cells (84).

Microglia/Macrophages

The contribution of microglia to MS is still highly debated. Studies in mice have shown that microglia are poor antigen presenting cells and not likely to activate infiltrating lymphocytes. Instead, microglia may contribute to the disease process via oxidative stress and produce proinflammatory cytokines that may activate astrocytes or cause oligodendrocytic damage. Microglia are highly phagocytic, and thus can remove myelin debris and cellular fragments, damaged axons, and dead cells. It is clear that microglia are activated in the CNS of MS patients, but whether they promote disease or facilitate repair is still not well delineated. One of the main hurdles for these investigations is that there is no unique marker to reliably distinguish microglia from infiltrating monocytes in neuroinflammation. Additionally, activated microglia are morphologically indistinguishable from infiltrating monocytes. RNA transcriptome analysis has yielded a number of markers that show preferential expression in microglia (**see section 2.1**). TMEM119 is the only marker so far examined in MS tissue and seems to be expressed by a subpopulation of myeloid cells within a lesion, and far from lesions [93]. However, there is still not a breadth of studies examining the specificity of TMEM119 in neuroinflammation, when all myeloid cells undergo major transcriptional changes [47]. Thus, below we will talk about microglia and macrophages as one population in active MS lesions, and specify TMEM119-expressing cells within the MS CNS.

Microglia/macrophages (M/Ms) in active MS lesions are heterogeneous and capable of performing a variety of activities that may promote or control inflammation and repair [94, 95]. M/Ms found within active MS lesions usually express markers associated with inflammatory macrophage functions, including

inducible nitric oxide synthase (iNOS), costimulatory molecules CD40, CD86, the Fc receptors CD32 and CD64, phagocytosis marker CD68 and p22phox, a subunit of NADPH oxidase [96, 97]. In addition, M/Ms may also express anti-inflammatory markers such as the mannose receptor CD206 and the scavenger receptor CD163 [96]. Approximately half of the myeloid cells within active lesions express TMEM119, suggesting these cells may be microglia. Interestingly, PY2R12, which is usually expressed in homeostatic microglia is not expressed in these cells, suggesting it is downregulated upon activation [93].

MS lesions are not static, and overtime grow outwards, eventually becoming chronically active. These lesions are slowly expanding and have a thin border of M/M. The center of these lesions appears quiescent and populated by lipid-laden (foamy) macrophages, many of them expressing CD206 and CD163 [94, 98]. However, M/Ms lining the rim of these lesions express iNOS and HLA-DR, suggesting they are inflammatory and promote T cell functions [99]. M/Ms at the rims of either active or chronically active plaques contain iron which has been suggested to promote MS pathology [100, 101]. In the normal CNS, most iron is found within oligodendrocytes or myelin. When iron is released after oligodendrocytic death and demyelination, it is internalized by ferritin+ microglia/macrophages which acquire a dystrophic phenotype [102]. Interestingly TMEM119+ cells that express low or no P2RY12 (likely activated microglia) are found within chronically active or slow expanding lesions and their density decreases inwards. Strikingly, there are no differences between overall M/M density and levels of activation between lesion types. [93, 96, 99].

Areas of the CNS that are far from the demyelinating lesions and often appearing normal (normal appearing white matter; NAWM) are also characterized by scattered microglial activation. Interestingly, ramified microglia were shown to express iNOS and were often close to injured axons [103]. However, microglia have also been documented to exhibit a suppressed and anti-inflammatory character [104]. Clusters of microglia or macrophages, known as microglial nodules, have been found in NAWM in close proximity to degenerating axons. These nodules appear in the absence of extensive inflammation,

astrogliosis or demyelination and their formation has been argued to be one of the early events in MS pathology [105]. Furthermore, P2RY12+ TMEM119+ microglia in the NAWM also expressing activation markers CD68 and p22phox are found in both MS and healthy controls' brains, suggesting that certain microglial populations are in an "intermediate" pre-activated state [93].

In addition to white matter, demyelination is also observed within the gray matter. MS gray matter is characterized by less infiltration by immune cells and less activation of M/Ms compared to that of white matter lesions. This type of demyelination has been mostly attributed to aberrant microglia functions such as ROS production via the NADPH oxidase activity. This mechanism seems to be more prominent in the gray matter compared to white matter lesions. In addition, cortical microglial activation can be observed via PET imaging by administering the traditional PK11195 and more recently the novel PBR28 ligands [106, 107].

In progressive forms of MS, M/Ms are activated both within the lesions and in the normal appearing white and gray matter and this has been linked to inflammatory cytokines produced in the meninges, likely by infiltrating B cells. [108, 109]. Activated complement component 3 fragments (C3d) are found within microglia clusters of slowly expanding lesions in progressive but not acute MS [110] and in close proximity of damaged axons. This suggests that C3 activation and deposition is not likely associated with lesion initiation, but rather a mechanism that facilitates the removal of axonal and cellular debris. Furthermore, the activation/phagocytosis marker CD68 is significantly increased in the NAWM in progressive forms of MS compared to that of relapsing-remitting MS and healthy controls [93].

Dendritic cells

Both cDCs and pDCs accumulate in the leptomeninges and lesions in MS patients. MoDCs, which are not present in homeostatic CNS, differentiate from infiltrating inflammatory monocytes within the CNS of MS patients. Studies in murine EAE showed that both cDCs and moDCs are found within the CNS infiltrates. cDCs express CD26 and ZBTB46, a transcription factor also expressed in human cDCs, while moDCs express

CD88 and CD64 [54, 99, 111]. Although these markers may be expressed by other cell-types, they are useful markers for identification of DC subsets. cDCs are the most efficient antigen presenting cells and are able to process larger myelin fragments to activate naïve and effector T cells. Both cDCs and moDCs progressively expand during the onset and peak of EAE in every CNS compartment. pDCs are not efficient antigen presenting cells, but are equipped to secrete inflammatory cytokines and promote an inflammatory environment to support cDCs and moDCs [112].

Granulocytes

Neutrophils are relatively rare in established MS lesions, thus their contribution to disease course has long been debated. Studies in EAE show that neutrophils are part of the inflammatory lesions, appear early in disease process [82, 113], and are increased in peripheral lymphoid organs and blood [113]. Neutrophils may promote early disease progression by increasing permeability of the BBB, possibly through secretion of matrix metalloproteinases, or the release of neutrophil extracellular traps (NETs) [114, 115]. Inactivation of neutrophil products, such as myeloperoxidase or neutrophil elastase, results in milder EAE course and associated optic neuritis [116, 117]. In agreement with the EAE data, CSF of newly diagnosed patients shows elevated neutrophil counts [118] and the CSF of patients with established disease contains increased levels of the neutrophil chemoattractant CXCL8 [119, 120]. Neutrophil elastase and chemokines that promote neutrophil recruitment, such as CXCL1 and CXCL5, are systemically elevated in relapsing MS patients and correlate with lesion burden and clinical disability [121]. Transcripts of the granulocyte-colony stimulating factor (G-CSF) which promotes the proliferation and differentiation of neutrophils (and other granulocytes) are found within lesions but not in NAWM [122] and treatment with G-CSF has been seen to worsen MS symptoms in patients [123, 124]. Thus, lack of neutrophil detection in MS lesions may be due to incorrect sampling timing.

Interestingly, mast cells are found in close proximity to MS lesions and were initially observed in 1890 by Neuman [125] and later by other groups [62, 126-128]. Their numbers are very low compared those of

the other myeloid subsets, thus not much is yet known about their contribution to disease progression. However, the ability of mast cells to secrete histamine and proteases may facilitate disease onset or relapses by promoting vascular permeability and tissue infiltration. In EAE, mice with spontaneous c-Kit mutations that lead to deletion of mast cells have shown that these cells may prevent, promote or have no effect on disease progression [129]. These conflicting data are likely due to the fact that none of these mouse strains are specific and efficient mast cell knockouts.

1.4. Effect of MS therapeutics on myeloid cells

A multitude of MS therapies are designed to dampen immune system activation. Although most of these therapies target lymphocytes, myeloid cells can also be affected directly or indirectly. This section will explore how current MS therapies affect myeloid cells.

IFN-β

IFN-β, the first FDA-approved biologic therapeutic for MS, is a pleiotropic cytokine exerting a plethora of effects on a variety of cells [130, 131]. Monocytes isolated from MS patients treated ex-vivo with IFN-β exhibit impaired inflammatory responses when stimulated with LPS/alum compared to monocytes isolated from healthy donors [132]. Ex-vivo treatment of DCs derived from MS patients or healthy donors with IFN-β reduced the expression of IL-1□ and IL-23 and upregulated the expression of IL12p35 and IL27p28, which resulted in reduced generation of Th17 cells [133]. Additionally, studies in EAE showed that deletion of type I IFNγ receptor (IFNAR), the receptor of IFN-β specifically on myeloid cells resulted in aggravated EAE disease [134].

IFN-β is one of the most common first-line MS treatments, however a large proportion of patients are not responsive. Interestingly, non-responders exhibit exaggerated upregulation of type I IFN responsive genes either at baseline or in response to IFN-β treatment compared to responders [135-137]. MS patients that upregulated the death-associated receptor TRAIL on monocytes after IFN-β treatment benefited more

than patients that did not [138]. Additionally, monocytes isolated from MS patients treated with IFN-β for prolonged periods of time (9 months to 6 years) upregulated the co-stimulatory molecules CD80, CD86, and CD40 [139], which was associated with responsiveness to treatment [140]. In a different study, however, there was a positive association between monocytic CD40 upregulation, early after IFN-β injections (9-12 hrs.) and relapses [141].

About 30% of MS patients treated with IFN-β also develop antidrug antibodies and thus are not responsive to treatment. Antidrug antibody generation was associated with decreased NOTCH2 signaling. NOTCH2, a regulator of monocyte differentiation from the inflammatory to anti-inflammatory phenotype, was markedly reduced on CD14+ monocytes from untreated MS patients that developed antidrug antibodies 12 months after IFN-β therapy initiation [142].

All the above suggest that defining myeloid cell subsets propensities with the context of MS before and after treatment initiation will be useful in determining whether IFN-β is a suitable treatment for specific patients.

Glatiramer Acetate

Glatiramer Acetate (GA) is a synthetic random copolymer, composed of glutamic acid, alanine lysine and tyrosine, employed as a treatment for relapsing-remitting MS. MS patients treated with GA show a shift towards Th2 responses and produce anti-inflammatory/pro-repair mediators, likely due to GA effects on myeloid subsets [143, 144]. Initial studies showed that GA binds to MHC-II altering the myelin antigen presentation capabilities resulting in impaired activation of autoreactive T cells [145, 146]. However, it was later shown that GA can also exert its anti-inflammatory effects independently of MHC-II [147]. Instead, GA was shown to promote the generation of anti-inflammatory monocytes which support regulatory T cell functions [147].

In support of this, monocytes isolated from the blood of GA-treated MS patients produced significantly higher amounts of IL-10, lower amounts of IL-12 and the levels of CD16+ anti-inflammatory monocytes

were restored to those of healthy controls [148, 149]. DCs from GA-treated MS patients exhibit reduced IL-12 production [150] and express lower levels of CD40, upregulation of which is associated with relapses [151]. Furthermore, the activity of myeloid derived suppressor cells, a population that suppresses inflammatory responses, is augmented in GA-treated MS patients [152], and GA-treated human microglia express IL-10 and reduce production of proinflammatory TNF [148]. Increased levels of circulating IL-27, a regulatory cytokine produced by myeloid cells in inflammatory conditions was recently linked to better GA therapeutic outcomes [153]. Another study showed increased levels of IL-27 in MS patients in circulation, CSF, and lesions, however there was no association with treatments [154].

Fingolimod

Fingolimod is the first oral therapy approved to treat relapsing remitting MS, and is more effective in reducing relapses than IFN-β [155]. Fingolimod (FTY720) is phosphorylated by sphingosine kinase, and its phosphorylated metabolite (FTY720-P) binds to the G-protein coupled sphingoshine-1-phosphate (S1P) receptors. S1P receptors are expressed on a variety of cells including neural, glial and endothelial cells in the CNS and most of the immune cells in the CNS and the periphery [156]. One of the mechanisms by which fingolimod reduces disease severity and relapses in MS is that it binds S1PR1, a type of S1P receptors, on lymphocytes and prevents their egress from lymphoid tissues [157].

Fingolimod's immunosuppressive effects are also exerted on myeloid cells. Incubation of murine macrophages or human monocytes with either the natural ligand of S1PR1, SP1, or fingolimod, respectively, reduced inflammatory responses after LPS exposure [158-160]. Although microglia, DCs and peripheral macrophages express similar patterns and levels of S1P receptors, FTY720 downregulated ERK phosphorylation only in DCs and macrophages. FTY720 also downregulated expression of the proinflammatory cytokine IL-12 and upregulated anti-inflammatory IL-10 in DCs and macrophages but not in microglia [159]. Flow cytometry analyses of DCs and monocytes isolated from MS patients before and during fingolimod-treatment showed decreased levels of activation markers (CD83, CD150 and HLA-DR).

Furthermore, fingolimod treatment reduced proinflammatory cytokine production, phagocytic activity of DCs and monocytes, and impaired priming of Th1 and Th17 cells [161]. Interestingly, monocytes isolated from fingolimod-treated MS patients exhibited reduced expression of proinflammatory micro-RNA miR-155 but also of antioxidant genes HMOX1 and OSGIN1 compared to untreated patients [162]. When monocyte-derived macrophages and microglia were examined in vitro, fingolimod reduced LPS-induced inflammatory cytokines and increased expression of antioxidants. These data suggest that the effects of fingolimod on myeloid cells in vivo may be an indirect effect. Fingolimod crosses the BBB [163] and therapeutic administration of fingolimod reduced TNF production by microglia and monocytes in EAE [158].

Dimethyl fumarate

Dimethyl fumarate (DMF) was approved as an oral first-line therapeutic for relapsing remitting MS in 2013. It is a methyl ester of fumaric acid, quickly metabolized to active monomethyl fumarate which activates transcription factor nuclear factor erythroid-derived 2 (Nrf2) and suppresses NF-B, to modulate oxidative stress [164]. DMF exerts its effects on multiple immune subsets [165].

Monocytes from DMF-treated RRMS patients express reduced levels of the pro-inflammatory micro-RNA miR-155, and DMF-treated human microglia and monocyte-derived macrophages had reduced production of pro-inflammatory cytokines after LPS stimulation, indicating direct regulatory effects [162]. DMF reduces neuroinflammation levels and cognitive deficits induced by systemic LPS administration [166]. In EAE, DMF promote the generation of anti-inflammatory monocytes and decreased macrophage infiltration into the CNS resulting in milder clinical score, Interestingly these effects were exerted independently of Nrf2 [167, 168].

Teriflunomide

Teriflunomide is a reversible inhibitor of dihydroorotate dehydrogenase (DHODH), a mitochondrial enzyme active in proliferating cells [169]. DHODH impairs proliferation of lymphocytes and exerts

nebulous effects on myeloid cells [170]. In EAE, teriflunomide reduced T cell and myeloid cell infiltration of the CNS [171]. In cultured primary microglia, teriflunomide downregulated expression of CD86 and expression of IL-10 [172]. Ex-vivo, teriflunomide treatment decreased production of IL-6 and CCL2 in activated monocytes from healthy individuals [173].

Furthermore, MS patients after 6 months of treatment showed increased IL-10 production and PD-L1 expression in monocytes, implying that teriflunomide induces anti-inflammatory and regulatory responses in these cells [174].

Monoclonal Antibodies

Several antibody-based therapies target lymphocytes have been recently developed. Below we will discuss whether and how these therapies affect myeloid cells.

Natalizumab

Natalizumab (NTZ) is an immunomodulatory antibody that limits immune cell infiltration into the CNS by blocking the interaction between the very late activation antigen-4 (VLA-4), an integrin expressed on lymphocytes and myeloid cells, and vascular adhesion molecule-1 (VCAM-1) [175]. As a result, fewer cells are able to migrate and infiltrate the CNS [176]. NTZ reduces relapses and lesion load but increases the risk for progressive multifocal leukoencephalopathy [177]. NTZ reduced the frequencies of mature activated pDCs, however this activation was not a direct effect of NTZ on pDC [178].

Triggering receptor expressed on myeloid cells 2 (TREM2) is an innate immune receptor associated with inflammatory responses and within the CNS expressed by microglia [179]. In neuroinflammation, microglia shed TREM2, which can be detected in CSF [180, 181]. NTZ reduced CSF soluble TREM-2 to baseline levels, indicating dampened microglial activation, which is associated with improved clinical outcome after 12 months of treatment [182]. It is not clear however whether there is a direct effect of NTZ on microglia.

Anti CD20 antibodies

There are multiple anti-CD20 monoclonal antibodies shown to ameliorate relapses in RRMS including rituximab, ocrelizumab and ofatumumab [183]. However, ocrelizumab is the only anti CD20 antibody that exerts beneficial effects in relapsing remitting and also in primary progressive MS [184]. A subset of GM-CSF producing memory B cells, more prevalent in MS patients than healthy controls, was shown to activate pro-inflammatory myeloid cells in vitro [185]. Following B cell depleting therapy in MS patients, the inflammatory myeloid response is diminished [185].

Alemtuzumab

Alemtuzumab is a monoclonal antibody that binds CD52 and effectively depletes CD52-expressing lymphocytes through antibody-dependent cell-mediated cytolysis. Both lymphocytes and myeloid cells express CD52, however myeloid cells are more resistant to alemtuzumab -mediated cytolysis thus their numbers are not affected by treatment [186]. Neutrophils, however, express CD52 and are subject to lysis during alemtuzumab treatment [187], occasionally leading to severe neutropenia [188].

1.5. Conclusion

The contribution of myeloid cells to MS progression is now widely appreciated. Their persistent elevated presence in lesions and activated phenotype regardless of tissue infiltration in relapsing and progressive MS suggest they play crucial roles in disease progression and chronicity. Although gaps in knowledge still exist, recent advances are making it easier for researchers and clinicians to dissect the roles of each myeloid subset in the disease process.

Current therapeutics have broad activities or specifically target lymphocyte functions. In many instances, however, their efficacy stems from their direct or indirect effects on myeloid cell functions. Future research focusing on modulation of myeloid populations and their activities will prove useful for the design of novel therapeutics for MS patients.

REFERENCES

1. Nayak D, Roth TL, McGavern DB. Microglia development and function. Annu Rev Immunol. 2014;32:367-402.

2. Schulz C, Gomez Perdiguero E, Chorro L, Szabo-Rogers H, Cagnard N, Kierdorf K, et al. A lineage of myeloid cells independent of Myb and hematopoietic stem cells. Science. 2012;336(6077):86-90.

3. Ginhoux F, Greter M, Leboeuf M, Nandi S, See P, Gokhan S, et al. Fate mapping analysis reveals that adult microglia derive from primitive macrophages. Science. 2010;330(6005):841-5.

4. Kierdorf K, Erny D, Goldmann T, Sander V, Schulz C, Perdiguero EG, et al. Microglia emerge from erythromyeloid precursors via Pu.1- and Irf8-dependent pathways. Nat Neurosci. 2013;16(3):273-80.

5. Rymo SF, Gerhardt H, Wolfhagen Sand F, Lang R, Uv A, Betsholtz C. A two-way communication between microglial cells and angiogenic sprouts regulates angiogenesis in aortic ring cultures. PLoS One. 2011;6(1):e15846.

6. Hammond TR, Robinton D, Stevens B. Microglia and the Brain: Complementary Partners in Development and Disease. Annu Rev Cell Dev Biol. 2018;34:523-44.

7. Torres L, Danver J, Ji K, Miyauchi JT, Chen D, Anderson ME, et al. Dynamic microglial modulation of spatial learning and social behavior. Brain Behav Immun. 2016;55:6-16.

8. Matcovitch-Natan O, Winter DR, Giladi A, Vargas Aguilar S, Spinrad A, Sarrazin S, et al. Microglia development follows a stepwise program to regulate brain homeostasis. Science. 2016;353(6301):aad8670.

9. Cunningham CL, Martinez-Cerdeno V, Noctor SC. Microglia regulate the number of neural precursor cells in the developing cerebral cortex. J Neurosci. 2013;33(10):4216-33.

10. Parkhurst CN, Yang G, Ninan I, Savas JN, Yates JR, 3rd, Lafaille JJ, et al. Microglia promote learning-dependent synapse formation through brain-derived neurotrophic factor. Cell. 2013;155(7):1596-609.

11. Paolicelli RC, Bolasco G, Pagani F, Maggi L, Scianni M, Panzanelli P, et al. Synaptic pruning by microglia is necessary for normal brain development. Science. 2011;333(6048):1456-8.

12. Stevens B, Allen NJ, Vazquez LE, Howell GR, Christopherson KS, Nouri N, et al. The classical complement cascade mediates CNS synapse elimination. Cell. 2007;131(6):1164-78.

13. Nandi S, Gokhan S, Dai XM, Wei S, Enikolopov G, Lin H, et al. The CSF-1 receptor ligands IL-34 and CSF-1 exhibit distinct developmental brain expression patterns and regulate neural progenitor cell maintenance and maturation. Dev Biol. 2012;367(2):100-13.

14. Kierdorf K, Prinz M. Microglia in steady state. J Clin Invest. 2017;127(9):3201-9.

15. Herz J, Filiano AJ, Smith A, Yogev N, Kipnis J. Myeloid Cells in the Central Nervous System. Immunity. 2017;46(6):943-56.

16. Zhan Y, Paolicelli RC, Sforazzini F, Weinhard L, Bolasco G, Pagani F, et al. Deficient neuron-microglia signaling results in impaired functional brain connectivity and social behavior. Nat Neurosci. 2014;17(3):400-6.

17. Marin-Teva JL, Dusart I, Colin C, Gervais A, van Rooijen N, Mallat M. Microglia promote the death of developing Purkinje cells. Neuron. 2004;41(4):535-47.

18. Araujo DM, Cotman CW. Basic FGF in astroglial, microglial, and neuronal cultures: characterization of binding sites and modulation of release by lymphokines and trophic factors. J Neurosci. 1992;12(5):1668-78.

19. Nakajima K, Honda S, Tohyama Y, Imai Y, Kohsaka S, Kurihara T. Neurotrophin secretion from cultured microglia. J Neurosci Res. 2001;65(4):322-31.

20. Trang T, Beggs S, Salter MW. Brain-derived neurotrophic factor from microglia: a molecular substrate for neuropathic pain. Neuron Glia Biol. 2011;7(1):99-108.

21. De Biase LM, Schuebel KE, Fusfeld ZH, Jair K, Hawes IA, Cimbro R, et al. Local Cues Establish and Maintain Region-Specific Phenotypes of Basal Ganglia Microglia. Neuron. 2017;95(2):341-56 e6.

22. Grabert K, Michoel T, Karavolos MH, Clohisey S, Baillie JK, Stevens MP, et al. Microglial brain region-dependent diversity and selective regional sensitivities to aging. Nat Neurosci. 2016;19(3):504-16.

23. Butovsky O, Weiner HL. Microglial signatures and their role in health and disease. Nat Rev Neurosci. 2018;19(10):622-35.

24. Hanisch UK. Functional diversity of microglia - how heterogeneous are they to begin with? Front Cell Neurosci. 2013;7:65.

25. Ransohoff RM, Cardona AE. The myeloid cells of the central nervous system parenchyma. Nature. 2010;468(7321):253-62.

26. Hammond TR, Dufort C, Dissing-Olesen L, Giera S, Young A, Wysoker A, et al. Single-Cell RNA Sequencing of Microglia throughout the Mouse Lifespan and in the Injured Brain Reveals Complex Cell-State Changes. Immunity. 2019;50(1):253-71 e6.

27. Masuda T, Sankowski R, Staszewski O, Bottcher C, Amann L, Scheiwe C, et al. Spatial and temporal heterogeneity of mouse and human microglia at single-cell resolution. Nature. 2019;566(7744):388-92.

28. Huang Y, Xu Z, Xiong S, Sun F, Qin G, Hu G, et al. Repopulated microglia are solely derived from the proliferation of residual microglia after acute depletion. Nat Neurosci. 2018;21(4):530-40.

29. Zhan L, Krabbe G, Du F, Jones I, Reichert MC, Telpoukhovskaia M, et al. Proximal recolonization by self-renewing microglia re-establishes microglial homeostasis in the adult mouse brain. PLoS Biol. 2019;17(2):e3000134.

30. Cronk JC, Filiano AJ, Louveau A, Marin I, Marsh R, Ji E, et al. Peripherally derived macrophages can engraft the brain independent of irradiation and maintain an identity distinct from microglia. J Exp Med. 2018;215(6):1627-47.

31. Chitu V, Gokhan S, Nandi S, Mehler MF, Stanley ER. Emerging Roles for CSF-1 Receptor and its Ligands in the Nervous System. Trends Neurosci. 2016;39(6):378-93.

32. Wu S, Xue R, Hassan S, Nguyen TML, Wang T, Pan H, et al. Il34-Csf1r Pathway Regulates the Migration and Colonization of Microglial Precursors. Dev Cell. 2018;46(5):552-63 e4.

33. Buttgereit A, Lelios I, Yu X, Vrohlings M, Krakoski NR, Gautier EL, et al. Sall1 is a transcriptional regulator defining microglia identity and function. Nat Immunol. 2016;17(12):1397-406.

34. Goldmann T, Wieghofer P, Jordao MJ, Prutek F, Hagemeyer N, Frenzel K, et al. Origin, fate and dynamics of macrophages at central nervous system interfaces. Nat Immunol. 2016;17(7):797-805.

35. Butovsky O, Jedrychowski MP, Moore CS, Cialic R, Lanser AJ, Gabriely G, et al. Identification of a unique TGF-beta-dependent molecular and functional signature in microglia. Nat Neurosci. 2014;17(1):131-43.

36. Hickman SE, Kingery ND, Ohsumi TK, Borowsky ML, Wang LC, Means TK, et al. The microglial sensome revealed by direct RNA sequencing. Nat Neurosci. 2013;16(12):1896-905.

37. Bachstetter AD, Morganti JM, Jernberg J, Schlunk A, Mitchell SH, Brewster KW, et al. Fractalkine and CX 3 CR1 regulate hippocampal neurogenesis in adult and aged rats. Neurobiol Aging. 2011;32(11):2030-44.

38. Sellner S, Paricio-Montesinos R, Spiess A, Masuch A, Erny D, Harsan LA, et al. Microglial CX3CR1 promotes adult neurogenesis by inhibiting Sirt 1/p65 signaling independent of CX3CL1. Acta Neuropathol Commun. 2016;4(1):102.

39. Vukovic J, Colditz MJ, Blackmore DG, Ruitenberg MJ, Bartlett PF. Microglia modulate hippocampal neural precursor activity in response to exercise and aging. J Neurosci. 2012;32(19):6435-43.

40. Fourgeaud L, Traves PG, Tufail Y, Leal-Bailey H, Lew ED, Burrola PG, et al. TAM receptors regulate multiple features of microglial physiology. Nature. 2016;532(7598):240-4.

41. Hagemeyer N, Hanft KM, Akriditou MA, Unger N, Park ES, Stanley ER, et al. Microglia contribute to normal myelinogenesis and to oligodendrocyte progenitor maintenance during adulthood. Acta Neuropathol. 2017;134(3):441-58.

42. Wlodarczyk A, Holtman IR, Krueger M, Yogev N, Bruttger J, Khorooshi R, et al. A novel microglial subset plays a key role in myelinogenesis in developing brain. EMBO J. 2017;36(22):3292-308.

43. Keaney J, Campbell M. The dynamic blood-brain barrier. FEBS J. 2015;282(21):4067-79.

44. Obermeier B, Daneman R, Ransohoff RM. Development, maintenance and disruption of the blood-brain barrier. Nat Med. 2013;19(12):1584-96.

45. Lou N, Takano T, Pei Y, Xavier AL, Goldman SA, Nedergaard M. Purinergic receptor P2RY12-dependent microglial closure of the injured blood-brain barrier. Proc Natl Acad Sci U S A. 2016;113(4):1074-9.

46. Katsumoto A, Lu H, Miranda AS, Ransohoff RM. Ontogeny and functions of central nervous system macrophages. J Immunol. 2014;193(6):2615-21.

47. Mrdjen D, Pavlovic A, Hartmann FJ, Schreiner B, Utz SG, Leung BP, et al. High-Dimensional Single-Cell Mapping of Central Nervous System Immune Cells Reveals Distinct Myeloid Subsets in Health, Aging, and Disease. Immunity. 2018;48(3):599.

48. Checchin D, Sennlaub F, Levavasseur E, Leduc M, Chemtob S. Potential role of microglia in retinal blood vessel formation. Invest Ophthalmol Vis Sci. 2006;47(8):3595-602.

49. Liu C, Wu C, Yang Q, Gao J, Li L, Yang D, et al. Macrophages Mediate the Repair of Brain Vascular Rupture through Direct Physical Adhesion and Mechanical Traction. Immunity. 2016;44(5):1162-76.

50. Kunis G, Baruch K, Miller O, Schwartz M. Immunization with a Myelin-Derived Antigen Activates the Brain's Choroid Plexus for Recruitment of Immunoregulatory Cells to the CNS and Attenuates Disease Progression in a Mouse Model of ALS. J Neurosci. 2015;35(16):6381-93.

51. Prinz M, Erny D, Hagemeyer N. Ontogeny and homeostasis of CNS myeloid cells. Nat Immunol. 2017;18(4):385-92.

52. Reboldi A, Coisne C, Baumjohann D, Benvenuto F, Bottinelli D, Lira S, et al. C-C chemokine receptor 6-regulated entry of TH-17 cells into the CNS through the choroid plexus is required for the initiation of EAE. Nat Immunol. 2009;10(5):514-23.

53. Zeisel A, Munoz-Manchado AB, Codeluppi S, Lonnerberg P, La Manno G, Jureus A, et al. Brain structure. Cell types in the mouse cortex and hippocampus revealed by single-cell RNA-seq. Science. 2015;347(6226):1138-42.

54. Mundt S, Mrdjen D, Utz SG, Greter M, Schreiner B, Becher B. Conventional DCs sample and present myelin antigens in the healthy CNS and allow parenchymal T cell entry to initiate neuroinflammation. Sci Immunol. 2019;4(31).

55. Waskow C, Liu K, Darrasse-Jeze G, Guermonprez P, Ginhoux F, Merad M, et al. The receptor tyrosine kinase Flt3 is required for dendritic cell development in peripheral lymphoid tissues. Nat Immunol. 2008;9(6):676-83.

56. Anandasabapathy N, Victora GD, Meredith M, Feder R, Dong B, Kluger C, et al. Flt3L controls the development of radiosensitive dendritic cells in the meninges and choroid plexus of the steady-state mouse brain. J Exp Med. 2011;208(8):1695-705.

57. Harpur CM, Kato Y, Dewi ST, Stankovic S, Johnson DN, Bedoui S, et al. Classical Type 1 Dendritic Cells Dominate Priming of Th1 Responses to Herpes Simplex Virus Type 1 Skin Infection. J Immunol. 2019;202(3):653-63.

58. Lee CH, Chen JS, Chiu HC, Hong CH, Liu CY, Ta YC, et al. Differential activation behavior of dermal dendritic cells underlies the strain-specific Th1 responses to single epicutaneous immunization. J Dermatol Sci. 2016;84(3):248-57.

59. Collin M, Bigley V. Human dendritic cell subsets: an update. Immunology. 2018;154(1):3-20.

60. Langlet C, Tamoutounour S, Henri S, Luche H, Ardouin L, Gregoire C, et al. CD64 expression distinguishes monocyte-derived and conventional dendritic cells and reveals their distinct role during intramuscular immunization. J Immunol. 2012;188(4):1751-60.

61. Malissen B, Tamoutounour S, Henri S. The origins and functions of dendritic cells and macrophages in the skin. Nat Rev Immunol. 2014;14(6):417-28.

62. Theoharides TC. Mast cells: the immune gate to the brain. Life Sci. 1990;46(9):607-17.

63. Silver R, Curley JP. Mast cells on the mind: new insights and opportunities. Trends Neurosci. 2013;36(9):513-21.

64. Kolaczkowska E, Kubes P. Neutrophil recruitment and function in health and inflammation. Nat Rev Immunol. 2013;13(3):159-75.

65. Geng S, Matsushima H, Okamoto T, Yao Y, Lu R, Page K, et al. Emergence, origin, and function of neutrophil-dendritic cell hybrids in experimentally induced inflammatory lesions in mice. Blood. 2013;121(10):1690-700.

66. Christoffersson G, Vagesjo E, Vandooren J, Liden M, Massena S, Reinert RB, et al. VEGF-A recruits a proangiogenic MMP-9-delivering neutrophil subset that induces angiogenesis in transplanted hypoxic tissue. Blood. 2012;120(23):4653-62.

67. Massena S, Christoffersson G, Vagesjo E, Seignez C, Gustafsson K, Binet F, et al. Identification and characterization of VEGF-A-responsive neutrophils expressing CD49d, VEGFR1, and CXCR4 in mice and humans. Blood. 2015;126(17):2016-26.

68. Tourki B, Halade G. Leukocyte diversity in resolving and nonresolving mechanisms of cardiac remodeling. FASEB J. 2017;31(10):4226-39.

69. Cronk JC, Derecki NC, Ji E, Xu Y, Lampano AE, Smirnov I, et al. Methyl-CpG Binding Protein 2 Regulates Microglia and Macrophage Gene Expression in Response to Inflammatory Stimuli. Immunity. 2015;42(4):679-91.

70. Frossi B, Mion F, Sibilano R, Danelli L, Pucillo CEM. Is it time for a new classification of mast cells? What do we know about mast cell heterogeneity? Immunol Rev. 2018;282(1):35-46.

71. Irani AM, Schwartz LB. Human mast cell heterogeneity. Allergy Proc. 1994;15(6):303-8.

72. Gupta K, Harvima IT. Mast cell-neural interactions contribute to pain and itch. Immunol Rev. 2018;282(1):168-87.

73. Silverman AJ, Asarian L, Khalil M, Silver R. GnRH, brain mast cells and behavior. Prog Brain Res. 2002;141:315-25.

74. Theoharides TC, Donelan J, Kandere-Grzybowska K, Konstantinidou A. The role of mast cells in migraine pathophysiology. Brain Res Brain Res Rev. 2005;49(1):65-76.

75. Crivellato E, Ribatti D. The mast cell: an evolutionary perspective. Biol Rev Camb Philos Soc. 2010;85(2):347-60.

76. Levy D. Migraine pain, meningeal inflammation, and mast cells. Curr Pain Headache Rep. 2009;13(3):237-40.

77. Chikahisa S, Kodama T, Soya A, Sagawa Y, Ishimaru Y, Sei H, et al. Histamine from brain resident MAST cells promotes wakefulness and modulates behavioral states. PLoS One. 2013;8(10):e78434.

78. Lenz KM, Pickett LA, Wright CL, Davis KT, Joshi A, McCarthy MM. Mast Cells in the Developing Brain Determine Adult Sexual Behavior. J Neurosci. 2018;38(37):8044-59.

79. Wingerchuk DM, Lucchinetti CF, Noseworthy JH. Multiple sclerosis: current pathophysiological concepts. Lab Invest. 2001;81(3):263-81.

80. Lassmann H, Bradl M. Multiple sclerosis: experimental models and reality. Acta Neuropathol. 2017;133(2):223-44.

81. Constantinescu CS, Farooqi N, O'Brien K, Gran B. Experimental autoimmune encephalomyelitis (EAE) as a model for multiple sclerosis (MS). Br J Pharmacol. 2011;164(4):1079-106.

82. Soulika AM, Lee E, McCauley E, Miers L, Bannerman P, Pleasure D. Initiation and progression of axonopathy in experimental autoimmune encephalomyelitis. J Neurosci. 2009;29(47):14965-79.

83. Chuluundorj D, Harding SA, Abernethy D, La Flamme AC. Expansion and preferential activation of the CD14(+)CD16(+) monocyte subset during multiple sclerosis. Immunol Cell Biol. 2014;92(6):509-17.

84. Gjelstrup MC, Stilund M, Petersen T, Moller HJ, Petersen EL, Christensen T. Subsets of activated monocytes and markers of inflammation in incipient and progressed multiple sclerosis. Immunol Cell Biol. 2018;96(2):160-74.

85. Karni A, Abraham M, Monsonego A, Cai G, Freeman GJ, Hafler D, et al. Innate immunity in multiple sclerosis: myeloid dendritic cells in secondary progressive multiple sclerosis are activated and drive a proinflammatory immune response. J Immunol. 2006;177(6):4196-202.

86. Nuyts AH, Lee WP, Bashir-Dar R, Berneman ZN, Cools N. Dendritic cells in multiple sclerosis: key players in the immunopathogenesis, key players for new cellular immunotherapies? Mult Scler. 2013;19(8):995-1002.

87. Dendrou CA, Fugger L, Friese MA. Immunopathology of multiple sclerosis. Nat Rev Immunol. 2015;15(9):545-58.

88. Popescu BF, Lucchinetti CF. Pathology of demyelinating diseases. Annu Rev Pathol. 2012;7:185-217.

89. Lucchinetti C, Bruck W, Parisi J, Scheithauer B, Rodriguez M, Lassmann H. Heterogeneity of multiple sclerosis lesions: implications for the pathogenesis of demyelination. Ann Neurol. 2000;47(6):707-17.

90. Mahad DH, Trapp BD, Lassmann H. Pathological mechanisms in progressive multiple sclerosis. Lancet Neurol. 2015;14(2):183-93.

91. Trapp BD, Peterson J, Ransohoff RM, Rudick R, Mork S, Bo L. Axonal transection in the lesions of multiple sclerosis. N Engl J Med. 1998;338(5):278-85.

92. Fischer MT, Sharma R, Lim JL, Haider L, Frischer JM, Drexhage J, et al. NADPH oxidase expression in active multiple sclerosis lesions in relation to oxidative tissue damage and mitochondrial injury. Brain. 2012;135(Pt 3):886-99.

93. Zrzavy T, Hametner S, Wimmer I, Butovsky O, Weiner HL, Lassmann H. Loss of 'homeostatic' microglia and patterns of their activation in active multiple sclerosis. Brain. 2017;140(7):1900-13.

94. Boven LA, Van Meurs M, Van Zwam M, Wierenga-Wolf A, Hintzen RQ, Boot RG, et al. Myelin-laden macrophages are anti-inflammatory, consistent with foam cells in multiple sclerosis. Brain. 2006;129(Pt 2):517-26.

95. Fan X, Zhang H, Cheng Y, Jiang X, Zhu J, Jin T. Double Roles of Macrophages in Human Neuroimmune Diseases and Their Animal Models. Mediators Inflamm. 2016;2016:8489251.

96. Gillen KM, Mubarak M, Nguyen TD, Pitt D. Significance and In Vivo Detection of Iron-Laden Microglia in White Matter Multiple Sclerosis Lesions. Front Immunol. 2018;9:255.

97. Vogel DY, Vereyken EJ, Glim JE, Heijnen PD, Moeton M, van der Valk P, et al. Macrophages in inflammatory multiple sclerosis lesions have an intermediate activation status. J Neuroinflammation. 2013;10:35.

98. Zhang Z, Zhang ZY, Schittenhelm J, Wu Y, Meyermann R, Schluesener HJ. Parenchymal accumulation of CD163+ macrophages/microglia in multiple sclerosis brains. J Neuroimmunol. 2011;237(1-2):73-9.

99. Giles DA, Washnock-Schmid JM, Duncker PC, Dahlawi S, Ponath G, Pitt D, et al. Myeloid cell plasticity in the evolution of central nervous system autoimmunity. Ann Neurol. 2018;83(1):131-41.

100. Mehta V, Pei W, Yang G, Li S, Swamy E, Boster A, et al. Iron is a sensitive biomarker for inflammation in multiple sclerosis lesions. PLoS One. 2013;8(3):e57573.

101. Popescu BF, Frischer JM, Webb SM, Tham M, Adiele RC, Robinson CA, et al. Pathogenic implications of distinct patterns of iron and zinc in chronic MS lesions. Acta Neuropathol. 2017;134(1):45-64.

102. Hametner S, Wimmer I, Haider L, Pfeifenbring S, Bruck W, Lassmann H. Iron and neurodegeneration in the multiple sclerosis brain. Ann Neurol. 2013;74(6):848-61.

103. Howell OW, Rundle JL, Garg A, Komada M, Brophy PJ, Reynolds R. Activated microglia mediate axoglial disruption that contributes to axonal injury in multiple sclerosis. J Neuropathol Exp Neurol. 2010;69(10):1017-33.

104. Melief J, Schuurman KG, van de Garde MD, Smolders J, van Eijk M, Hamann J, et al. Microglia in normal appearing white matter of multiple sclerosis are alerted but immunosuppressed. Glia. 2013;61(11):1848-61.

105. Singh S, Metz I, Amor S, van der Valk P, Stadelmann C, Bruck W. Microglial nodules in early multiple sclerosis white matter are associated with degenerating axons. Acta Neuropathol. 2013;125(4):595-608.

106. Herranz E, Gianni C, Louapre C, Treaba CA, Govindarajan ST, Ouellette R, et al. Neuroinflammatory component of gray matter pathology in multiple sclerosis. Ann Neurol. 2016;80(5):776-90.

107. Politis M, Giannetti P, Su P, Turkheimer F, Keihaninejad S, Wu K, et al. Increased PK11195 PET binding in the cortex of patients with MS correlates with disability. Neurology. 2012;79(6):523-30.

108. Abdelhak A, Weber MS, Tumani H. Primary Progressive Multiple Sclerosis: Putting Together the Puzzle. Front Neurol. 2017;8:234.

109. Howell OW, Reeves CA, Nicholas R, Carassiti D, Radotra B, Gentleman SM, et al. Meningeal inflammation is widespread and linked to cortical pathology in multiple sclerosis. Brain. 2011;134(Pt 9):2755-71.

110. Michailidou I, Naessens DM, Hametner S, Guldenaar W, Kooi EJ, Geurts JJ, et al. Complement C3 on microglial clusters in multiple sclerosis occur in chronic but not acute disease: Implication for disease pathogenesis. Glia. 2017;65(2):264-77.

111. Shemer A, Grozovski J, Tay TL, Tao J, Volaski A, Suss P, et al. Engrafted parenchymal brain macrophages differ from microglia in transcriptome, chromatin landscape and response to challenge. Nat Commun. 2018;9(1):5206.

112. Said A, Weindl G. Regulation of Dendritic Cell Function in Inflammation. J Immunol Res. 2015;2015:743169.

113. Pierson ER, Wagner CA, Goverman JM. The contribution of neutrophils to CNS autoimmunity. Clin Immunol. 2018;189:23-8.

114. Brinkmann V, Reichard U, Goosmann C, Fauler B, Uhlemann Y, Weiss DS, et al. Neutrophil extracellular traps kill bacteria. Science. 2004;303(5663):1532-5.

115. Naegele M, Tillack K, Reinhardt S, Schippling S, Martin R, Sospedra M. Neutrophils in multiple sclerosis are characterized by a primed phenotype. J Neuroimmunol. 2012;242(1-2):60-71.

116. Saadoun S, Waters P, MacDonald C, Bell BA, Vincent A, Verkman AS, et al. Neutrophil protease inhibition reduces neuromyelitis optica-immunoglobulin G-induced damage in mouse brain. Ann Neurol. 2012;71(3):323-33.

117. Woodberry T, Bouffler SE, Wilson AS, Buckland RL, Brustle A. The Emerging Role of Neutrophil Granulocytes in Multiple Sclerosis. J Clin Med. 2018;7(12).

118. Kostic M, Dzopalic T, Zivanovic S, Zivkovic N, Cvetanovic A, Stojanovic I, et al. IL-17 and glutamate excitotoxicity in the pathogenesis of multiple sclerosis. Scand J Immunol. 2014;79(3):181-6.

119. Campbell SJ, Meier U, Mardiguian S, Jiang Y, Littleton ET, Bristow A, et al. Sickness behaviour is induced by a peripheral CXC-chemokine also expressed in multiple sclerosis and EAE. Brain Behav Immun. 2010;24(5):738-46.

120. Ishizu T, Osoegawa M, Mei FJ, Kikuchi H, Tanaka M, Takakura Y, et al. Intrathecal activation of the IL-17/IL-8 axis in opticospinal multiple sclerosis. Brain. 2005;128(Pt 5):988-1002.

121. Rumble JM, Huber AK, Krishnamoorthy G, Srinivasan A, Giles DA, Zhang X, et al. Neutrophil-related factors as biomarkers in EAE and MS. J Exp Med. 2015;212(1):23-35.

122. Lock C, Hermans G, Pedotti R, Brendolan A, Schadt E, Garren H, et al. Gene-microarray analysis of multiple sclerosis lesions yields new targets validated in autoimmune encephalomyelitis. Nat Med. 2002;8(5):500-8.

123. Burt RK, Fassas A, Snowden J, van Laar JM, Kozak T, Wulffraat NM, et al. Collection of hematopoietic stem cells from patients with autoimmune diseases. Bone Marrow Transplant. 2001;28(1):1-12.

124. Openshaw H, Lund BT, Kashyap A, Atkinson R, Sniecinski I, Weiner LP, et al. Peripheral blood stem cell transplantation in multiple sclerosis with busulfan and cyclophosphamide conditioning: report of toxicity and immunological monitoring. Biol Blood Marrow Transplant. 2000;6(5A):563-75.

125. J. N. Ueber das Vorkommen der sogenannten „Mastzellen" bei pathologischen Veränderungen des Gehirns. Archiv für pathologische Anatomie und Physiologie und für klinische Medicin. 1890;122(2):378-08.

126. Ibrahim MZ, Reder AT, Lawand R, Takash W, Sallouh-Khatib S. The mast cells of the multiple sclerosis brain. J Neuroimmunol. 1996;70(2):131-8.

127. Olsson Y. Mast cells in plaques of multiple sclerosis. Acta Neurol Scand. 1974;50(5):611-8.

128. Toms R, Weiner HL, Johnson D. Identification of IgE-positive cells and mast cells in frozen sections of multiple sclerosis brains. J Neuroimmunol. 1990;30(2-3):169-77.

129. Brown MA, Weinberg RB. Mast Cells and Innate Lymphoid Cells: Underappreciated Players in CNS Autoimmune Demyelinating Disease. Front Immunol. 2018;9:514.

130. Calabresi PA, Stone LA, Bash CN, Frank JA, McFarland HF. Interferon beta results in immediate reduction of contrast-enhanced MRI lesions in multiple sclerosis patients followed by weekly MRI. Neurology. 1997;48(5):1446-8.

131. Jacobs LD, Cookfair DL, Rudick RA, Herndon RM, Richert JR, Salazar AM, et al. Intramuscular interferon beta-1a for disease progression in relapsing multiple sclerosis. The Multiple Sclerosis Collaborative Research Group (MSCRG). Ann Neurol. 1996;39(3):285-94.

132. Guarda G, Braun M, Staehli F, Tardivel A, Mattmann C, Forster I, et al. Type I interferon inhibits interleukin-1 production and inflammasome activation. Immunity. 2011;34(2):213-23.

133. Ramgolam VS, Sha Y, Jin J, Zhang X, Markovic-Plese S. IFN-beta inhibits human Th17 cell differentiation. J Immunol. 2009;183(8):5418-27.

134. Prinz M, Schmidt H, Mildner A, Knobeloch KP, Hanisch UK, Raasch J, et al. Distinct and nonredundant in vivo functions of IFNAR on myeloid cells limit autoimmunity in the central nervous system. Immunity. 2008;28(5):675-86.

135. Bustamante MF, Nurtdinov RN, Rio J, Montalban X, Comabella M. Baseline gene expression signatures in monocytes from multiple sclerosis patients treated with interferon-beta. PLoS One. 2013;8(4):e60994.

136. Comabella M, Lunemann JD, Rio J, Sanchez A, Lopez C, Julia E, et al. A type I interferon signature in monocytes is associated with poor response to interferon-beta in multiple sclerosis. Brain. 2009;132(Pt 12):3353-65.

137. Zula JA, Green HC, Ransohoff RM, Rudick RA, Stark GR, van Boxel-Dezaire AH. The role of cell type-specific responses in IFN-beta therapy of multiple sclerosis. Proc Natl Acad Sci U S A. 2011;108(49):19689-94.

138. Hebb AL, Moore CS, Bhan V, Robertson GS. Effects of IFN-B on TRAIL and Decoy Receptor Expression in Different Immune Cell Populations from MS Patients with Distinct Disease Subtypes. Autoimmune Dis. 2010;2011:485752.

139. Marckmann S, Wiesemann E, Hilse R, Trebst C, Stangel M, Windhagen A. Interferon-beta up-regulates the expression of co-stimulatory molecules CD80, CD86 and CD40 on monocytes: significance for treatment of multiple sclerosis. Clin Exp Immunol. 2004;138(3):499-506.

140. Wiesemann E, Deb M, Trebst C, Hemmer B, Stangel M, Windhagen A. Effects of interferon-beta on co-signaling molecules: upregulation of CD40, CD86 and PD-L2 on monocytes in relation to clinical response to interferon-beta treatment in patients with multiple sclerosis. Mult Scler. 2008;14(2):166-76.

141. Sellebjerg F, Krakauer M, Limborg S, Hesse D, Lund H, Langkilde A, et al. Endogenous and recombinant type I interferons and disease activity in multiple sclerosis. PLoS One. 2012;7(6):e35927.

142. Adriani M, Nytrova P, Mbogning C, Hassler S, Medek K, Jensen PEH, et al. Monocyte NOTCH2 expression predicts IFN-beta immunogenicity in multiple sclerosis patients. JCI Insight. 2018;3(11).

143. Prod'homme T, Zamvil SS. The Evolving Mechanisms of Action of Glatiramer Acetate. Cold Spring Harb Perspect Med. 2019;9(2).

144. Weber MS, Hohlfeld R, Zamvil SS. Mechanism of action of glatiramer acetate in treatment of multiple sclerosis. Neurotherapeutics. 2007;4(4):647-53.

145. Fridkis-Hareli M, Teitelbaum D, Gurevich E, Pecht I, Brautbar C, Kwon OJ, et al. Direct binding of myelin basic protein and synthetic copolymer 1 to class II major histocompatibility complex molecules on living antigen-presenting cells--specificity and promiscuity. Proc Natl Acad Sci U S A. 1994;91(11):4872-6.

146. Teitelbaum D, Fridkis-Hareli M, Arnon R, Sela M. Copolymer 1 inhibits chronic relapsing experimental allergic encephalomyelitis induced by proteolipid protein (PLP) peptides in mice and interferes with PLP-specific T cell responses. J Neuroimmunol. 1996;64(2):209-17.

147. Weber MS, Prod'homme T, Youssef S, Dunn SE, Rundle CD, Lee L, et al. Type II monocytes modulate T cell-mediated central nervous system autoimmune disease. Nat Med. 2007;13(8):935-43.

148. Kim HJ, Ifergan I, Antel JP, Seguin R, Duddy M, Lapierre Y, et al. Type 2 monocyte and microglia differentiation mediated by glatiramer acetate therapy in patients with multiple sclerosis. J Immunol. 2004;172(11):7144-53.

149. Chuluundorj D, Harding SA, Abernethy D, La Flamme AC. Glatiramer acetate treatment normalized the monocyte activation profile in MS patients to that of healthy controls. Immunol Cell Biol. 2017;95(3):297-305.

150. Hussien Y, Sanna A, Soderstrom M, Link H, Huang YM. Glatiramer acetate and IFN-beta act on dendritic cells in multiple sclerosis. J Neuroimmunol. 2001;121(1-2):102-10.

151. Sellebjerg F, Hesse D, Limborg S, Lund H, Sondergaard HB, Krakauer M, et al. Dendritic cell, monocyte and T cell activation and response to glatiramer acetate in multiple sclerosis. Mult Scler. 2013;19(2):179-87.

152. van der Touw W, Kang K, Luan Y, Ma G, Mai S, Qin L, et al. Glatiramer Acetate Enhances Myeloid-Derived Suppressor Cell Function via Recognition of Paired Ig-like Receptor B. J Immunol. 2018;201(6):1727-34.

153. Mindur JE, Valenzuela RM, Yadav SK, Boppana S, Dhib-Jalbut S, Ito K. IL-27: a potential biomarker for responders to glatiramer acetate therapy. J Neuroimmunol. 2017;304:21-8.

154. Lalive PH, Kreutzfeldt M, Devergne O, Metz I, Bruck W, Merkler D, et al. Increased interleukin-27 cytokine expression in the central nervous system of multiple sclerosis patients. J Neuroinflammation. 2017;14(1):144.

155. Cohen JA, Barkhof F, Comi G, Hartung HP, Khatri BO, Montalban X, et al. Oral fingolimod or intramuscular interferon for relapsing multiple sclerosis. N Engl J Med. 2010;362(5):402-15.

156. Chun J, Kihara Y, Jonnalagadda D, Blaho VA. Fingolimod: Lessons Learned and New Opportunities for Treating Multiple Sclerosis and Other Disorders. Annu Rev Pharmacol Toxicol. 2019;59:149-70.

157. Brinkmann V, Billich A, Baumruker T, Heining P, Schmouder R, Francis G, et al. Fingolimod (FTY720): discovery and development of an oral drug to treat multiple sclerosis. Nat Rev Drug Discov. 2010;9(11):883-97.

158. Di Dario M, Colombo E, Govi C, De Feo D, Messina MJ, Romeo M, et al. Myeloid cells as target of fingolimod action in multiple sclerosis. Neurol Neuroimmunol Neuroinflamm. 2015;2(6):e157.

159. Durafourt BA, Lambert C, Johnson TA, Blain M, Bar-Or A, Antel JP. Differential responses of human microglia and blood-derived myeloid cells to FTY720. J Neuroimmunol. 2011;230(1-2):10-6.

160. Hughes JE, Srinivasan S, Lynch KR, Proia RL, Ferdek P, Hedrick CC. Sphingosine-1-phosphate induces an antiinflammatory phenotype in macrophages. Circ Res. 2008;102(8):950-8.

161. Thomas K, Sehr T, Proschmann U, Rodriguez-Leal FA, Haase R, Ziemssen T. Fingolimod additionally acts as immunomodulator focused on the innate immune system beyond its prominent effects on lymphocyte recirculation. J Neuroinflammation. 2017;14(1):41.

162. Michell-Robinson MA, Moore CS, Healy LM, Osso LA, Zorko N, Grouza V, et al. Effects of fumarates on circulating and CNS myeloid cells in multiple sclerosis. Ann Clin Transl Neurol. 2016;3(1):27-41.

163. Foster CA, Howard LM, Schweitzer A, Persohn E, Hiestand PC, Balatoni B, et al. Brain penetration of the oral immunomodulatory drug FTY720 and its phosphorylation in the central nervous system during experimental autoimmune encephalomyelitis: consequences for mode of action in multiple sclerosis. J Pharmacol Exp Ther. 2007;323(2):469-75.

164. Linker RA, Lee DH, Ryan S, van Dam AM, Conrad R, Bista P, et al. Fumaric acid esters exert neuroprotective effects in neuroinflammation via activation of the Nrf2 antioxidant pathway. Brain. 2011;134(Pt 3):678-92.

165. Mills EA, Ogrodnik MA, Plave A, Mao-Draayer Y. Emerging Understanding of the Mechanism of Action for Dimethyl Fumarate in the Treatment of Multiple Sclerosis. Front Neurol. 2018;9:5.

166. Paraiso HC, Kuo PC, Curfman ET, Moon HJ, Sweazey RD, Yen JH, et al. Dimethyl fumarate attenuates reactive microglia and long-term memory deficits following systemic immune challenge. J Neuroinflammation. 2018;15(1):100.

167. Schulze-Topphoff U, Varrin-Doyer M, Pekarek K, Spencer CM, Shetty A, Sagan SA, et al. Dimethyl fumarate treatment induces adaptive and innate immune modulation independent of Nrf2. Proc Natl Acad Sci U S A. 2016;113(17):4777-82.

168. Schilling S, Goelz S, Linker R, Luehder F, Gold R. Fumaric acid esters are effective in chronic experimental autoimmune encephalomyelitis and suppress macrophage infiltration. Clin Exp Immunol. 2006;145(1):101-7.

169. Bar-Or A, Pachner A, Menguy-Vacheron F, Kaplan J, Wiendl H. Teriflunomide and its mechanism of action in multiple sclerosis. Drugs. 2014;74(6):659-74.

170. Bar-Or A. Teriflunomide (Aubagio(R)) for the treatment of multiple sclerosis. Exp Neurol. 2014;262 Pt A:57-65.

171. Merrill JE, Hanak S, Pu SF, Liang J, Dang C, Iglesias-Bregna D, et al. Teriflunomide reduces behavioral, electrophysiological, and histopathological deficits in the Dark Agouti rat model of experimental autoimmune encephalomyelitis. J Neurol. 2009;256(1):89-103.

172. Wostradowski T, Prajeeth CK, Gudi V, Kronenberg J, Witte S, Brieskorn M, et al. In vitro evaluation of physiologically relevant concentrations of teriflunomide on activation and proliferation of primary rodent microglia. J Neuroinflammation. 2016;13(1):250.

173. Li L, Liu J, Delohery T, Zhang D, Arendt C, Jones C. The effects of teriflunomide on lymphocyte subpopulations in human peripheral blood mononuclear cells in vitro. J Neuroimmunol. 2013;265(1-2):82-90.

174. Medina S, Sainz de la Maza S, Villarrubia N, Alvarez-Lafuente R, Costa-Frossard L, Arroyo R, et al. Teriflunomide induces a tolerogenic bias in blood immune cells of MS patients. Ann Clin Transl Neurol. 2019;6(2):355-63.

175. Polman CH, O'Connor PW, Havrdova E, Hutchinson M, Kappos L, Miller DH, et al. A randomized, placebo-controlled trial of natalizumab for relapsing multiple sclerosis. N Engl J Med. 2006;354(9):899-910.

176. Planas R, Jelcic I, Schippling S, Martin R, Sospedra M. Natalizumab treatment perturbs memory- and marginal zone-like B-cell homing in secondary lymphoid organs in multiple sclerosis. Eur J Immunol. 2012;42(3):790-8.

177. Metz I, Radue EW, Oterino A, Kumpfel T, Wiendl H, Schippling S, et al. Pathology of immune reconstitution inflammatory syndrome in multiple sclerosis with natalizumab-associated progressive multifocal leukoencephalopathy. Acta Neuropathol. 2012;123(2):235-45.

178. Kivisakk P, Francois K, Mbianda J, Gandhi R, Weiner HL, Khoury SJ. Effect of natalizumab treatment on circulating plasmacytoid dendritic cells: a cross-sectional observational study in patients with multiple sclerosis. PLoS One. 2014;9(7):e103716.

179. Painter MM, Atagi Y, Liu CC, Rademakers R, Xu H, Fryer JD, et al. TREM2 in CNS homeostasis and neurodegenerative disease. Mol Neurodegener. 2015;10:43.

180. Kleinberger G, Yamanishi Y, Suarez-Calvet M, Czirr E, Lohmann E, Cuyvers E, et al. TREM2 mutations implicated in neurodegeneration impair cell surface transport and phagocytosis. Sci Transl Med. 2014;6(243):243ra86.

181. Piccio L, Buonsanti C, Cella M, Tassi I, Schmidt RE, Fenoglio C, et al. Identification of soluble TREM-2 in the cerebrospinal fluid and its association with multiple sclerosis and CNS inflammation. Brain. 2008;131(Pt 11):3081-91.

182. Ohrfelt A, Axelsson M, Malmestrom C, Novakova L, Heslegrave A, Blennow K, et al. Soluble TREM-2 in cerebrospinal fluid from patients with multiple sclerosis treated with natalizumab or mitoxantrone. Mult Scler. 2016;22(12):1587-95.

183. Greenfield AL, Hauser SL. B-cell Therapy for Multiple Sclerosis: Entering an era. Ann Neurol. 2018;83(1):13-26.

184. Montalban X, Hauser SL, Kappos L, Arnold DL, Bar-Or A, Comi G, et al. Ocrelizumab versus Placebo in Primary Progressive Multiple Sclerosis. N Engl J Med. 2017;376(3):209-20.

185. Li R, Rezk A, Miyazaki Y, Hilgenberg E, Touil H, Shen P, et al. Proinflammatory GM-CSF-producing B cells in multiple sclerosis and B cell depletion therapy. Sci Transl Med. 2015;7(310):310ra166.

186. Rao SP, Sancho J, Campos-Rivera J, Boutin PM, Severy PB, Weeden T, et al. Human peripheral blood mononuclear cells exhibit heterogeneous CD52 expression levels and show differential sensitivity to alemtuzumab mediated cytolysis. PLoS One. 2012;7(6):e39416.

187. Ambrose LR, Morel AS, Warrens AN. Neutrophils express CD52 and exhibit complement-mediated lysis in the presence of alemtuzumab. Blood. 2009;114(14):3052-5.

188. Baker D, Giovannoni G, Schmierer K. Marked neutropenia: Significant but rare in people with multiple sclerosis after alemtuzumab treatment. Mult Scler Relat Disord. 2017;18:181-3.

Chapter 2:

CSF1R antagonism results in increased supraspinal infiltration in EAE

Marilyn Wang, Sofia E. Caryotakis, Glendalyn G. Smith, Alan V. Nguyen, David E. Pleasure, Athena M. Soulika

Published in the Journal of Neuroinflammation

Abstract

Background

Colony stimulating factor 1 receptor (CSF1R) signaling is crucial for the maintenance and function of various myeloid subsets. CSF1R antagonism was previously shown to mitigate clinical severity in experimental autoimmune encephalomyelitis (EAE). The associated mechanisms are still not well delineated.

Methods

To assess the effect of CSF1R signaling, we employed the CSF1R antagonist PLX5622 formulated in chow (PLX5622 diet, PD) and its control chow (control diet, CD). We examined the effect of PD in steady state and EAE by analyzing cells isolated from peripheral immune organs and from the CNS via flow cytometry. We determined CNS infiltration sites and assessed the extent of demyelination using immunohistochemistry of cerebella and spinal cords. Transcripts of genes associated with neuroinflammation were also analyzed in these tissues.

Results

In addition to microglial depletion, PD treatment reduced dendritic cells and macrophages in peripheral immune organs, both during steady state and during EAE. Furthermore, CSF1R antagonism modulated numbers and relative frequencies of T effector cells both in the periphery and in the CNS during the early stages of the disease. Classical neurological symptoms were milder in PD compared to CD mice. Interestingly, a subset of PD mice developed atypical EAE symptoms. Unlike previous studies, we observed that the CNS of PD mice was infiltrated by increased numbers of peripheral cells compared to that of CD mice. Immunohistochemical analysis showed that CNS infiltrates in PD mice were mainly localized in the

cerebellum while in CD mice infiltrates were primarily localized in the spinal cords during the onset of neurological deficits. Accordingly, during the same timepoint, cerebella of PD but not of CD mice had extensive demyelinating lesions, while spinal cords of CD but not of PD mice were heavily demyelinated.

Conclusions

Our findings suggest that CSF1R activity modulates the cellular composition of immune cells both in the periphery and within the CNS, and affects lesion localization of during the early EAE stages.

2.1 Introduction

Colony stimulating factor 1 receptor (CSF1R) is a tyrosine kinase receptor that promotes the development, survival, proliferation, migration, and differentiation of various myeloid cells such as monocytes, macrophages, dendritic cells (DCs), and osteoclasts [1, 2]. Its known cognate ligands are colony stimulating factor 1 (CSF1) and interleukin 34 (IL34). Although their expression patterns differ [3], and IL34 also signals via protein tyrosine phosphatase zeta (PTP-z) [4], these ligands induce relatively similar (albeit not identical) effects [5, 6].

Within the healthy central nervous system (CNS), CSF1R is expressed by microglia [5, 7, 8], and is necessary for their viability [9]. In addition, CSF1R is expressed by DCs [10, 11] and macrophages [12] in the choroid plexus and meninges. Although expression of CSF1R in neurons has been debated [5], it is now recognized that certain neurons express CSF1R in steady state, and is upregulated in injury [13, 14].

The importance of CSF1R signaling in development is underlined by seminal studies showing that CSF1R deficiency and *Csf1*-null mutations lead to perinatal death [15]. Small molecule antagonists have been successfully and widely employed to elucidate the effects of CSF1R signaling in preclinical models [16-26]. These antagonists were originally developed to deplete tumor-associated macrophages, thus promoting a more pro-inflammatory and anti-tumor environment [27, 28]. PLX3397 (Plexxikon, Inc), in particular, is now FDA approved for the treatment of the rare and highly fatal tenosynovial giant cell tumors [29, 30]. PLX3397 was later shown to deplete microglia, and was used in neuroimmunological studies [9]. However, in addition to CSF1R, PLX3397 also targets c-KIT and FLT3 kinases [31], and has poor blood brain barrier (BBB) permeability [9, 23]. Other CSF1R antagonists, such as BLZ945 and PLX5622, were later developed, exhibiting improved potency and specificity [32]. PLX5622 is one of the most selective and potent (IC_{50}<10nM) CSF1R antagonists, readily crosses the BBB, and is suitable for neuroimmunological studies [23, 33].

Both CSF1 and CSF1R are upregulated within and around demyelinating lesions of progressive multiple sclerosis (MS) patients compared to the white matter of non-MS controls [34]. CSF1R antagonism was shown to mitigate experimental autoimmune encephalomyelitis (EAE) severity by many groups [16, 17, 35], and this was initially attributed to microglia depletion [16, 34]. However, due to its broad expression, it is unlikely that the contribution of CSF1R to neuroinflammation is limited to microglia depletion. Indeed, thorough analysis of the effects of CSF1R antagonists has shown that other myeloid subsets are depleted both in steady state and in inflammation [17-20, 36]. Furthermore, even if CSF1R antagonism does not affect viability, it can affect cellular functions either directly or indirectly. For example, CSF1R antagonism impairs monocyte differentiation to macrophages [37, 38], and affects phagocytosis [18, 39]. Therefore, a characterization of multiple cell subsets is necessary to define the effects of CSF1R activity in neuroinflammation.

To test the effects of CSF1R antagonism in the initiation and progression of EAE, we employed PLX5622. Mice were analyzed both in steady state (i.e., treated with PLX5622 but not induced with EAE) and before and after the onset of EAE clinical symptoms. We show that in addition to microglia depletion, PLX5622 treatment modulated steady state frequencies and/or numbers of various myeloid cells in the CNS, spleen, bone marrow, and skin. In agreement with other studies [16, 17, 35], we show that PLX5622 diminished EAE clinical severity. This was accompanied by decreased peripheral activation in the secondary lymphoid organs (SLOs) during the preclinical phase of EAE. Contrary to other studies, we found increased numbers of infiltrating leukocytes in the CNS of PLX5622-treated mice compared to controls. Among the CNS infiltrating cells, relative frequencies and numbers of inflammatory myeloid subsets were increased in the PLX5622 group compared to controls. Interestingly, CNS infiltrates were mainly localized in the cerebellum of PLX5622-treated mice, and mainly in the spinal cord of control mice. These data highlight an underappreciated effect of CSF1R in EAE, and suggest that CSF1R signaling affects the regional localization of inflammatory foci in neuroinflammation.

2.2 Materials and Methods

Animals

C57BL/6 mice were obtained from Jackson Laboratory, and bred at the Mouse Biology Program at the University of California, Davis. Animal procedures were approved by the Institutional Animal Care and Use Committee of UC Davis. Animals were age- and sex-matched for each experiment.

Compounds

PLX5622 (Plexxikon, Inc.) was formulated at 1200 mg/kg in AIN-76A chow by Research Diets, Inc. PLX5622 diet and AIN-76A control diet were given to mice ad libitum.

Rodent myelin oligodendrocyte glycoprotein peptide, amino acids 35-55 (MOG_{35-55}), was obtained from Vivitide (now Biosynth).

MOG_{35-55} EAE induction

Mice were fed PLX5622 diet or control diet for 7 days before EAE induction. Both male and female mice were used in this study. Age- (10-13 week-old) and sex-matched mice were EAE-induced using two subcutaneous flank injections of a total of 300 µg MOG_{35-55} in complete Freund's adjuvant [incomplete Freund's adjuvant (ThermoFisher) containing 5 mg/ml of heat-killed *Mycobacterium tuberculosis* (BD Difco Adjuvants)]. On days 0 and 2 after induction, mice also received intraperitoneal injections of 200 ng of pertussis toxin. Mice were weighed and assessed for clinical symptoms for classical EAE on a 5-point scale: 0 no detectable symptoms; 1 waddling gait, normal tail; 2 full limp tail, waddling gait; 3 hind limb paresis; 4 full hind limb paralysis; 5 death [40-43]. Half point scores were assigned when the severity of clinical symptoms were in between full-scale points.

Single cell suspension preparation and flow cytometric analysis

Animals were anesthetized with an intraperitoneal injection of ketamine (150 mg/kg) and xylazine (16 mg/kg), and exsanguinated via transcardial perfusion using ice-cold PBS, as we have previously described [40, 43]. Following PBS perfusion, bone marrow or spleen and lymph nodes were passed through a 100 µm cell strainer in PBS. Red blood cells were lysed using ammonium-chloride-potassium (ACK) lysis buffer (Quality Biological Inc) and cells were resuspended in complete RPMI [(RPMI 1640 containing 10% FBS (Hyclone), 2 mM L-glutamine, 0.1 mM nonessential amino acids, 100 U penicillin-streptomycin, 1 mM sodium pyruvate (Gibco), and 50 µM 2-mercaptoethanol (Sigma)].

For T cell recall analysis, 300,000 spleen and lymph node cells/well were incubated in 96 well plates, in the presence or absence of 100 µg/ml MOG_{35-55} for 16 hours in a total volume of 200 µL. All cells were then incubated in the presence of brefeldin A and monensin (Biolegend) for 5 hours before immunostaining for flow cytometry analysis.

Pooled whole brain and whole spinal cord tissues were minced and incubated with 0.04 units of Liberase TL (Roche) and 10 µg of DNase I (Roche) in 5 ml PBS for 45 minutes at 37°C. Shaved and depilated dorsal skin adjacent to the sites of immunization were minced and incubated with 0.4 U/ml Dispase II (Roche), for 2 hours, at 37°C. 1 mg/ml collagenase (Roche) was added and incubated for an additional 30 minutes [44, 45].

Immune cells were isolated using a 40/70% (v/v) Percoll gradient (GE Healthcare) and resuspended in cRPMI. For CNS infiltrating T cell analysis, cells were incubated in the presence or absence of 50 ng/ml phorbol 12-myristate 13-acetate (MilliporeSigma) and 750 ng/ml ionomycin (CalBioChem), as well as brefeldin A and monensin (Biolegend) for 3 hours, and cells were immunostained. Live cells were detected using Zombie Red viability stain (ThermoFisher), after which cells were stained for extracellular markers, and fixed using 4% PFA at room temperature for 20 minutes before analysis. Cytokines were detected via intracellular staining using the BD Biosciences Cytofix/Cytoperm kit. FoxP3 was detected following cell fixation and nuclear permeabilization using the eBioscience FoxP3/Transcription factor buffer set. Cells

were analyzed using the Attune NxT flow cytometer. Frequencies reported represented percentages of cell populations within their respective mother gates.

Antibodies used are listed in Table 1

Evans blue analysis

Within 24 hours of onset of typical EAE symptoms, mice were injected intravenously with 200 µL of 0.3% Evans blue dye (Sigma) dissolved in saline. Mice were anesthetized and perfused with PBS after 90 minutes [40]. Whole spinal cord and brain tissues were isolated and imaged immediately.

Quantitative polymerase chain reaction (qPCR)

Lumbar spinal cords and cerebella were isolated at onset and acute EAE and stored in RNA*later* (Thermofisher Scientific). Tissues were homogenized in Qiazol (Qiagen), extracted using phenol-chloroform, and mRNA was purified using the RNeasy mini kit (Qiagen), according to the manufacturer's instructions. cDNA was synthesized using the Quantitect Reverse Transcription kit (Qiagen) according to manufacturer's instructions. qPCR was performed using an AriaMX real-time PCR system (Agilent) using SYBR Green Master Mix (Qiagen). Transcript expression levels were normalized using HSP90 [41]. Primers used in the study are listed in Table 2.

Immunohistochemical analysis

Animals were anesthetized via intraperitoneal injection of ketamine and xylazine, and perfusion via cardiac puncture was performed using ice-cold PBS, as we previously described [40, 43]. CNS regions of interest were isolated, and tissues were post-fixed overnight in 4% PFA. After washing with PBS, tissues were cryoprotected in 30% sucrose for 3 days, and frozen in OCT.

Cerebellar and lumbar spinal cord cryosections (10 µm) were collected during EAE onset, dried for 1 hour at room temperature, and blocked with 10% donkey serum for 1 hour at room temperature. Following washes in PBS containing 0.1% Tween 20 (PBS-T), tissues were incubated overnight at 4°C with primary antibodies against IBA1 (Wako Chemicals), CD3 (Santa Cruz Biotechnology), Ly6G (BD Pharmingen), and CD11b (BD Pharmingen). For MBP (BD Pharmingen) staining, slides were dipped in cold methanol for 30 min at -20°C before initial washes and before blocking. Following washes in PBS-T, tissues were incubated with secondary antibodies conjugated with FITC, Rhodamine-X, or Cy5 (Jackson ImmunoResearch) for 1 hour at room temperature, followed by DAPI counterstain. Tissues were mounted with Fluoromount-G (Electron Microscopy Sciences) and 20x images were acquired using the Nikon C2 scanning confocal microscope, stitched into whole tissue section images, and processed using the Nikon NIS-Elements AR software (version 4.60).

Immunohistochemical quantification

Cells counts and fluorescence intensities were detected in whole tissue sections using Imaris software version 9.2 (Oxford Instruments). Cell counts (CD3+ or Ly6G+ cells) were calculated per mm^2 of white matter area. Fluorescence intensities (for IBA1 and CD11b) were measured using Fiji ImageJ software (NIH) and shown as mean fluorescence intensity per pixel (MFI).

Demyelination was assessed via MBP immunostaining. Areas devoid of MBP immunoreactivity and total white matter areas were traced using Fiji ImageJ software (NIH); demyelination is shown as percentage of demyelinated area within the total white matter area.

In all immunohistochemical quantification, cerebellar and lumbar spinal cord tissues were matched per mouse and were collected during the onset of neurological deficits. At least two were sections averaged per tissue and 7-8 mice per group were analyzed.

Sholl Analysis

Cerebella and lumbar spinal cord tissues were isolated during EAE onset, immunostained with IBA1 and scanned using a 60x oil objective on the Nikon C2 scanning confocal microscope. The simple neurite tracing tool on Fiji ImageJ software (NIH) was used to trace IBA1+ branches. Two images per section, 4-8 microglia per section, two sections per tissue and 6-7 mice were employed.

Statistical Analysis

To determine statistical significance for EAE clinical course, we employed the Mann-Whitney U test. Experiments were repeated at least 5 times with at least 4-6 mice per gender per group per timepoint. Significance for cumulative and peak disease scores, flow cytometry, cell number and MFI quantification, and Sholl analysis was calculated with two-tailed Student's t-test. When not normally distributed, data were log transformed. Significance for transcript differences was calculated with one-way ANOVA. P values were statistically significant if <0.05.

2.3 Results

CSF1R antagonism depletes microglia and modulates other myeloid cell populations in the steady state CNS

Mice were placed on either 1200 mg/kg PLX5622 diet (PD) or control diet (CD) for seven days (Figure 1A; schema). Flow cytometric analysis of pooled spinal cord and brain (CNS) confirmed that PD mice showed statistically significantly decreased total CNS cell numbers compared with CD mice (CD: $1.63x10^5$ vs PD: $6.71x10^4$, p=0.0006) (Figure 1B). In agreement with previous studies [9, 18], this was mainly due to a 90% decrease of microglial (CD45loCD11b+) numbers in the PD CNS compared to CD (CD: $1.31x10^5$ vs PD:$1.33x10^4$; p=0.00000019) (Figure 1B). Microglia were effectively depleted in the cerebellum and the spinal cord (Figure 1C and Additional File 1A)

Other immune cell populations are sparse in the steady state CNS; small numbers of macrophages [46], monocytes [47], T cells, [48], and DCs [10] can be found in the meningeal spaces and the choroid plexus, while neutrophils are occasionally present and limited to the meningeal spaces [49]. PD mice had elevated frequencies and numbers of lymphocytes, neutrophils, and DCs compared to CD mice (Additional file 1B). This analysis, however, is limited by the small number of non-microglia immune cells in the CNS.

CSF1R antagonism reshapes immune cell populations in peripheral tissues in steady state

Compared to CD, PD mice showed no statistically significant differences in total cell numbers neither in the spleen (CD: $1.07x10^8$ vs PD: $7.37 x10^7$; p=0.06) (Figure 2A) nor the bone marrow (BM) (CD: $4.13x10^7$ vs PD: $4.03x10^7$; p=0.8) (Figure 2B). PD increased frequencies of neutrophils (CD45+CD11b+Ly6G+) in both the spleen and the BM, but not their absolute numbers. This suggests that the changes in neutrophil frequencies are due to a non-neutrophil cell population depletion.

PD increased total monocyte (CD45+CD11b+Ly6G-CD11c-MHCII-) frequencies and reduced total macrophage (CD45+CD11b+Ly6G-CD11c-MHCII+) frequencies and numbers both in spleen and in the BM compared to CD (Figure 2A and B). Frequencies of Ly6C+ monocytes increased, while Ly6C- monocytes and Ly6C+ and Ly6C- macrophages decreased in the spleens of PD compared to CD group (Figure 2A). BM DC (CD45hiCD11b+Ly6G-CD11c+MHCII+) frequencies and numbers decreased in PD compared to CD mice (Figure 2B). Additionally, the frequencies of Ly6C+ macrophages, and the numbers of Ly6C+ and Ly6C- macrophages decreased in the BM of the PD group. All of these are in agreement with a previous study by Lei et al [18]. However, unlike Lei et al. [18], we did not observe significant differences in CD4+ T and CD8+ T cells neither in the spleen nor in the BM between the two groups (data not shown). This may be due to the shorter period of PD treatment in our study (1 week) versus the one by Lei et al. (3 weeks).

Analysis of healthy caudal dorsal skin (pooled epidermis and dermis) showed that CSF1R antagonism did not change the total number of cells per milligram of tissue (Figure 2C). PD, however, diminished total

macrophages (CD45+CD11b+Ly6G-CD11c-MHCII+) and langerin+ cells (CD45+CD11b+Ly6G-CD11c+MHCII+langerin+), a population which includes Langerhans cells in the epidermis and langerin+ DCs in the dermis (Figure 2C). This is in agreement with studies showing that CSF1R signaling is mandatory for Langerhans cells' viability [50-52]. Frequencies of total monocytes and Ly6C+ monocytes increased in PD skin, but their numbers did not change between the groups. Furthermore, the numbers of total DCs and of Ly6C- macrophages were decreased in the PD group (Figure 2C).

CSF1R antagonism ameliorates EAE clinical course

To examine the role of CSF1R signaling in the onset and progression of EAE, age- and sex-matched mice were placed on CD or PD for 7 days before EAE induction and maintained on their respective diets up to the end of the experiment (Figure 3A; schema).

In agreement with previous studies [17, 35], PD mice exhibited delayed disease onset and milder severity of classical EAE clinical symptoms (Figure 3B, Additional file 2), and lower peak (CD: 3.8 ± 1.1 vs PD: 2.1 ± 1.7; $p<0.0001$) and cumulative disease scores (CD: 25.4 ± 17.3 vs PD: 10.9 ± 13.4; $p<0.0001$), compared to the CD group (Figure 3C).

Interestingly, 35% of PD mice exhibited atypical EAE neurological deficits such as seizures, ataxia, repetitive axial rotation, and anxiety and fear responses, such as freezing and strong startle reflexes; these mice exhibited no or very mild classical EAE clinical scores. Atypical EAE symptoms were never observed in CD mice. Unexpectedly, 60% of PD mice with atypical EAE (corresponding to 21% of total PD mice employed) died prior to development of conventional EAE symptoms, and before day 14 post EAE induction (pi) (not shown). PD mice that died prior to development of severe conventional EAE were not included in subsequent clinical scoring analysis. The rest of PD mice later also developed classical EAE deficits and none of these mice died as a result of EAE. We observed no deaths in the CD group.

No differences in EAE clinical course were noted between male and female mice in either group.

Flow cytometric analysis of pooled brain and spinal cord tissues (per mouse) before clinical EAE symptoms appear (pre-onset; days 7-9 pi) showed that 70% of CD45loCD11b+ cells (a population that is mostly microglia) were depleted in PD mice (CD: $3.46x10^5$ vs PD: $1.03x10^5$; p=0.0000015) (Figure 3D). Further analysis showed that the depleted population was predominantly CD45loCD11b+Ly6C-, a population that has been suggested to denote mostly microglia, while CD45loCD11b+Ly6C+ denotes mostly infiltrating macrophages [53] (Figure 3E).

CSF1R antagonism diminishes peripheral activation in secondary lymphoid organs in EAE

To determine whether the milder EAE course in PD mice was due to impaired immune responses in the periphery, we employed flow cytometry to analyze single cell suspensions of pooled spleen and draining lymph nodes (herein referred to as the secondary lymphoid organs, SLOs), before clinical EAE symptoms appear (day 7-9 pi).

Absolute numbers of total cells in the SLOs of PD mice were reduced compared to CD mice (CD: $1.93x10^8 \pm 9.28x10^7$ vs PD: $1.27x10^8 \pm 5.02x10^7$; p=0.006), and this was associated with statistically significant reductions of both myeloid and lymphoid cell numbers (Figure 4A). We further analyzed myeloid cell subsets using the gating strategy shown in Figure 4B. CSF1R antagonism increased neutrophil frequencies, but not their absolute numbers (Figure 4C). PD decreased total macrophage and DC frequencies and absolute numbers (Figure 4D). Although the frequencies of classical DCs (cDCs; CD45+CD11b+Ly6G-CD11c+MHCII+CD26+) increased while those of monocyte-derived DCs (moDCs; CD45+CD11b+Ly6G-CD11c+MHCII+CD88+) decreased, the absolute numbers of both these subsets decreased (Figure 4E). CSF1R antagonism statistically significantly decreased the numbers of Ly6C+ (inflammatory) monocytes [54] and macrophages in PD mice (Figure 4F).

Analysis of lymphocytic subsets (gating strategy shown in Figure 5A) showed that there were no differences in total CD4+ T cells between the two groups (Figure 5B). PD, however, decreased frequencies

and numbers of MOG-specific T effectors (Th1, Th17, and Th1/17) (Figure 5C). Interestingly, the log10 ratio of Th17:Th1 was increased in PD compared to CD mice. This ratio was greater than 1 in PD and lower than 1 in CD mice (Figure 5D). MOG-specific Tregs were decreased (Figure 5E) while the ratio of MOG-specific Tregs to T effectors was elevated in the SLOs of PD compared to CD mice during preclinical EAE (Figure 5F).

During later stages of the disease (acute EAE; day 20-22 pi) the frequencies and absolute numbers of neutrophils, total monocytes, and Ly6C+ monocytes were elevated in PD compared to CD mice (Additional file 3A). There were no differences in DCs (Additional file 3A) and T cell (Additional file 3B) populations in the SLOs during this timepoint.

CSF1R antagonism depletes myeloid cell populations in the bone marrow and skin in EAE

To determine if immune cell frequencies and numbers were affected by CSF1R antagonism in tissues other than the SLOs, we also analyzed bone marrow and dorsal skin (adjacent to the site of immunization) during preclinical and acute EAE.

There were no differences in the absolute numbers of total bone marrow cells, neither before the onset nor during acute EAE (Additional file 4). Neutrophil frequencies but not numbers were elevated, while DC and macrophage numbers were diminished in the PD bone marrow during preclinical EAE compared to controls (Additional file 4A). Additionally, Ly6C+ monocytes and Ly6C+ and Ly6C- macrophages were decreased in the preclinical phase (Additional file 4A), but not during acute EAE (Additional file 4B).

In the skin, neutrophil frequencies were increased in preclinical EAE (Additional file 5A). Langerin+ cells, total macrophages, and Ly6C+ inflammatory macrophages were reduced in PD compared to CD mice, both during the preclinical phase and acute disease (Additional file 5A and B). DCs, and particularly skin langerin+ DCs, are recruited into the SLOs and are powerful antigen presenting cells [52], thus reduction in these cell types may contribute to the priming impairments in PD mice. Total monocytes were increased

only in acute EAE (Additional file 5B). Immunohistochemical analysis confirmed that the skin of PD mice contained fewer CD11b+IBA1+ macrophages (Additional file 5C).

CSF1R antagonism increases CNS infiltration by peripheral immune cells

Single cell suspensions from pooled brain and spinal cord tissues (per mouse) were analyzed by flow cytometry before clinical symptom onset or during acute EAE.

Despite efficient microglial depletion, the absolute numbers of total CNS cells before neurological deficits onset were higher in PD compared to CD mice (CD: $6.17x10^5 \pm 3.63x10^5$ vs PD: $12.5x10^5 \pm 11.4 \times 10^5$; p=0.02) (Figure 6A). This was due to increased numbers of infiltrating leukocytes (CD45hi) in the CNS of PD compared to CD mice (CD: $2.23x10^5 \pm 2.04x10^5$ vs PD: $10.6x10^5 \pm 10.8x10^5$; p=0.001) (Figure 6A). Both infiltrating myeloid and lymphocyte subsets increased in the CNS of PD compared to CD mice (Figure 6A). We further analyzed the CNS infiltrating myeloid cells (gating strategy shown in Figure 6B). Frequencies and numbers of neutrophils were elevated in the CNS of PD mice compared to CD mice (Figure 6C). Although there were no differences in frequencies, numbers of total DCs, monocytes, and macrophages were elevated in the CNS of PD mice (Figure 6D). Both frequencies and numbers of cDCs and Ly6C+ monocytes and numbers of Ly6C+ and Ly6C- macrophages were elevated in PD mice (Figure 6E and F).

CNS infiltrating lymphocytes (CD45hiCD11b-) were further analyzed as shown in Figure 7A. The relative frequencies of CD4+ T cells were lower in PD compared to CD mice in preclinical EAE (Figure 7B). However, and as a result of increased overall infiltration (Figure 6A), the absolute numbers of both CD4+ T and CD8+ T cells were increased in PD mice (Figure 7B). The relative frequencies of Th1 cells were not different between the groups, while those of Th17 and Th1/17 subsets were decreased in the CNS of PD compared to CD mice (Figure 7C). However, the numbers of Th1 cells were elevated, while there were no changes in Th17, and Th1/17 numbers in PD compared to CD mice (Figure 7C). This resulted in lower log10 ratios of

Th17:Th1 in the CNS of PD compared to CD mice during preclinical EAE (Figure 7D). These ratios were greater than 1 in the CD and lower than 1 in the PD mice (Figure 7D).

Frequencies and absolute numbers of Tregs were increased (Figure 7E) and accordingly, Treg:Teff ratios were significantly higher in preclinical EAE in the CNS of PD compared to CD mice (Figure 7F).

During acute EAE (day 20-22 pi), the numbers of total CNS cells were decreased in the PD mice (Figure 8A). There were no statistically significant differences between the two groups in the numbers of infiltrating leukocytes (CD45hi cells) (CD: $1.37x10^6 \pm 1.1x10^6$ vs PD: $1.54x10^6 \pm 1.60x10^6$; p=0.74), suggesting that the decrease in total cells is due to microglia depletion (Figure 8A). At this timepoint, there were no differences in neutrophils and monocytes (Figure 8B and C). Although the frequencies of both cDCs and moDCs were now reduced, their numbers were not different in PD compared to CD mice (Figure 8D). The numbers of Ly6C+ inflammatory monocytes and macrophages were increased, while those of Ly6C- monocytes were decreased (Figure 8E). Numbers of total CD4+ T cells and Th1 cells remained elevated in the CNS of the PD compared to CD group (Figure 9A and B). The log10 ratio of Th17:Th1 remained decreased in the PD compared to CD group and these ratios were lower than 1 in both groups during this timepoint (Figure 9C).

Unlike the preclinical phase, Treg populations were now similar between the groups (Figure 9D), and the Treg:Teff ratios were lower in the CNS of PD compared to CD mice (Figure 9E).

These suggest that the CNS of PD mice is characterized by more robust infiltration, initiating during the preclinical EAE phase and lingering during the acute phase, albeit in lower intensity and breadth. However, PD mice consistently displayed milder neurological deficit scores compared to CD mice.

CSF1R signaling dictates the localization of inflammatory foci in the CNS in EAE

To address the seemingly conflicting data of increased CNS infiltration in PD mice but milder classical EAE clinical symptoms compared to CD mice, we initially hypothesized that the infiltrating cells may not

efficiently penetrate the CNS of PD mice. To examine whether this was the case, we employed Evans blue dye (Eb) as we have previously described [40]. For this analysis, we employed mice within 24 hrs after the first symptom of EAE appeared in CD mice. At this timepoint, the majority of PD mice had no classical EAE symptoms. As expected, spinal cords of CD mice had extensive Eb infiltrated areas. However, PD spinal cords showed minor Eb foci. In contrast, we observed increased Eb areas in the cerebellum of PD mice, but mild Eb presence in the cerebellum of CD mice (Additional file 6).

At EAE onset, IBA1+ cells in the CD lumbar spinal cords were readily detected while, as expected, they were largely absent from the EAE PD spinal cord (Figure 10A and B) (CD: 6.17 vs PD: 0.626; p=0.01). IBA1+ cells in CD spinal cords displayed activated morphology (yet not ameboid) [55] maintaining some degree of branching, thick short processes, and larger somas (Figure 10A; bottom left inserts). In the spinal cords of PD mice, there were few IBA1+ cells in the white matter, which exhibited low or no branching and an ameboid morphology, and were mostly located at the edge of the tissue (coinciding with the very few and small inflammatory foci), suggesting they are mostly monocyte-derived macrophages (Figure 10A; bottom right inserts). Sholl analysis showed that IBA1+ cells in PD spinal cords exhibited lower levels of complexity compared with IBA1+ cells in CD spinal cords (Figure 10C).

In the cerebellum, IBA1+ cells were readily detected in both CD and PD mice (Figure 10D and E) (CD: 4.25 vs PD: 3.32; p=0.24) at EAE onset. In CD mice, however, IBA1+ cells exhibited higher degree of complexity and moderately activated morphology (Figure 10D; bottom left insert). In PD cerebella, IBA1+ cells exhibited almost exclusively amoeboid morphology (Figure 10D; bottom right insert), likely representing infiltrating cells that have migrated from the periphery within the tissue parenchyma. Thus, the increased IBA1 MFI in PD cerebella is due to infiltrating monocyte-derived macrophages, while IBA1 MFI in CD cerebella is the result of microglia and some infiltrating monocyte derived macrophages (Figure 10E). Sholl analysis confirmed that the majority of CD cerebellar IBA1+ cells exhibited significantly higher levels of complexity and are presumably microglia (Figure 10F).

Accordingly, immunohistochemical analysis of lumbar spinal cords of CD EAE mice showed increased CD11b (all myeloid cells) MFI (Figure 11A; graph on the right), and increased numbers of T cells (CD3+) (Figure 11A; graph on far right), and of neutrophils (Ly6G+) (Figure 11B; graph on right), compared to PD EAE spinal cords. Only a few cells were detected within the PD spinal cord parenchyma and meninges (Figure 11A and B). This was confirmed via qPCR analysis showing that *Cd3e*, as well as *Cd4* and *Cd8a,* transcripts were increased in CD compared to PD spinal cords during EAE onset (Additional file 7A).

CD11b fluorescence intensity (Figure 11C; graph on the right) and numbers of CD3e+ T cells (Figure 11C; graph on far right) and neutrophils, (Figure 11D; graph on the right) were significantly increased in the cerebellum of PD compared to CD mice at EAE onset. Infiltration of cerebella was detected both in the perivascular cuffs and within the tissue parenchyma (Figure 11C and D).

These data were confirmed via qPCR analysis showing that *Cd3e* transcripts were increased in PD cerebella compared to that of the CD group. *Cd8a* transcripts were also increased, but no difference was detected in *Cd4* transcripts in PD compared to CD cerebella (Additional file 7A). Although the increased *Cd4* transcripts in the CD group may be suggestive of CD4+ T cell infiltration, this increase is likely due to *Cd4* mRNA expression in microglia which has been previously documented in numerous RNAseq studies [56-59].

All the above show that during EAE onset, infiltration was more prominent in the spinal cords of CD mice and in the cerebella of PD mice. However, one CD mouse, which acutely developed severe neurological deficits (typical EAE score of 3.5 from score 0 within 24 hours; a very rare event in model), showed extreme infiltration in both the cerebellum and the spinal cord in levels that were higher than any other mouse in either group during this timepoint. This mouse was excluded from the analysis due to the abnormal disease pattern.

MBP immunoreactivity revealed increased demyelination in the spinal cord of CD compared to PD mice at EAE onset (Figure 12A). On the contrary, there were significantly smaller demyelinated areas in the cerebellum of CD compared to PD mice (Figure 12B).

All the above indicate that peripheral immune cells in PD mice enter the CNS but preferentially localize within the supraspinal regions, instead of lumbar spinal cords as is the case for the control mice.

Effect of CSF1R antagonism in immune related transcripts in the CNS of mice with EAE

Our next step was to determine a possible mechanism underlying the preferential recruitment of peripheral immune cells into the cerebellum instead of the spinal cord of PD mice with EAE.

We initially examined whether the relative CSF1R levels are affected by PD. CNS *Csf1r* transcripts were significantly decreased in the PD compared to the CD group (Figure 13A). This downregulation is likely due to the depletion of CSF1R-expressing microglia and other myeloid cell subsets. Interestingly, *Csf1r* levels in the cerebellum of CD mice were significantly upregulated compared to healthy tissue during both onset and acute EAE phases, but not in the spinal cord (Figure 13A). It is likely that this differential *Csf1r* upregulation may reflect a compartment-dependent modulation of microglia activity. The expression of the CSF1R ligands *Csf1* and *Il34* in the CNS were equivalent between CD and PD mice (Figure 13A).

Flow cytometric analysis showed that the remaining/surviving microglia and infiltrating monocytes/macrophages express high levels of CSF1R (CD115) in the CNS, but to a lesser degree in the periphery of PD compared to CD mice (Figure 13B and C). CSF1R signaling is required for survival of macrophages [60] and of a Ly6C- subset of monocytes [37], and the differentiation of monocytes to macrophages [61].

Despite this dramatic increase of CSF1R expression in CNS infiltrating monocytes and macrophages in PD mice, this was not sufficient to increase *Csf1r* levels in the CNS to similar levels as those of CD CNS tissues (Figure 13A). In addition, a caveat of flow cytometric CSF1R detection is that the CSF1R (CD115) antibody

binding may be inhibited by CSF1R natural ligands [2], which may result in impaired detection of CSF1R in cells isolated from CD tissues.

Transcripts of *Csf1r* have been previously detected in neutrophils [62], however, we did not detect CSF1R expression in neutrophils by flow cytometry (Figure 13B and C).

We then examined whether we could detect regional differences in the levels of transcripts of cytokines, chemokines, and transcription factors associated with EAE and MS [63, 64] (Figure 14). We employed the whole cerebellum, a tissue which even when heavily infiltrated, contains large areas devoid of infiltration; thus, the signal of certain transcripts may be "diluted". On the other hand, lumbar EAE spinal cord tissues contain heavily lesioned areas, thus the contribution of transcripts from unaffected tissue areas is small.

Interestingly, *Csf3*, encoding for G-CSF, was elevated in the PD cerebellum, and CD spinal cord during disease onset (Figure 14A). G-CSF has been previously shown to be expressed in the CNS around the time of clinical disease onset, and is associated with neutrophilic infiltration [43, 65] and neutrophilic survival [66]. These suggest that increased cerebellar *Csf3* transcripts promote preferential cerebellar neutrophilic infiltration in PD mice.

During disease onset, transcripts of *Cxcr3* and of its ligands *Cxcl9* and *Cxcl11* were decreased in the PD spinal cords, suggesting a decrease in Th1-associated chemokines compared to CD (Figure 14B). Interestingly, *Cxcl10* and *Ifng* levels were elevated in the cerebellum of PD mice. In addition, CSF1R antagonism resulted in statistically significant transcript increases of *Il1b* and *Ccr6* (a receptor expressed on both Th17 and Tregs [67-69]) in the cerebellum of PD compared to CD mice (Figure 14C).

Icam1, which is heavily involved with leukocyte cell arrest, subsequent diapedesis, polarization and crawling across the BBB [70-72], and *Vcam1*, which is involved with Th1 and Th17 cell arrest [73], were both elevated in the cerebellum of PD mice but not in their spinal cords compared to CD mice during EAE onset (Figure 14D). Although their ligands (*Itgal* and *Itga4*, respectively) were not differentially

upregulated between the groups (Figure 14D), the differences in *Icam1* and *Vcam1* expression suggest that these molecules may orchestrate the localization of CNS infiltrates in EAE.

Additional transcripts of genes associated with EAE induction and progression were tested but did not show differences in expression between the two groups during disease onset (Additional file 7B).

2.4 Discussion

CSF1R antagonists were originally developed to deplete tumor-associated macrophages, which promote tumor growth, survival, angiogenesis, treatment resistance, and metastasis [74-76]. Tumors treated with CSF1R antagonists are infiltrated by increased CD4+ T cells, pro-inflammatory macrophages, and other pro-inflammatory leukocytes [21, 22, 77]. As a result, administration of these antagonists as part of combination therapy enhances the efficacy of anti-cancer therapeutics manifold [77].

Along with other tissue macrophages, small molecule CSF1R antagonists can also effectively deplete microglia [32], and have been shown to ameliorate EAE clinical course [16, 17, 35]. The mechanism of action is still nebulous. Studies have shown that the dampening of EAE clinical symptoms in mice treated with CSF1R antagonists is associated with depletion of microglia and CNS-associated macrophages, as well as decreased CNS infiltration and peripheral myeloid cell maturation [16, 17, 35].

Using PLX5622 diet (PD) and in agreement with previous studies [16, 35], we also observed efficient microglial depletion and milder EAE clinical course in PD mice compared to controls. However, and contrary to other studies [16, 17, 35], PD mice exhibited increased CNS infiltration and increased presence of myeloid subsets, including inflammatory monocytes, neutrophils, and cDCs, and T cell subsets (both T effectors and Tregs) compared to controls (CD) before and during EAE onset.

Interestingly, we observed that during disease onset spinal cords of PD mice were largely devoid of infiltration, while their cerebella were severely infiltrated. As expected, at the same timepoint, infiltration was mainly localized in the spinal cords of controls. Accordingly, larger demyelinated areas were detected

in the spinal cords of CD compared to PD mice, while increased demyelination was detected in the cerebella of PD compared to CD mice.

Unlike damage to the spinal cord, which presents with motor deficits [78], cerebellar infiltration manifests in deficits in cognitive, emotional, and behavioral function, induction of fear and anxiety [79, 80], and impairments in balance and proprioception [81-84]. We observed that one third of EAE PD mice developed seizures, exhibited hypersensitivity for startle response, freezing behavior, and repetitive axial rotation. At the time of atypical EAE onset, PD mice exhibited mild or no classical EAE symptoms. Furthermore, although we detected some cerebellar infiltration in CD mice, these mice never developed atypical EAE symptoms.

Our data are in apparent disagreement with previous studies by Montilla et al. [35], who also used PLX5622 and Hwang et al. [17], who used BLZ945, a CSF1R antagonist that acts similarly to PLX5622 [32]. BLZ945 and PLX5622 have similar potency (both have an IC_{50} <10nM) [85-87] and CNS penetration properties [17, 35]. Both of the previous studies showed decreased infiltration of the CNS in mice that were treated with CSF1R antagonists. However, Montilla et al. examined only spinal cords, which we show were not effectively infiltrated in PD mice. In contrast, we used pooled brains and spinal cords for our flow cytometry analysis. Although Hwang et al. also used pooled brains and spinal cords, they documented dramatically lower numbers of infiltrating cells in mice that received BLZ945.

We also observed mild differences between our study and the previous studies in peripheral immune responses. In addition to decreases in macrophage populations, we show that PD mice exhibited decreased numbers of DCs in the SLOs during preclinical EAE, as shown by Hwang et al [17]. Although we detected increased neutrophil and monocyte frequencies in PD SLOs, these did not translate in differences in absolute numbers, in agreement with Montilla, but in disagreement with Hwang et al. Montilla et al. and Hwang et al. did not detect differences in total peripheral CD4+ T cells but no information on CD4+ T cell subsets was provided [17, 35]. In agreement with these studies, we did not detect differences in total

peripheral CD4+ T cell numbers either. However, we observed significant decreases in both frequencies and absolute numbers of T effectors and T regulatory cells in the SLOs of PD mice compared with controls during preclinical EAE. This suggests that in the absence of antigen presenting cells (which are depleted in the PD mice), T cells did not differentiate effectively.

One of the reasons for the discrepancies between our study and the Hwang et al. study could be that they initiated CSF1R blockade on the day of EAE induction, while we did so seven days earlier better approximating the Montilla study in which treatment was initiated three weeks before EAE induction. It is likely that in the Hwang study there may not have been enough time for myeloid cells to adopt to the CSF1R blockade both in the SLOs and after these enter the CNS. Indeed, the Hwang study shows that mice treated with BLZ945 starting on day 0 eventually developed clinical deficits during the later EAE stages, however no information on the make-up and numbers of CNS infiltrating cells was provided.

Interestingly, immunohistological analysis of PD lumbar spinal cords at later stages of the disease (day 37 post EAE induction; day 44 on PD) showed increased microglial presence compared to preclinical and acute EAE stages (Additional File 8). After depletion, microglia repopulation occurs via proliferation of surviving/remaining microglia [88]. In inflammatory conditions peripheral myeloid cells may give rise to microglia-like cells that are phenotypically similar but transcriptionally different than microglia, and may not survive long-term [89-91]. In this study repopulation occurred while the mice were still on PD, suggesting that the newly appearing microglia derived from a CSF1R- independent mechanism. Whether the repopulation occurs from PD surviving microglia or residual infiltrating monocyte derived macrophages is still unclear.

The Hwang et al. study [17] further showed that treatment initiation after clinical symptom onset ameliorated the disease progression for the following 7 or 14 days, but there is no information on whether the mice relapsed later (i.e., after the mice were at least three weeks on the treatment). Interestingly, we

did not detect differences in the clinical scores when mice were placed on PD after clinical symptoms appeared (data not shown).

Other factors that impact disease development and progression of EAE include differences in the local environment, such as microbiota and mouse husbandry, and in the formulation of immunization reagents.

The mechanism(s) behind preferential recruitment of peripheral cells to the cerebellum instead of the spinal cord in PD mice remain to be elucidated. Increases in neutrophil frequencies, an indirect effect of prolonged CSF1R blockade, both in the periphery and the CNS of PD mice compared to controls, are associated with preferential infiltration of the supraspinal regions and with atypical EAE [92-94]. Previous studies have shown that CSF1R blockade increases G-CSF levels [95], a cytokine responsible for the survival, proliferation, maturation, and function of neutrophils [96]. Indeed, *Csf3* was elevated in the PD cerebellum and diminished in the PD spinal cords during the onset of clinical symptoms. Neutrophils are also known to recruit other leukocytes, especially inflammatory monocytes, to sites of inflammation by upregulating cell adhesion molecules such as ICAM1 and VCAM1, and secreting chemokines such as CXCL9 and CXCL10 [97, 98]. Indeed, we detected elevation of *Icam1, Vcam1 and Cxcl10* transcripts in the cerebellum of PD mice at EAE onset. Increased neutrophil frequencies may have promoted the recruitment of increased numbers of monocytes and other immune cells detected in the cerebellum in our study.

A complementary explanation stems from the study by Stromnes et al. [99], which shows that T cells with a log10 ratio of Th17:Th1>1 in the periphery tend to localize in supraspinal areas while T cells with log10 ratio of Th17:Th1<1 tend to localize in the spinal cord [99]. These ratios were also confirmed in the brains and spinal cords of mice with EAE [99]. We also show that T cells in the SLOs of PD mice during the preclinical stage of EAE had log10 ratios of Th17:Th1 higher than 1, which could partly explain the changes in lesion localization. The increase in Th17:Th1 ratios may be related to the PD-mediated depletion of Th1-promoting cells in peripheral tissues such as moDCs [100-103], or skin langerin+ DCs [104].

Our analysis of the effects of CSF1R antagonism on myeloid and lymphoid compartments extends current understanding about CSF1R effects in neuroinflammation. Although FDA-approved CSF1R antagonists do not penetrate the CNS as effectively as PLX5622, their prolonged use may be detrimental. The pleiotropism of CSF1R signaling likely has other yet undiscovered effects both in steady state and in disease settings that warrant further investigations.

2.5 References

1. Stanley, E.R. and V. Chitu, *CSF-1 receptor signaling in myeloid cells.* Cold Spring Harb Perspect Biol, 2014. **6**(6).
2. Grabert, K., et al., *A Transgenic Line That Reports CSF1R Protein Expression Provides a Definitive Marker for the Mouse Mononuclear Phagocyte System.* J Immunol, 2020. **205**(11): p. 3154-3166.
3. Chihara, T., et al., *IL-34 and M-CSF share the receptor Fms but are not identical in biological activity and signal activation.* Cell Death Differ, 2010. **17**(12): p. 1917-27.
4. Nandi, S., et al., *Receptor-type protein-tyrosine phosphatase zeta is a functional receptor for interleukin-34.* J Biol Chem, 2013. **288**(30): p. 21972-86.
5. Chitu, V., et al., *Emerging Roles for CSF-1 Receptor and its Ligands in the Nervous System.* Trends Neurosci, 2016. **39**(6): p. 378-393.
6. Lin, W., et al., *Function of CSF1 and IL34 in Macrophage Homeostasis, Inflammation, and Cancer.* Front Immunol, 2019. **10**: p. 2019.
7. Guilbert, L.J. and E.R. Stanley, *Specific interaction of murine colony-stimulating factor with mononuclear phagocytic cells.* J Cell Biol, 1980. **85**(1): p. 153-9.
8. Nandi, S., et al., *The CSF-1 receptor ligands IL-34 and CSF-1 exhibit distinct developmental brain expression patterns and regulate neural progenitor cell maintenance and maturation.* Dev Biol, 2012. **367**(2): p. 100-13.
9. Elmore, M.R., et al., *Colony-stimulating factor 1 receptor signaling is necessary for microglia viability, unmasking a microglia progenitor cell in the adult brain.* Neuron, 2014. **82**(2): p. 380-97.
10. Quintana, E., et al., *DNGR-1(+) dendritic cells are located in meningeal membrane and choroid plexus of the noninjured brain.* Glia, 2015. **63**(12): p. 2231-48.

11. Chinnery, H.R., M.J. Ruitenberg, and P.G. McMenamin, *Novel characterization of monocyte-derived cell populations in the meninges and choroid plexus and their rates of replenishment in bone marrow chimeric mice.* J Neuropathol Exp Neurol, 2010. **69**(9): p. 896-909.

12. Mrdjen, D., et al., *High-Dimensional Single-Cell Mapping of Central Nervous System Immune Cells Reveals Distinct Myeloid Subsets in Health, Aging, and Disease.* Immunity, 2018. **48**(3): p. 599.

13. Wang, Y., O. Berezovska, and S. Fedoroff, *Expression of colony stimulating factor-1 receptor (CSF-1R) by CNS neurons in mice.* J Neurosci Res, 1999. **57**(5): p. 616-32.

14. Luo, J., et al., *Colony-stimulating factor 1 receptor (CSF1R) signaling in injured neurons facilitates protection and survival.* J Exp Med, 2013. **210**(1): p. 157-72.

15. Chitu, V. and E.R. Stanley, *Regulation of Embryonic and Postnatal Development by the CSF-1 Receptor.* Curr Top Dev Biol, 2017. **123**: p. 229-275.

16. Nissen, J.C., et al., *Csf1R inhibition attenuates experimental autoimmune encephalomyelitis and promotes recovery.* Exp Neurol, 2018. **307**: p. 24-36.

17. Hwang, D., et al., *CSF-1 maintains pathogenic but not homeostatic myeloid cells in the central nervous system during autoimmune neuroinflammation.* Proc Natl Acad Sci U S A, 2022. **119**(14): p. e2111804119.

18. Lei, F., et al., *CSF1R inhibition by a small-molecule inhibitor is not microglia specific; affecting hematopoiesis and the function of macrophages.* Proc Natl Acad Sci U S A, 2020. **117**(38): p. 23336-23338.

19. Funk, K.E. and R.S. Klein, *CSF1R antagonism limits local restimulation of antiviral CD8(+) T cells during viral encephalitis.* J Neuroinflammation, 2019. **16**(1): p. 22.

20. Spiteri, A.G., et al., *PLX5622 Reduces Disease Severity in Lethal CNS Infection by Off-Target Inhibition of Peripheral Inflammatory Monocyte Production.* Front Immunol, 2022. **13**: p. 851556.

21. Mok, S., et al., *Inhibition of CSF-1 receptor improves the antitumor efficacy of adoptive cell transfer immunotherapy.* Cancer Res, 2014. **74**(1): p. 153-161.

22. Ngiow, S.F., et al., *Co-inhibition of colony stimulating factor-1 receptor and BRAF oncogene in mouse models of BRAF(V600E) melanoma.* Oncoimmunology, 2016. **5**(3): p. e1089381.

23. Spangenberg, E., et al., *Sustained microglial depletion with CSF1R inhibitor impairs parenchymal plaque development in an Alzheimer's disease model.* Nat Commun, 2019. **10**(1): p. 3758.

24. Hu, B., et al., *Insights Into the Role of CSF1R in the Central Nervous System and Neurological Disorders.* Front Aging Neurosci, 2021. **13**: p. 789834.

25. Gratuze, M., et al., *Activated microglia mitigate Abeta-associated tau seeding and spreading.* J Exp Med, 2021. **218**(8).

26. Zhang, D., et al., *Microglial activation contributes to cognitive impairments in rotenone-induced mouse Parkinson's disease model.* J Neuroinflammation, 2021. **18**(1): p. 4.

27. Cannarile, M.A., et al., *Colony-stimulating factor 1 receptor (CSF1R) inhibitors in cancer therapy.* J Immunother Cancer, 2017. **5**(1): p. 53.

28. Tan, I.L., et al., *CSF1R inhibition depletes tumor-associated macrophages and attenuates tumor progression in a mouse sonic Hedgehog-Medulloblastoma model.* Oncogene, 2021. **40**(2): p. 396-407.

29. Tap, W.D., et al., *Pexidartinib versus placebo for advanced tenosynovial giant cell tumour (ENLIVEN): a randomised phase 3 trial.* Lancet, 2019. **394**(10197): p. 478-487.

30. Lamb, Y.N., *Pexidartinib: First Approval.* Drugs, 2019. **79**(16): p. 1805-1812.

31. Smith, C.C., et al., *Characterizing and Overriding the Structural Mechanism of the Quizartinib-Resistant FLT3 "Gatekeeper" F691L Mutation with PLX3397.* Cancer Discov, 2015. **5**(6): p. 668-79.

32. Green, K.N., J.D. Crapser, and L.A. Hohsfield, *To Kill a Microglia: A Case for CSF1R Inhibitors.* Trends Immunol, 2020. **41**(9): p. 771-784.

33. Feng, R., et al., *Self-renewing macrophages in dorsal root ganglia contribute to promote nerve regeneration.* Proc Natl Acad Sci U S A, 2023. **120**(7): p. e2215906120.

34. Hagan, N., et al., *CSF1R signaling is a regulator of pathogenesis in progressive MS.* Cell Death Dis, 2020. **11**(10): p. 904.

35. Montilla, A., et al., *Microglia and meningeal macrophages depletion delays the onset of experimental autoimmune encephalomyelitis.* Cell Death Dis, 2023. **14**(1): p. 16.

36. Lin, H., et al., *Discovery of a cytokine and its receptor by functional screening of the extracellular proteome.* Science, 2008. **320**(5877): p. 807-11.

37. Hume, D.A. and K.P. MacDonald, *Therapeutic applications of macrophage colony-stimulating factor-1 (CSF-1) and antagonists of CSF-1 receptor (CSF-1R) signaling.* Blood, 2012. **119**(8): p. 1810-20.

38. Sehgal, A., K.M. Irvine, and D.A. Hume, *Functions of macrophage colony-stimulating factor (CSF1) in development, homeostasis, and tissue repair.* Semin Immunol, 2021. **54**: p. 101509.

39. Delaney, C., et al., *Attenuated CSF-1R signalling drives cerebrovascular pathology.* EMBO Mol Med, 2021. **13**(2): p. e12889.

40. Lee, E., et al., *IFN-gamma signaling in the central nervous system controls the course of experimental autoimmune encephalomyelitis independently of the localization and composition of inflammatory foci.* J Neuroinflammation, 2012. **9**: p. 7.

41. Mills Ko, E., et al., *Deletion of astroglial CXCL10 delays clinical onset but does not affect progressive axon loss in a murine autoimmune multiple sclerosis model.* J Neuroinflammation, 2014. **11**: p. 105.

42. Moreno, M., et al., *Conditional ablation of astroglial CCL2 suppresses CNS accumulation of M1 macrophages and preserves axons in mice with MOG peptide EAE.* J Neurosci, 2014. **34**(24): p. 8175-85.

43. Soulika, A.M., et al., *Initiation and progression of axonopathy in experimental autoimmune encephalomyelitis.* J Neurosci, 2009. **29**(47): p. 14965-79.

44. Nguyen, A.V., et al., *Montelukast, an Antagonist of Cysteinyl Leukotriene Signaling, Impairs Burn Wound Healing.* Plast Reconstr Surg, 2022. **150**(1): p. 92e-104e.

45. Nguyen, A.V., et al., *Skin-Resident beta2AR Signaling Delays Burn Wound Healing.* J Invest Dermatol, 2021. **141**(8): p. 2098-2101 e4.

46. Goldmann, T., et al., *Origin, fate and dynamics of macrophages at central nervous system interfaces.* Nat Immunol, 2016. **17**(7): p. 797-805.

47. Mildner, A., et al., *Ly-6G+CCR2- myeloid cells rather than Ly-6ChighCCR2+ monocytes are required for the control of bacterial infection in the central nervous system.* J Immunol, 2008. **181**(4): p. 2713-22.

48. Filiano, A.J., S.P. Gadani, and J. Kipnis, *How and why do T cells and their derived cytokines affect the injured and healthy brain?* Nat Rev Neurosci, 2017. **18**(6): p. 375-384.

49. Cugurra, A., et al., *Skull and vertebral bone marrow are myeloid cell reservoirs for the meninges and CNS parenchyma.* Science, 2021. **373**(6553).

50. Wang, Y., et al., *IL-34 is a tissue-restricted ligand of CSF1R required for the development of Langerhans cells and microglia.* Nat Immunol, 2012. **13**(8): p. 753-60.

51. Lonardi, S., et al., *CSF1R Is Required for Differentiation and Migration of Langerhans Cells and Langerhans Cell Histiocytosis.* Cancer Immunol Res, 2020. **8**(6): p. 829-841.

52. Merad, M., F. Ginhoux, and M. Collin, *Origin, homeostasis and function of Langerhans cells and other langerin-expressing dendritic cells.* Nat Rev Immunol, 2008. **8**(12): p. 935-47.

53. Church, K.A., et al., *Models of microglia depletion and replenishment elicit protective effects to alleviate vascular and neuronal damage in the diabetic murine retina.* J Neuroinflammation, 2022. **19**(1): p. 300.

54. King, I.L., T.L. Dickendesher, and B.M. Segal, *Circulating Ly-6C+ myeloid precursors migrate to the CNS and play a pathogenic role during autoimmune demyelinating disease.* Blood, 2009. **113**(14): p. 3190-7.

55. Jonas, R.A., et al., *The spider effect: morphological and orienting classification of microglia in response to stimuli in vivo.* PLoS One, 2012. **7**(2): p. e30763.

56. Chiu, I.M., et al., *A neurodegeneration-specific gene-expression signature of acutely isolated microglia from an amyotrophic lateral sclerosis mouse model.* Cell Rep, 2013. **4**(2): p. 385-401.

57. Pan, J., et al., *Transcriptomic profiling of microglia and astrocytes throughout aging.* J Neuroinflammation, 2020. **17**(1): p. 97.

58. Pulido-Salgado, M., et al., *RNA-Seq transcriptomic profiling of primary murine microglia treated with LPS or LPS + IFNgamma.* Sci Rep, 2018. **8**(1): p. 16096.

59. Zhang, Y., et al., *An RNA-sequencing transcriptome and splicing database of glia, neurons, and vascular cells of the cerebral cortex.* J Neurosci, 2014. **34**(36): p. 11929-47.

60. Cecchini, M.G., et al., *Role of colony stimulating factor-1 in the establishment and regulation of tissue macrophages during postnatal development of the mouse.* Development, 1994. **120**(6): p. 1357-1372.

61. Dai, X.M., et al., *Targeted disruption of the mouse colony-stimulating factor 1 receptor gene results in osteopetrosis, mononuclear phagocyte deficiency, increased primitive progenitor cell frequencies, and reproductive defects.* Blood, 2002. **99**(1): p. 111-20.

62. Sasmono, R.T., et al., *Mouse neutrophilic granulocytes express mRNA encoding the macrophage colony-stimulating factor receptor (CSF-1R) as well as many other macrophage-specific transcripts and can transdifferentiate into macrophages in vitro in response to CSF-1.* J Leukoc Biol, 2007. **82**(1): p. 111-23.

63. Imitola, J., T. Chitnis, and S.J. Khoury, *Cytokines in multiple sclerosis: from bench to bedside.* Pharmacol Ther, 2005. **106**(2): p. 163-77.

64. Wang, K., et al., *The Properties of Cytokines in Multiple Sclerosis: Pros and Cons.* Am J Med Sci, 2018. **356**(6): p. 552-560.

65. Rumble, J.M., et al., *Neutrophil-related factors as biomarkers in EAE and MS.* J Exp Med, 2015. **212**(1): p. 23-35.

66. Basu, S., et al., *Evaluation of role of G-CSF in the production, survival, and release of neutrophils from bone marrow into circulation.* Blood, 2002. **100**(3): p. 854-61.

67. Hu, J., et al., *C-C motif chemokine ligand 20 regulates neuroinflammation following spinal cord injury via Th17 cell recruitment.* J Neuroinflammation, 2016. **13**(1): p. 162.

68. Liao, F., et al., *CC-chemokine receptor 6 is expressed on diverse memory subsets of T cells and determines responsiveness to macrophage inflammatory protein 3 alpha.* J Immunol, 1999. **162**(1): p. 186-94.

69. Yamazaki, T., et al., *CCR6 regulates the migration of inflammatory and regulatory T cells.* J Immunol, 2008. **181**(12): p. 8391-401.

70. Abadier, M., et al., *Cell surface levels of endothelial ICAM-1 influence the transcellular or paracellular T-cell diapedesis across the blood-brain barrier.* Eur J Immunol, 2015. **45**(4): p. 1043-58.

71. Steiner, O., et al., *Differential roles for endothelial ICAM-1, ICAM-2, and VCAM-1 in shear-resistant T cell arrest, polarization, and directed crawling on blood-brain barrier endothelium.* J Immunol, 2010. **185**(8): p. 4846-55.

72. Felix, R., et al., *Role of colony-stimulating factor-1 in bone metabolism.* J Cell Biochem, 1994. **55**(3): p. 340-9.

73. Haghayegh Jahromi, N., et al., *Intercellular Adhesion Molecule-1 (ICAM-1) and ICAM-2 Differentially Contribute to Peripheral Activation and CNS Entry of Autoaggressive Th1 and Th17 Cells in Experimental Autoimmune Encephalomyelitis.* Front Immunol, 2019. **10**: p. 3056.

74. Noy, R. and J.W. Pollard, *Tumor-associated macrophages: from mechanisms to therapy.* Immunity, 2014. **41**(1): p. 49-61.

75. DeNardo, D.G., et al., *Leukocyte complexity predicts breast cancer survival and functionally regulates response to chemotherapy.* Cancer Discov, 2011. **1**(1): p. 54-67.

76. Ries, C.H., et al., *Targeting tumor-associated macrophages with anti-CSF-1R antibody reveals a strategy for cancer therapy.* Cancer Cell, 2014. **25**(6): p. 846-59.

77. Yan, D., et al., *Inhibition of colony stimulating factor-1 receptor abrogates microenvironment-mediated therapeutic resistance in gliomas.* Oncogene, 2017. **36**(43): p. 6049-6058.

78. Wujek, J.R., et al., *Axon loss in the spinal cord determines permanent neurological disability in an animal model of multiple sclerosis.* J Neuropathol Exp Neurol, 2002. **61**(1): p. 23-32.

79. Otsuka, S., et al., *Roles of Cbln1 in Non-Motor Functions of Mice.* J Neurosci, 2016. **36**(46): p. 11801-11816.

80. Sacchetti, B., T. Sacco, and P. Strata, *Reversible inactivation of amygdala and cerebellum but not perirhinal cortex impairs reactivated fear memories.* European Journal of Neuroscience, 2007. **25**(9): p. 2875-2884.

81. Proske, U. and S.C. Gandevia, *The kinaesthetic senses.* J Physiol, 2009. **587**(Pt 17): p. 4139-46.

82. Wolpert, D.M., Z. Ghahramani, and M.I. Jordan, *An internal model for sensorimotor integration.* Science, 1995. **269**(5232): p. 1880-2.

83. Wolpert, D.M., R.C. Miall, and M. Kawato, *Internal models in the cerebellum.* Trends Cogn Sci, 1998. **2**(9): p. 338-47.

84. Miall, R.C., et al., *Disruption of state estimation in the human lateral cerebellum.* PLoS Biol, 2007. **5**(11): p. e316.

85. Dagher, N.N., et al., *Colony-stimulating factor 1 receptor inhibition prevents microglial plaque association and improves cognition in 3xTg-AD mice.* J Neuroinflammation, 2015. **12**: p. 139.

86. Pyonteck, S.M., et al., *CSF-1R inhibition alters macrophage polarization and blocks glioma progression.* Nat Med, 2013. **19**(10): p. 1264-72.

87. van der Wildt, B., et al., *BLZ945 derivatives for PET imaging of colony stimulating factor-1 receptors in the brain.* Nucl Med Biol, 2021. **100-101**: p. 44-51.

88. Huang, Y., et al., *Repopulated microglia are solely derived from the proliferation of residual microglia after acute depletion.* Nat Neurosci, 2018. **21**(4): p. 530-540.

89. Getts, D.R., et al., *Ly6c+ "inflammatory monocytes" are microglial precursors recruited in a pathogenic manner in West Nile virus encephalitis.* J Exp Med, 2008. **205**(10): p. 2319-37.

90. Ajami, B., et al., *Infiltrating monocytes trigger EAE progression, but do not contribute to the resident microglia pool.* Nat Neurosci, 2011. **14**(9): p. 1142-9.

91. Lund, H., et al., *Competitive repopulation of an empty microglial niche yields functionally distinct subsets of microglia-like cells.* Nat Commun, 2018. **9**(1): p. 4845.

92. Liu, Y., et al., *Preferential Recruitment of Neutrophils into the Cerebellum and Brainstem Contributes to the Atypical Experimental Autoimmune Encephalomyelitis Phenotype.* J Immunol, 2015. **195**(3): p. 841-52.

93. Stoolman, J.S., et al., *An IFNgamma/CXCL2 regulatory pathway determines lesion localization during EAE.* J Neuroinflammation, 2018. **15**(1): p. 208.

94. Yan, Z., et al., *Deficiency of Socs3 leads to brain-targeted EAE via enhanced neutrophil activation and ROS production.* JCI Insight, 2019. **5**(9).

95. Swierczak, A., et al., *The promotion of breast cancer metastasis caused by inhibition of CSF-1R/CSF-1 signaling is blocked by targeting the G-CSF receptor.* Cancer Immunol Res, 2014. **2**(8): p. 765-76.

96. Martin, K.R., et al., *G-CSF - A double edge sword in neutrophil mediated immunity.* Semin Immunol, 2021. **54**: p. 101516.

97. Soehnlein, O., et al., *Neutrophil secretion products pave the way for inflammatory monocytes.* Blood, 2008. **112**(4): p. 1461-71.

98. Zhou, J., et al., *Neutrophils promote mononuclear cell infiltration during viral-induced encephalitis.* J Immunol, 2003. **170**(6): p. 3331-6.

99. Stromnes, I.M., et al., *Differential regulation of central nervous system autoimmunity by T(H)1 and T(H)17 cells.* Nat Med, 2008. **14**(3): p. 337-42.

100. Leon, B., M. Lopez-Bravo, and C. Ardavin, *Monocyte-derived dendritic cells formed at the infection site control the induction of protective T helper 1 responses against Leishmania.* Immunity, 2007. **26**(4): p. 519-31.

101. Sanarico, N., et al., *Human monocyte-derived dendritic cells differentiated in the presence of IL-2 produce proinflammatory cytokines and prime Th1 immune response.* J Leukoc Biol, 2006. **80**(3): p. 555-62.

102. Tanaka, H., et al., *Human monocyte-derived dendritic cells induce naive T cell differentiation into T helper cell type 2 (Th2) or Th1/Th2 effectors. Role of stimulator/responder ratio.* J Exp Med, 2000. **192**(3): p. 405-12.

103. Zou, W., et al., *Macrophage-Derived Dendritic Cells Have Strong Th1-Polarizing Potential Mediated by β-Chemokines Rather Than IL-12.* The Journal of Immunology, 2000. **165**(8): p. 4388-4396.

104. King, I.L., M.A. Kroenke, and B.M. Segal, *GM-CSF-dependent, CD103+ dermal dendritic cells play a critical role in Th effector cell differentiation after subcutaneous immunization.* J Exp Med, 2010. **207**(5): p. 953-61.

2.6 Figures and tables

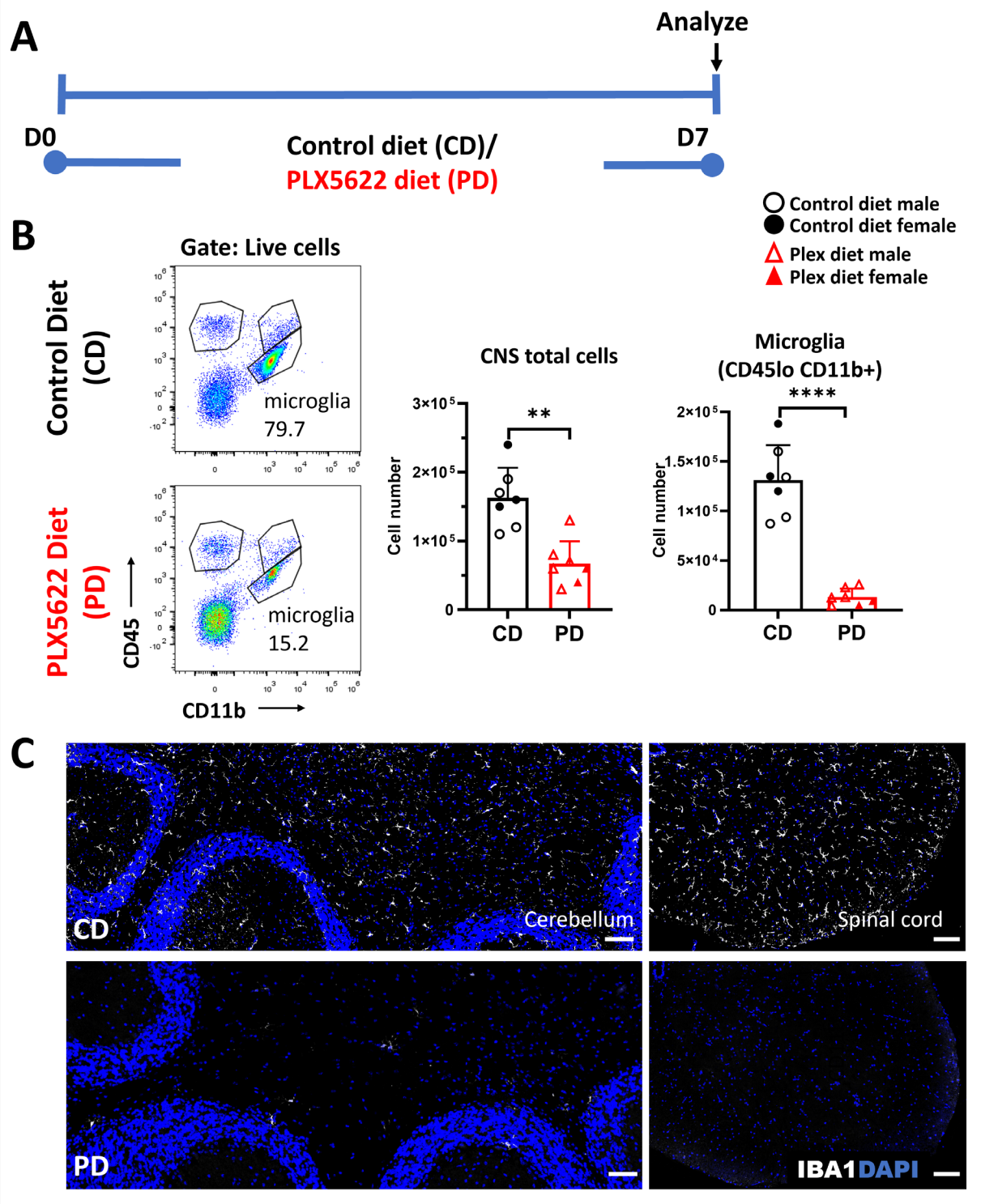

Figure 1: CSF1R antagonism depletes microglia at steady state.

A Experimental schema depicting that healthy C57BL/6 mice were maintained on control diet (CD) or PLX5622 diet (PD) for seven days. Tissues were then collected and analyzed by flow cytometry and immunohistochemistry. **B** Flow cytometric analysis shows that both total CNS cells and CD11b+CD45lo (microglia) numbers are reduced in PD compared to CD mice in steady state. **C** Immunohistochemical staining of cerebellum (left) and spinal cord (right) tissues confirms robust IBA1+ cell depletion in PD mice. Scale bars represent 100 µm. Results are shown as means ±SD, n=6-7; **p<0.005, ****p<0.00005.

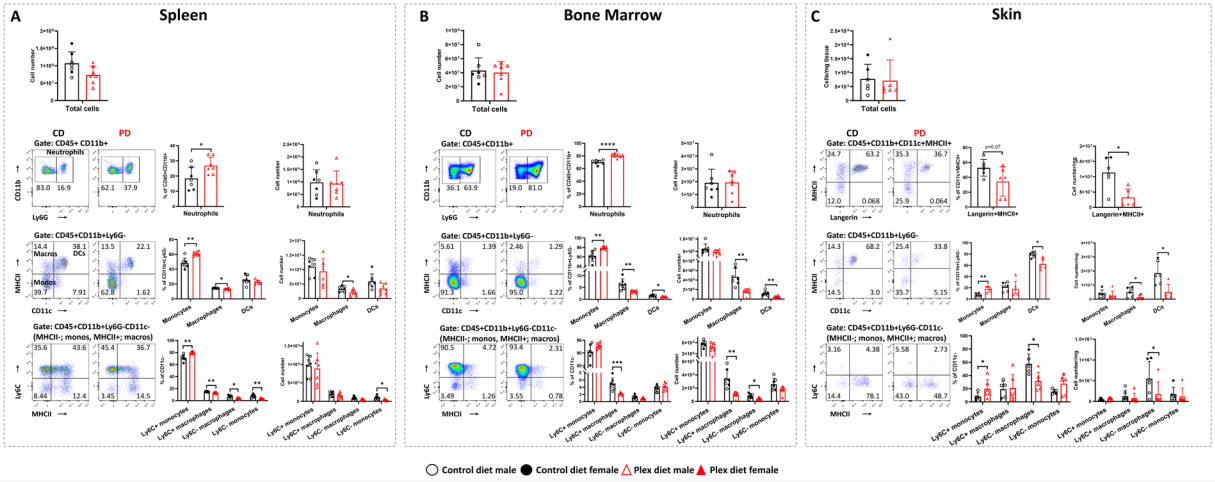

Figure 2: Effect of PLX5622 on myeloid cell subsets in peripheral immune tissues in steady state.

Flow cytometric analysis of single cells isolated from spleen, bone marrow, and skin in CD and PD mice. Neutrophils (CD45+CD11b+Ly6G+), monocytes (monos; CD45+CD11b+CD11c-Ly6G-MHCII-Ly6C+), macrophages (macros; CD45+CD11b+CD11c-Ly6G-MHCII+) and dendritic cells (DCs; CD45+CD11b+CD11c+MHCII+) were analyzed in **A** spleen and **B** bone marrow. Monocytes and macrophage subsets were further classified as Ly6C+ (inflammatory) or Ly6C- (non-inflammatory). **C** In skin, dendritic cells (CD45+CD11b+CD11c+MHCII+), langerin+ cells (CD45+CD11b+Ly6G-CD11c+MHCII+langerin+; includes Langerhans cells in the epidermis and langerin+ DCs in the dermis), and monocyte/macrophage populations were analyzed. Monocytes and macrophage subsets were further classified as Ly6C+ or Ly6C-.

Representative flow plots are shown. Both male and female mice were employed. Results are shown as means ±SD, n=6-7; *p<0.05, **p<0.005, ****p<0.00005.

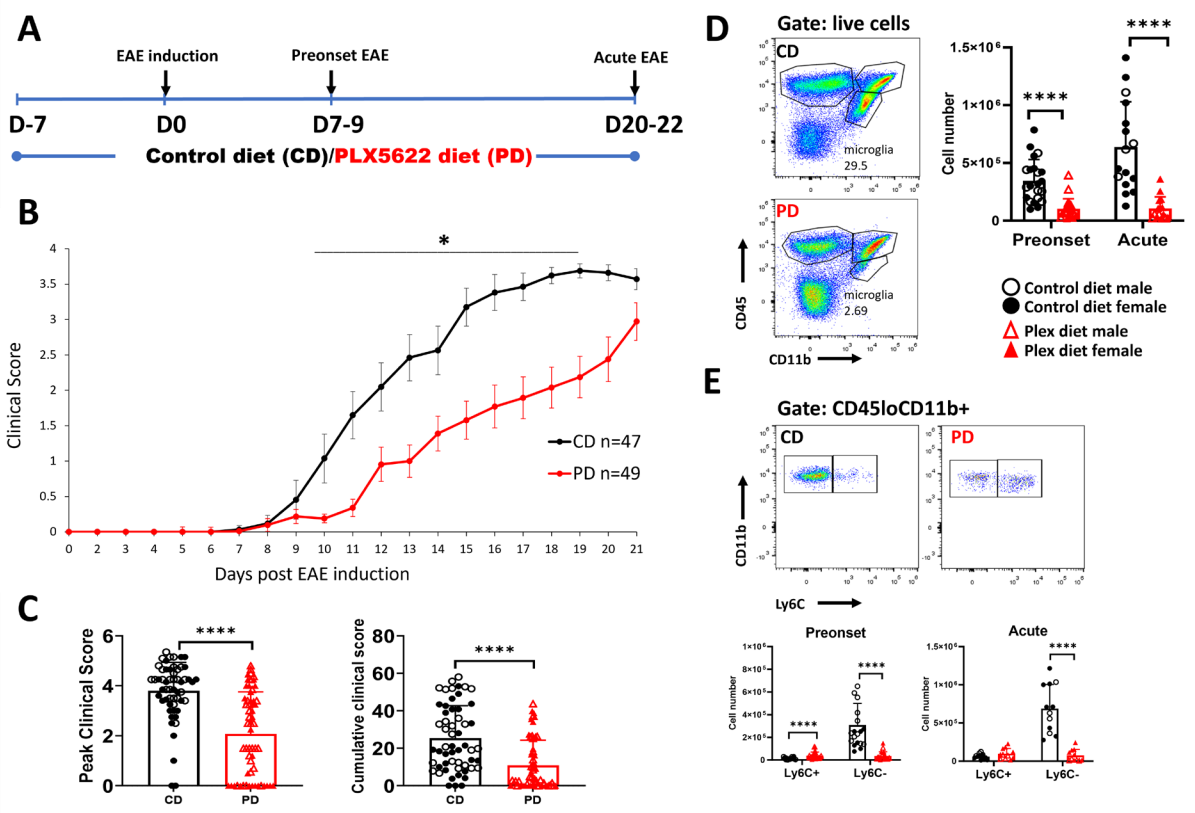

Figure 3: CSF1R antagonism ameliorates EAE clinical severity.

A Schema of experimental design. **B** Classical EAE neurological symptoms onset was delayed, and severity was milder in PD compared to CD mice. **C** Peak and cumulative EAE scores were lower in PD compared to CD mice. **D** Microglia (CD45loCD11b+) are depleted in pooled brain and spinal cord tissues of PD mice in preclinical and acute EAE. **E** Analysis of Ly6C expression in CD45loCD11b+ cells shows that CD45loCD11b+Ly6C- cells were preferentially depleted in the CNS of PD mice.

Representative flow plots are shown. Both male and female mice were employed. Results are shown as means ± SD; n= 44-47 CD, 40-49 PD; *p<0.05, ****p<0.0005.

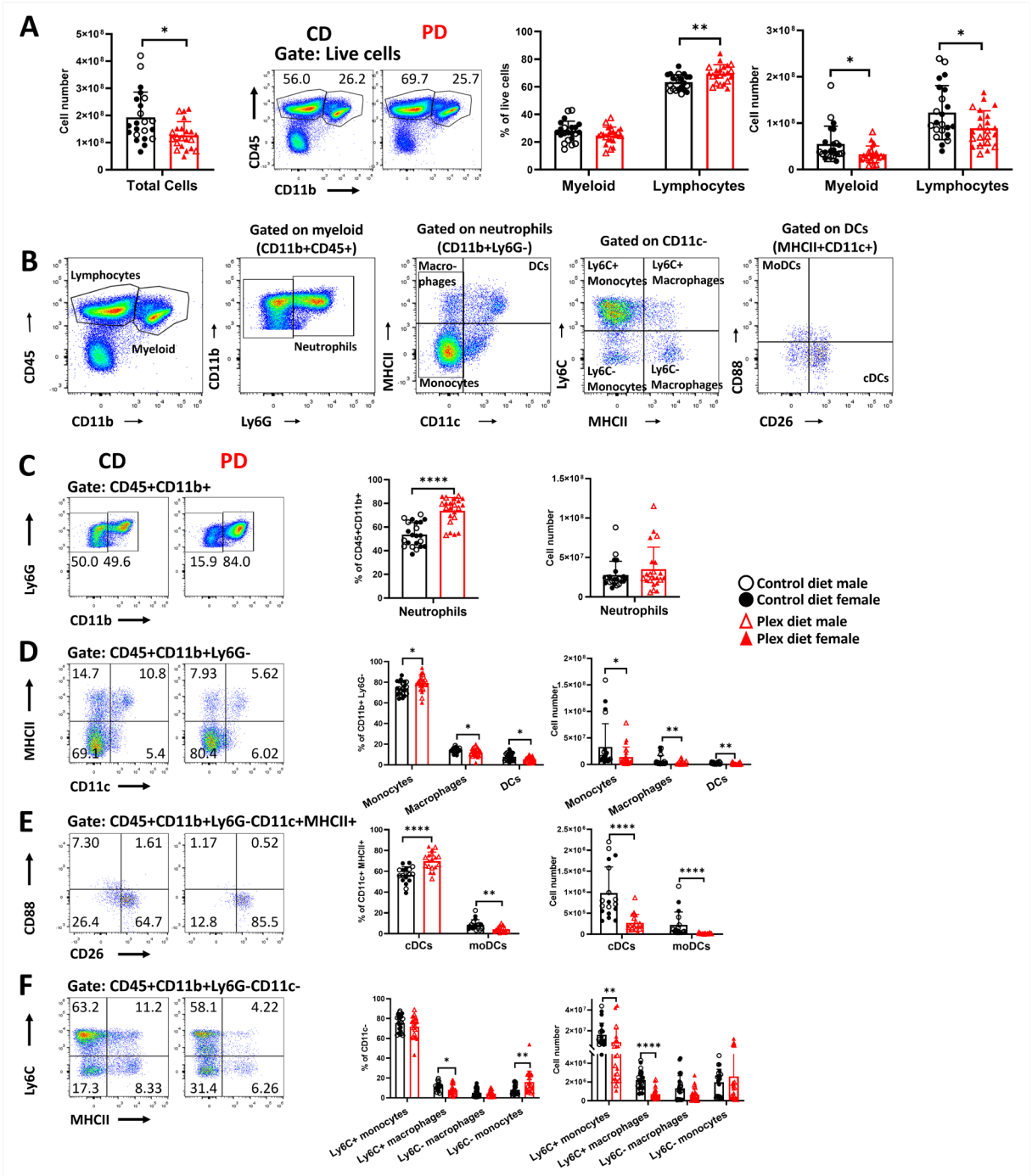

Figure 4: PD depletes macrophages and DCs in secondary lymphoid organs (SLOs) in preclinical EAE.

Pooled spleen and draining lymph nodes (SLOs) were analyzed before clinical symptom onset (preonset EAE). **A** Numbers of total cells, and of myeloid (CD45+CD11b+), and lymphocytic (CD45+CD11b-) cells were lower in the SLOs of PD compared to those of CD mice. **B** Gating strategy for flow cytometry analysis of

SLO myeloid cells in EAE. **C** Neutrophil (CD45+CD11b+Ly6G+) frequencies were increased but not their numbers in PD mice compared to CD mice. **D** Frequencies of all monocytes (CD45+CD11b+Ly6G-CD11c-MHCII-) were increased but their numbers were decreased in SLOs of PD compared to those of CD mice. Both frequencies and numbers of total DCs (CD45+CD11b+Ly6G-CD11c+MHCII+), and of total macrophages (CD45+CD11b+Ly6G-CD11c-MHCII+) were decreased in PD compared to CD. **E** Frequencies of classical DCs (cDCs; CD45+CD11b+Ly6G-CD11c+MHCII+CD26+CD88-) were increased, and those of monocyte-derived DCs (moDCs; CD45+CD11b+Ly6G-CD11c+MHCII+CD26-CD88+) were decreased but the absolute numbers of both subsets were decreased in the PD SLOs compared to CD. **F** Ly6C+ monocyte and macrophage subsets (CD45+CD11b+Ly6G-CD11c-MHCII+Ly6C+) were decreased in the PD SLOs compared to those of CD mice.

Representative flow plots are shown. Both male and female mice were employed. Data are shown as means ± SD, n=22; *p<0.05, **p<0.005, ****p<0.00005.

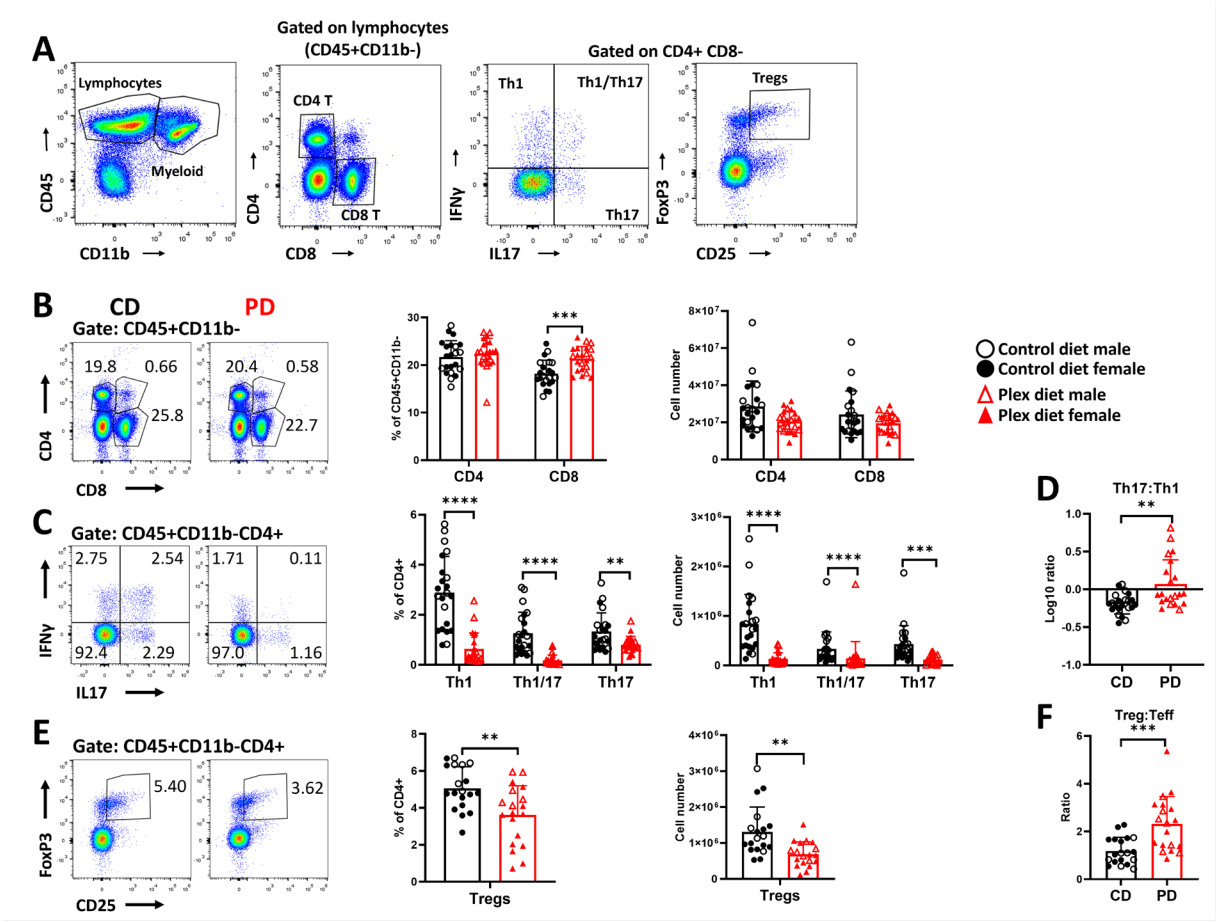

Figure 5: Impaired T effector cell generation in the SLOs of PD mice in preclinical EAE

A Gating strategy for flow cytometry analysis of T cell subsets in the EAE SLOs **B** Frequencies and numbers of CD4+ and CD8+ T cells in the SLOs of CD and PD mice. **C** Frequencies and numbers of MOG-specific CD4 T cell (CD45+CD11b-CD4+) subsets Th1 (IFNγ+), Th17 (IL17+), Th1/17 (IFNγ+IL17+) were decreased in the PD compared to CD SLOs. **D** Log10 ratios of Th17:Th1 were increased in the SLOs of PD compared to CD. **E** Both frequencies and absolute numbers of Tregs (CD25+FoxP3+) were decreased in PD SLOs compared to CD. **F** Ratios of Treg:Teff were increased in PD SLOs compared to CD.

Representative flow plots are shown. Both male and female mice were employed. Data are shown as means ± SD, n=22; **p<0.005, ***p<0.0005, ****p<0.00005.

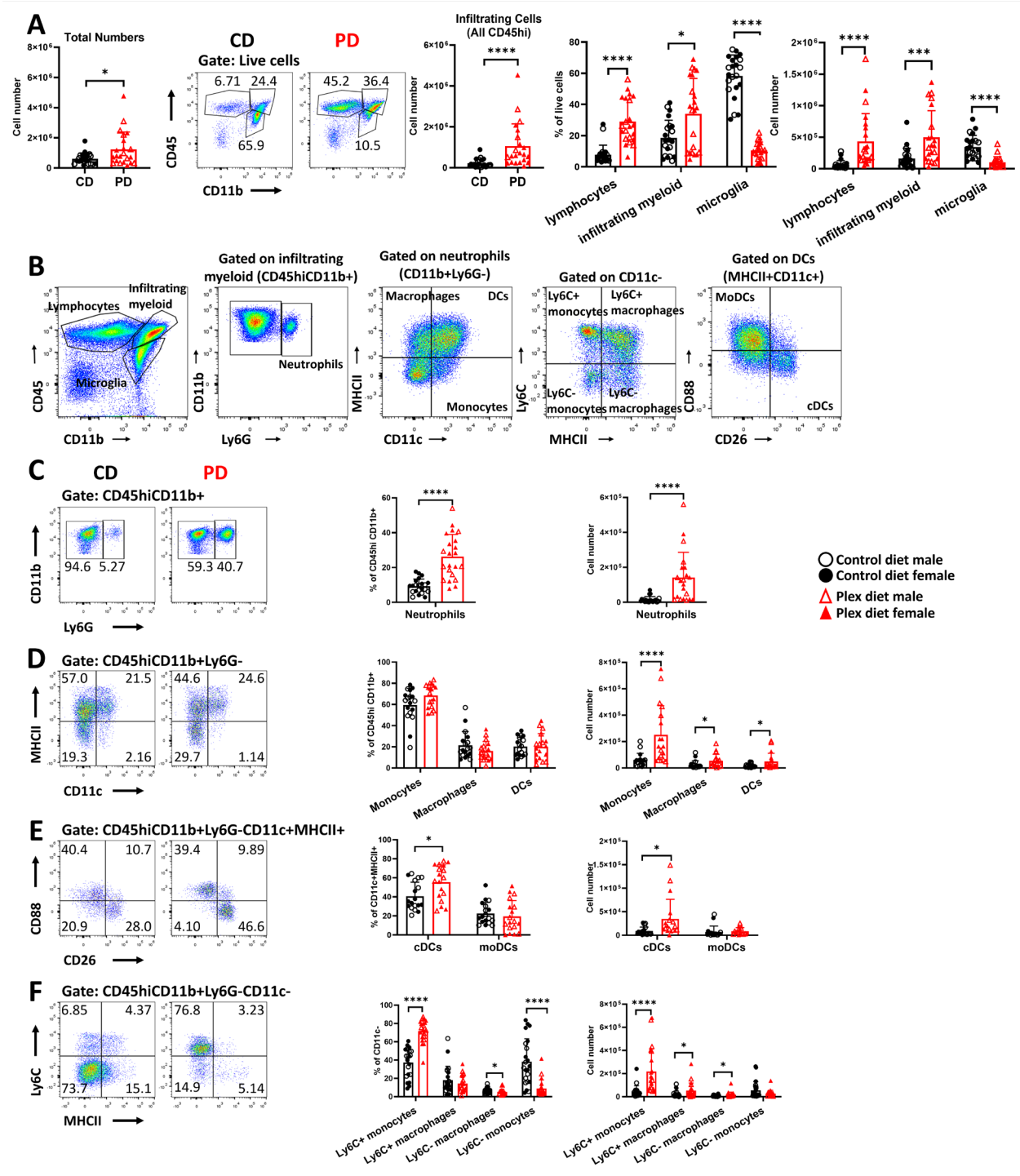

Figure 6: CSF1R antagonism increases CNS infiltration by myeloid cells before neurological symptoms appear in EAE.

Single cells isolated from pooled brain and spinal cord tissues were analyzed by flow cytometry for myeloid subsets before onset of neurological deficits (preonset) **A** Numbers of total cells, and of infiltrating immune cells (CD45hi), which include myeloid cells (CD45hiCD11b+) and lymphocytes (CD45hiCD11b-) were increased while microglia were decreased in the CNS of PD compared to CD mice in preclinical EAE. **B** Gating strategy for flow cytometric analysis of myeloid cells in the CNS. **C** Frequencies and absolute numbers of neutrophils (CD45hiCD11b+Ly6G+) were increased in the CNS of PD mice with during preonset EAE compared with CD mice. **D** No differences in the frequencies of total monocytes (CD45hiCD11b+Ly6G-CD11c-MHCII-), total macrophages (CD45hiCD11b+Ly6G-CD11c-MHCII+) and total DCs (CD45hiCD11b+Ly6G-CD11c+MHCII+) were detected but their numbers were increased in the CNS of PD compared to CD. **E** Frequencies and numbers of cDCs (CD45hiCD11b+Ly6G-CD11c+MHCII+CD26+CD88-), but not of moDCs (CD45hiCD11b+Ly6G-CD11c+MHCII+CD26+CD88+) were increased in the CNS of PD compared to CD mice. **F** Numbers of Ly6C+ monocytes, and of both Ly6C+ and Ly6C- macrophages were increased in the CNS of PD compared to CD mice in preclinical EAE.

Representative flow plots are shown. Both male and female mice were employed. Data are shown as means ± SD, n=22; *p<0.05, ***p<0.0005, ****p<0.00005.

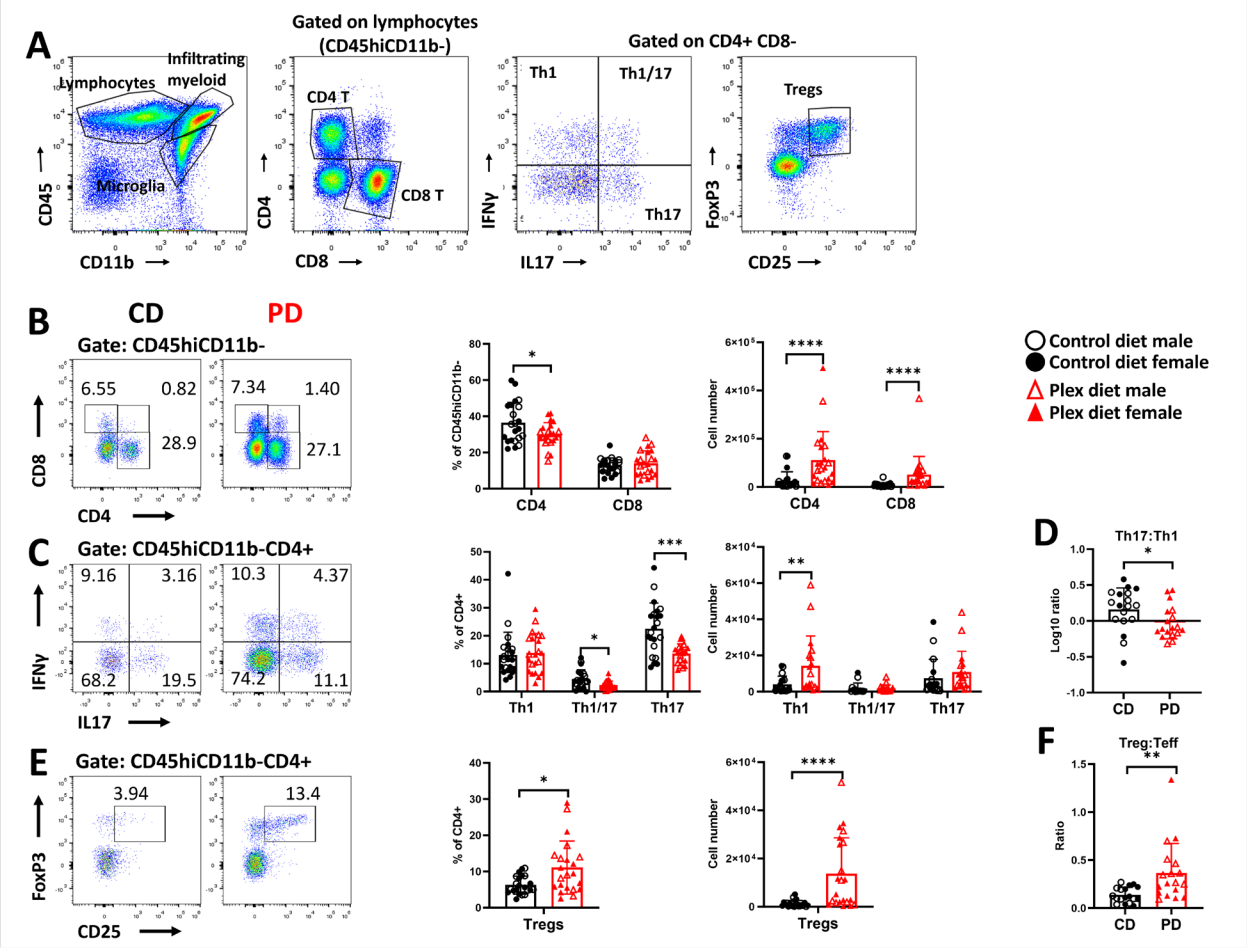

Figure 7: CSF1R antagonism increases CNS infiltration by lymphocytes before neurological symptoms appear in EAE.

Single cells isolated from pooled brain and spinal cord tissues were analyzed by flow cytometry for T cell subsets before onset of neurological deficits (preonset). **A** Gating strategy for flow cytometric analysis of T cells in the EAE CNS. **B** Frequencies of both CD4+, but not of CD8+ T cells decreased, but the numbers of both subsets increased in the CNS of PD compared to CD mice. **C** Frequencies of Th1 cells were not different between the groups, but their absolute numbers were increased in the CNS of PD compared with CD. Although the frequencies of Th1/17 and Th17 cells were decreased their absolute numbers were not different in the CNS of PD compared to CD mice. **D** Log10 Th17:Th1 ratios were below 1 in the CNS of PD mice, while in CD they were greater than 1. **E** Both frequencies and numbers of Tregs were increased in

the CNS of PD compared to CD mice. **F** Treg:Teffector ratios were increased in the CNS of PD mice compared to CD before EAE onset.

Representative flow plots are shown. Both male and female mice were employed. Data are shown as means ± SD, n=22; *p<0.05, **p<0.005, ***p<0.0005.

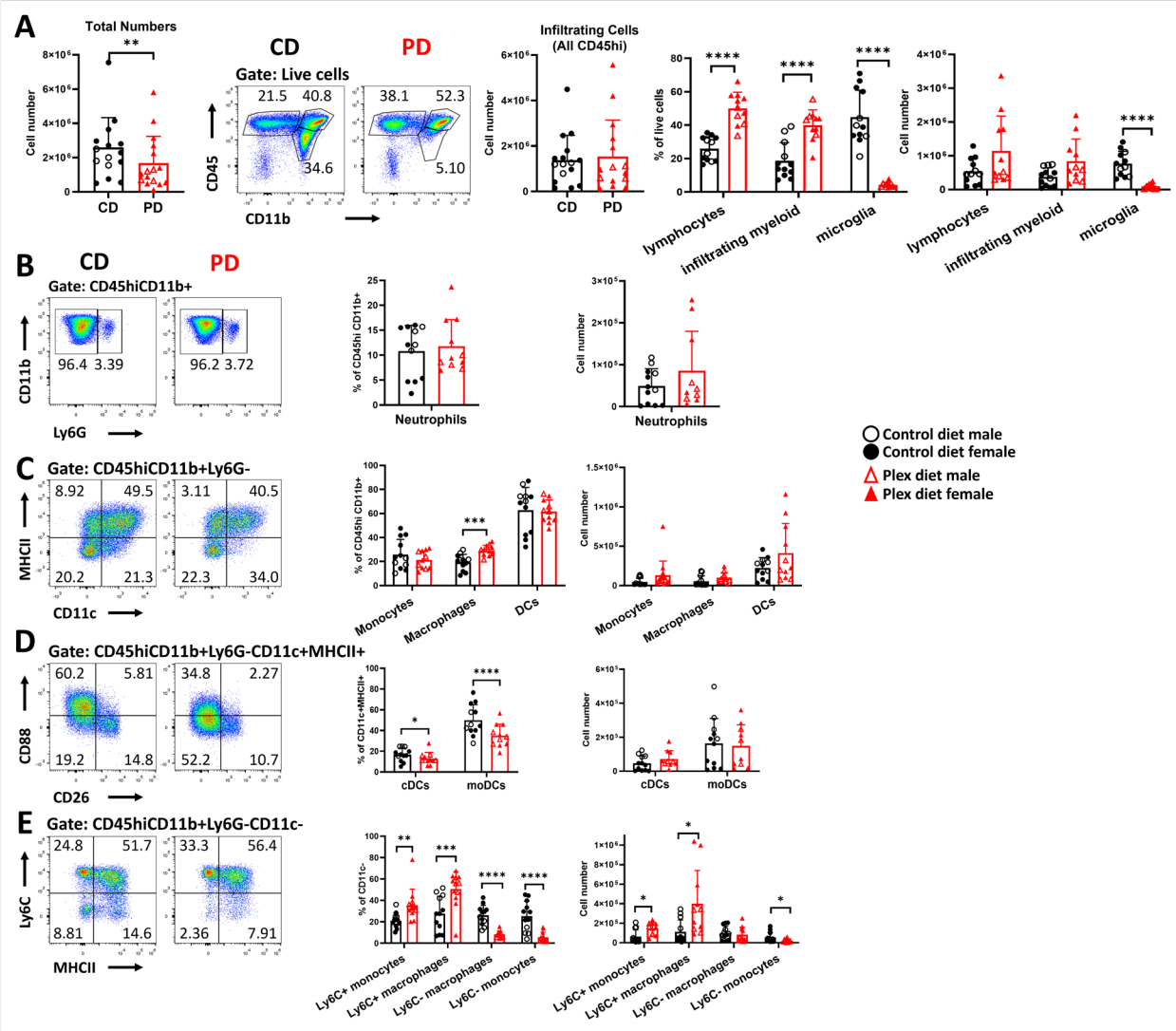

Figure 8: Only mild differences in the myeloid cell populations persist in the CNS of PD mice in acute EAE.

Single cells isolated from pooled brain and spinal cord tissues were analyzed by flow cytometry during acute EAE. **A** Numbers of total cells were lower in the PD CNS compared to CD. There were no differences in the numbers of total infiltrating cells (CD45hi). Although the frequencies of myeloid cells (CD45hiCD11b+) and lymphocytes (CD45hiCD11b-) remained higher in PD compared to CD mice, their numbers were not different between the groups in acute EAE. Microglia frequencies and numbers remained low in PD compared to CD mice. **B** No differences in frequencies and absolute numbers of neutrophils were detected between the groups at this timepoint. **C** Although the frequencies of total macrophages (CD45hiCD11b+Ly6G-CD11c- MHCII+) were increased in the PD mice, there were no differences in absolute numbers. No differences were detected in total monocytes (CD45hiCD11b+Ly6G-CD11c- MHCII-) and total DCs (CD45hiCD11b+Ly6G-CD11c+MHCII+) between the groups. **D** Frequencies of cDCs and moDCs decreased, but their absolute numbers were not different in PD compared to CD. **E** Frequencies of Ly6C+ monocytes and macrophages were increased while Ly6C- monocytes and macrophages were decreased in the CNS of PD compared to CD mice during acute EAE. Representative flow plots are shown. Both male and female mice were employed. Data are shown as means ± SD, n= 12; *p<0.05, **p<0.005, ***p<0.0005, ****p<0.00005.

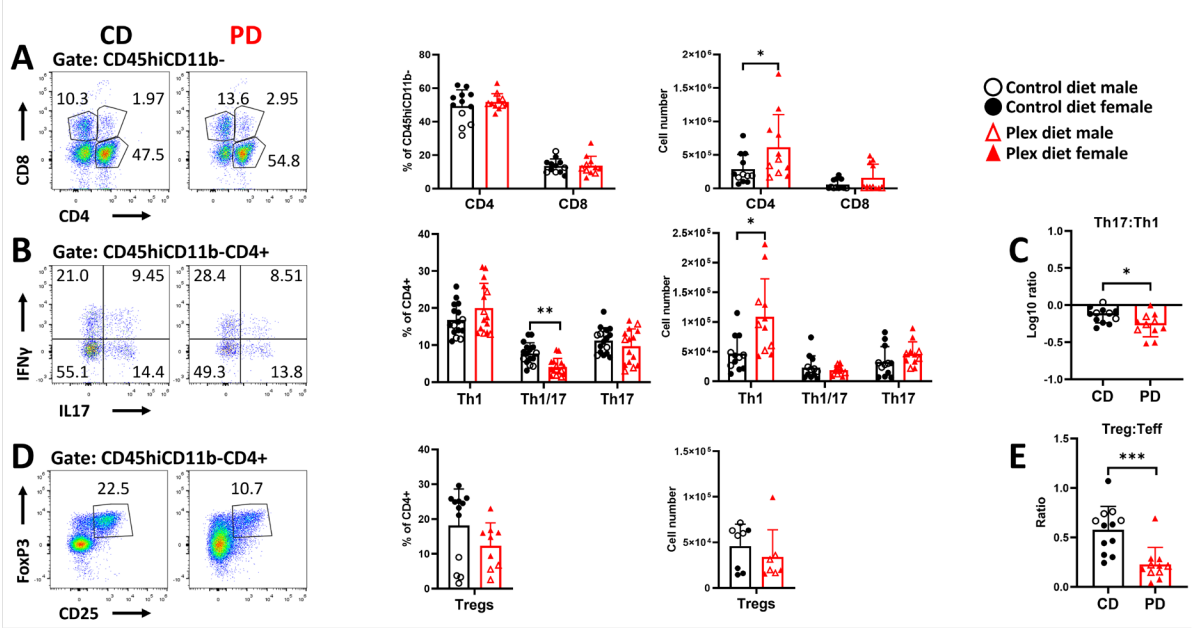

Figure 9: Mild differences in T cell populations persist in the CNS of PD mice during acute EAE.

Single cells isolated from pooled brain and spinal cord tissues were analyzed by flow cytometry during acute EAE. **A** Although there were no differences in the CD4+ and CD8+ T cell frequencies, the numbers of CD4+ T cells were increased in the CNS of PD mice compared to CD. **B** Only numbers of Th1 cells remained elevated during acute EAE within the CNS of PD compared to CD mice. **C** Log10 Th17:Th1 ratios were below 1 for both groups and were significantly lower in the CNS of PD compared to CD mice. **D** There were no differences in the Treg populations between the groups. **E** Treg:Teff ratios were decreased in the CNS of PD compared to CD group.

Representative flow plots are shown. Both male and female mice were employed. Data are shown as means ± SD, n=12; *p<0.05, **p<0.005, ***p<0.0005

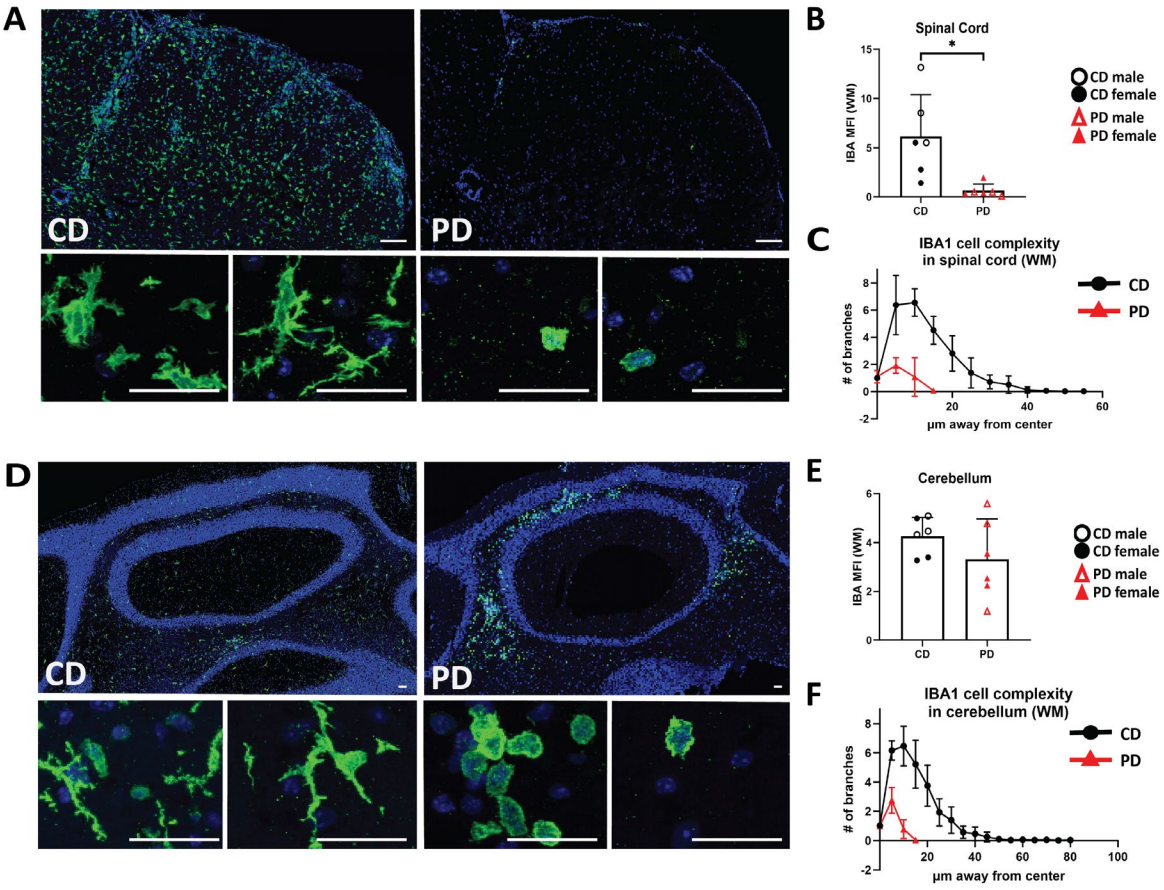

Figure 10: IBA1+ cells in the PD CNS of EAE mice have activated morphology and low complexity.

CNS sections of CD and PD mice isolated during EAE onset were immunostained for IBA1. **A/D** Representative images of IBA1 immunoreactivity in lumbar spinal cords (A) and cerebellar (D) tissues of mice. **B/E.** Quantification of IBA1 MFI of lumbar spinal cord (B) and cerebellar (E) tissues of CD and PD mice. **C/F** Sholl analysis of IBA1+ cells near inflammatory foci shows low complexity and activated morphology in PD mice, but increased complexity in CD mice. (C: spinal cord; F cerebellum).

Scale bars denote 100 µm in whole tissue images and 25 µm in enlarged cellular-level images**.** Data are shown as means ± SD, n=6-7 mice; 2 sections per tissue; 4-8 microglia per section; *p<0.05.

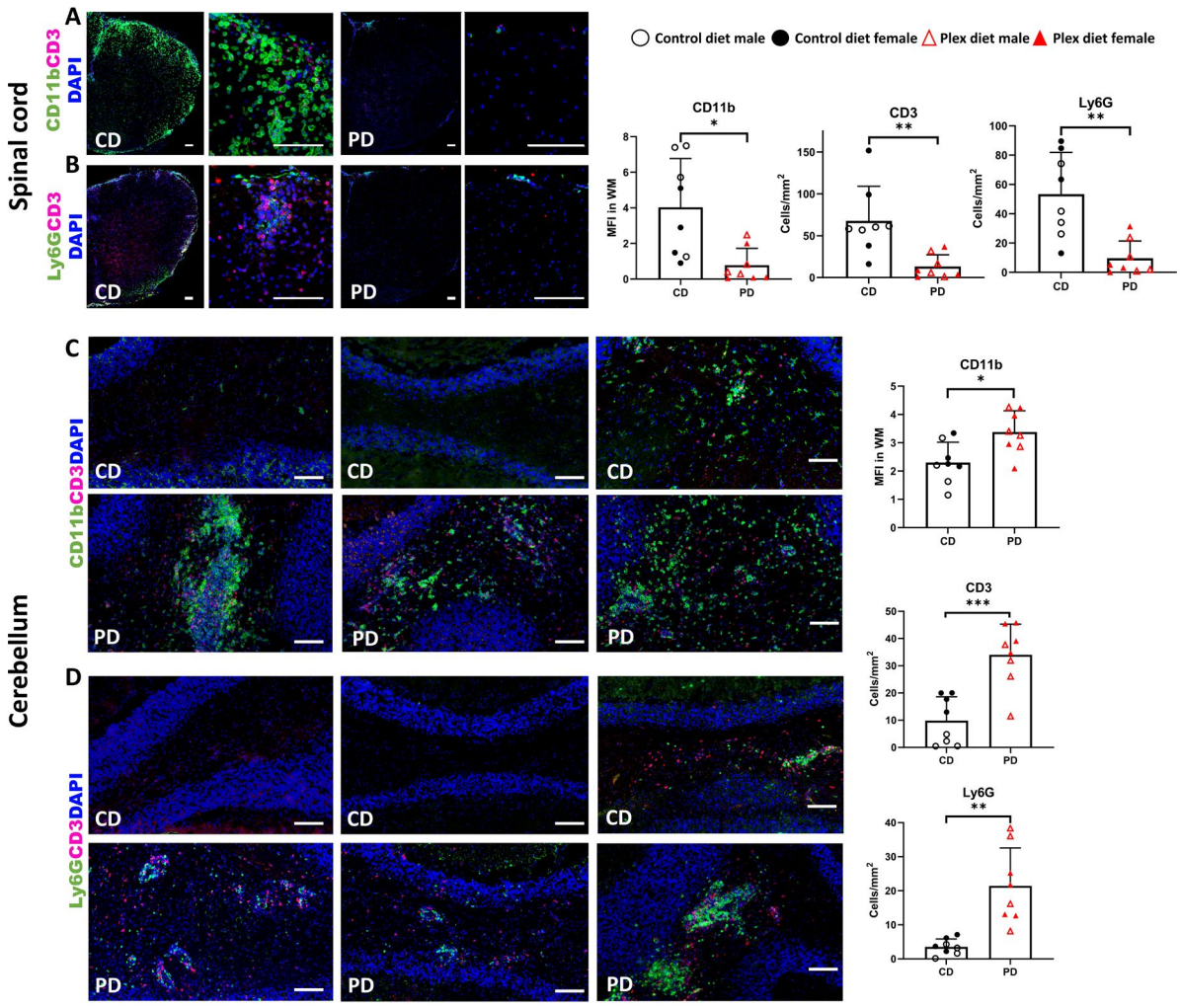

Figure 11: CNS infiltration is prominent in the cerebellum of PD mice during EAE.

Lumbar spinal cords and cerebella were isolated at neurological deficit onset and analyzed via immunohistochemistry for mean fluorescence intensity (MFI) of CD11b (myeloid cells), and for counts of CD3+ T cells, and Ly6G+ neutrophils. **A/B** Spinal cords of CD mice show increased infiltration by myeloid cells, T cells (A), and neutrophils (B), while these cells are sparsely detected in the parenchyma or in the meninges of the PD spinal cords. Quantification is shown in graphs on the right. **C/D** Cerebella of CD mice are only mildly infiltrated by myeloid cells, T cells (C), and neutrophils (D), while these cells are found in large numbers in the cerebellum of PD mice. Quantification is shown in graphs on the right.

Scale bars denote 100 µm. Both male and female mice were employed. Data are shown as means ± SD, n=8; at least 2 sections per tissue; *p<0.05, **p<0.005, ***p<0.0005.

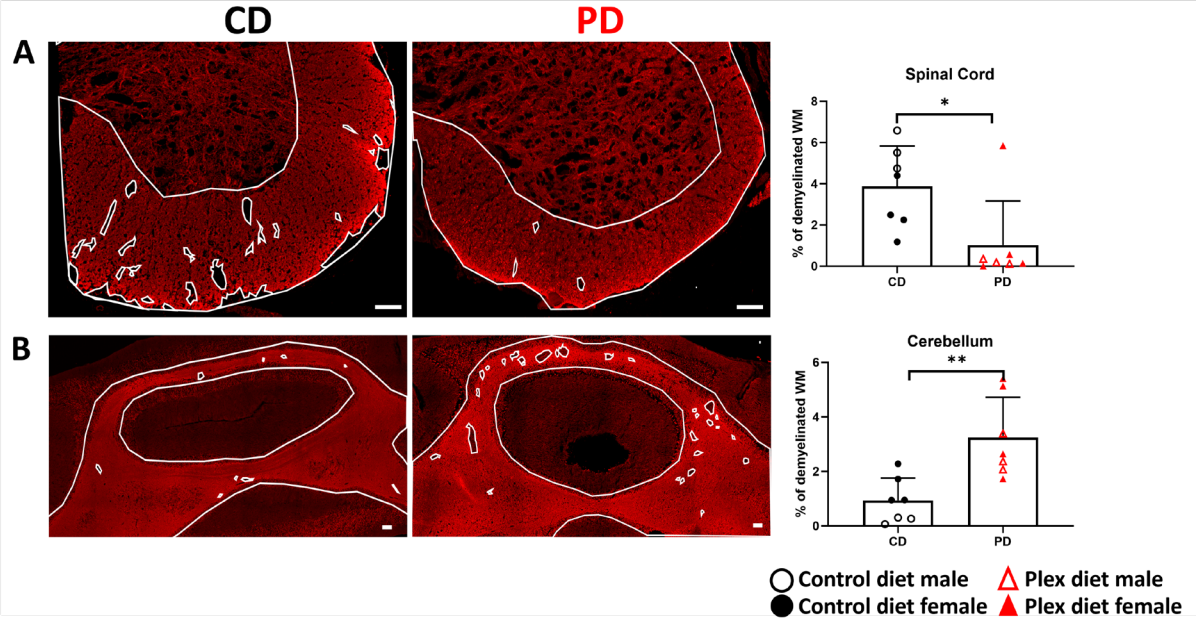

Figure 12: Increased demyelination in the cerebellum and decreased demyelination in the spinal cord of PD mice during EAE onset.

Myelin was detected in lumbar spinal cord and cerebellar tissues isolated from mice during EAE onset via MBP immunostaining. Demyelinated areas (i.e., white matter devoid of MBP immunoreactivity; demarcated with small white borders) are readily detected in the spinal cords of CD but not in the spinal cords of PD (A) and cerebella of PD mice but not cerebella of CD mice (B). Quantification shows percentage of MBP devoid white matter (WM) with all WM area (graphs on the right).

Scale bars denote 100 µm. Data are shown as means ± SD, n=7; at least 2 sections per tissue; *p<0.05, **p<0.005.

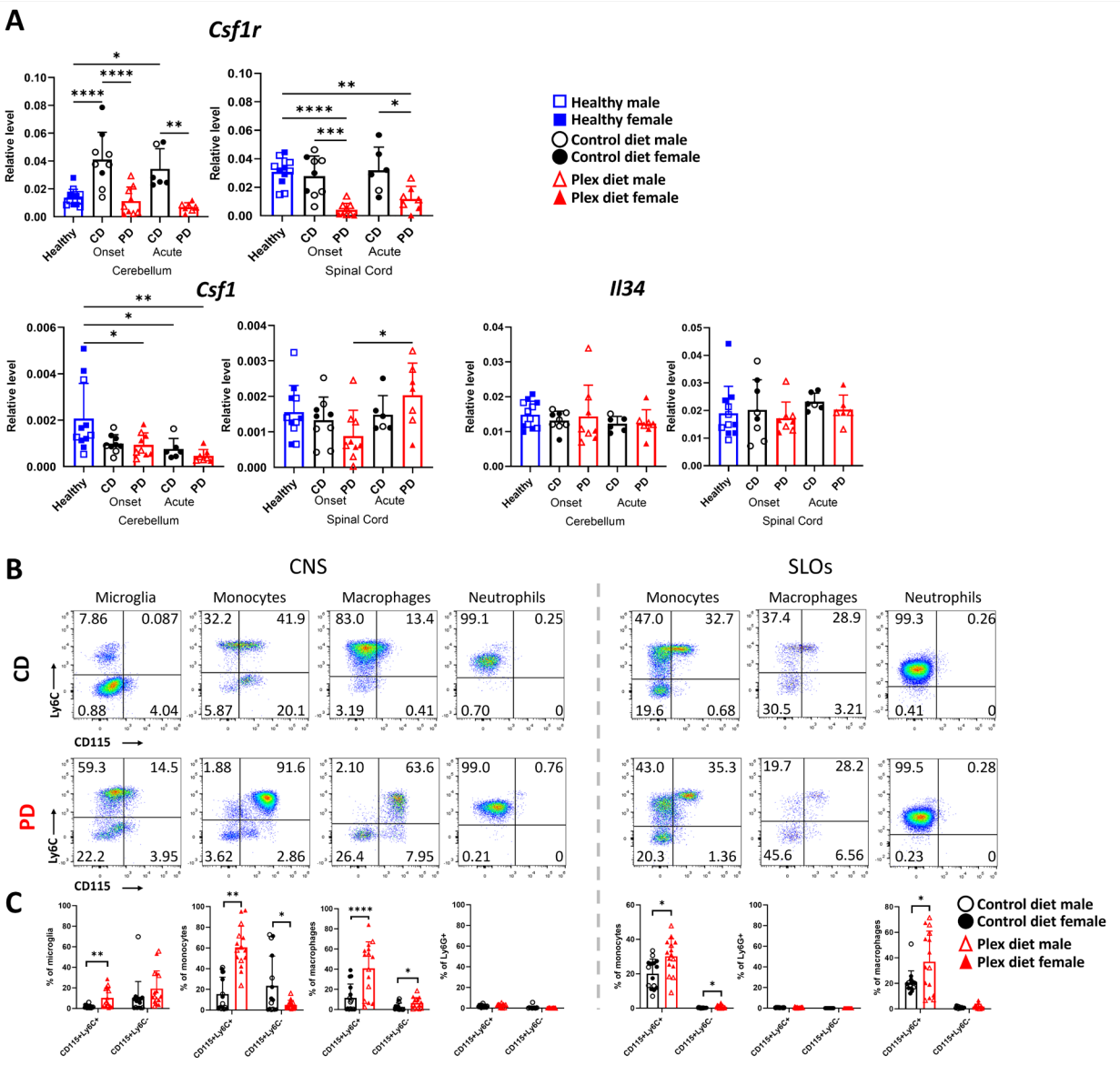

Figure 13: Effect of CSF1R antagonism on the expression of CSF1R and its ligands during EAE.

A *Csf1r* transcript levels are lower in the PD compared to CD CNS during EAE. There were no differences in the transcripts of *Csf1* and *Il34*. **B** CSF1R (CD115) expression was detected using flow cytometry in Ly6C+ and Ly6C- microglia, monocytes, macrophages, and neutrophils in pooled brain and spinal cord (CNS), and SLOs during EAE. **C** Quantification of B.

Data are shown as means ±SD, A: n=9-12; B: n=16 *p<0.05, **p<0.005, ***p<0.0005, ****p<0.00005.

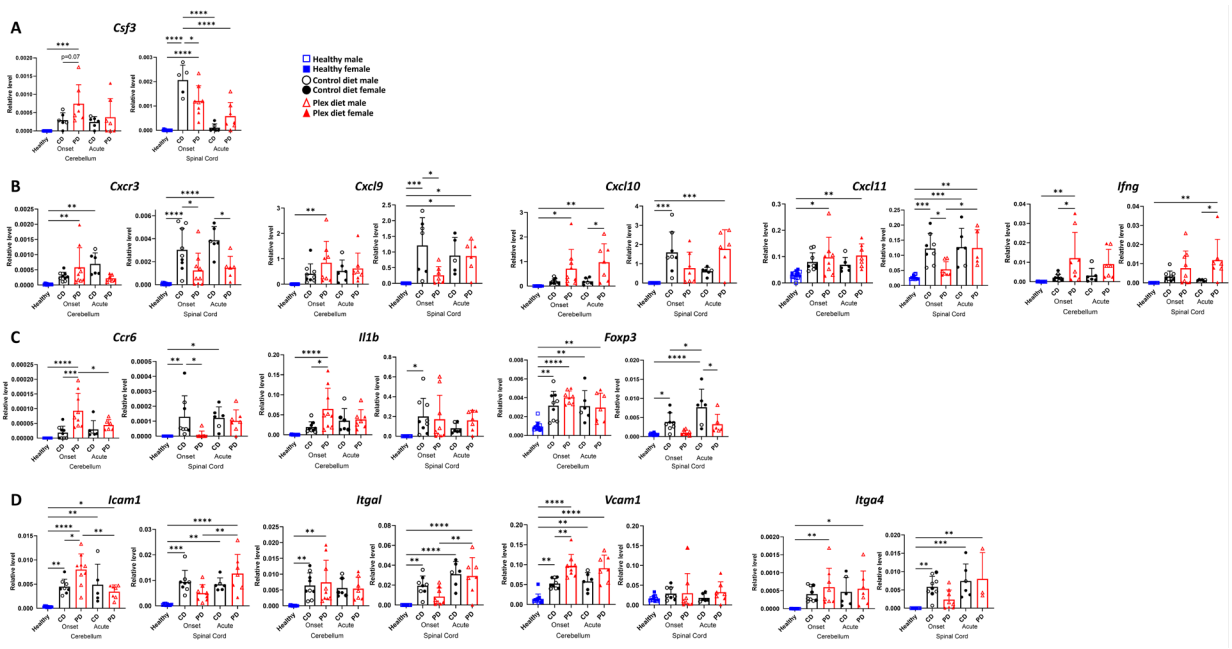

Figure 14: CSF1R antagonism differentially affects gene expression in CNS compartments. A-D Cerebella and spinal cords were isolated from CD and PD mice at onset and acute EAE and RNA transcripts were analyzed by quantitative PCR.

Data are shown as means ±SD, n=6-12; *p<0.05, **p<0.005, ***p<0.0005, ****p<0.00005.

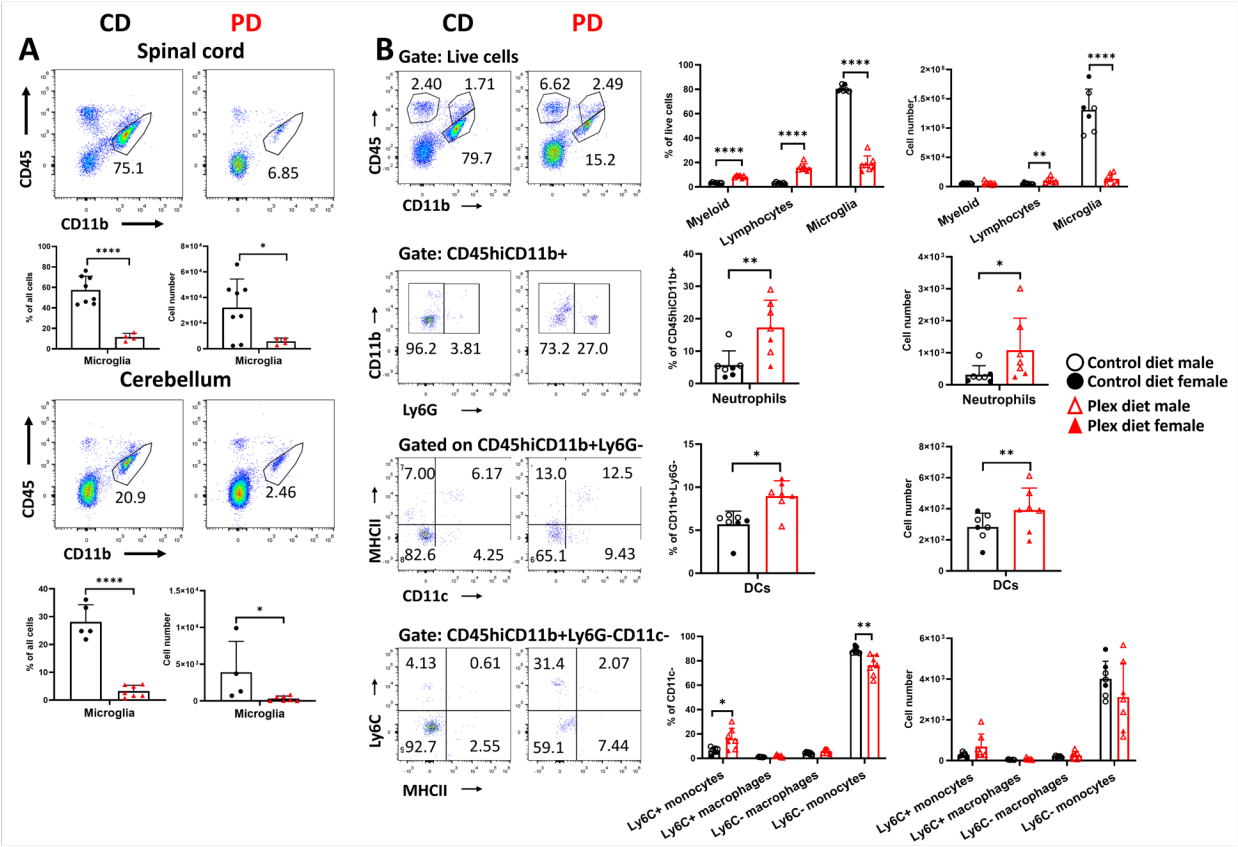

Additional file 1: Effect of CSF1R antagonism on CNS immune cell populations in steady state.

A Microglia are depleted efficiently in the PD spinal cord and cerebellum. **B** Effect of PD on microglia and CNS-associated myeloid cells and lymphocytes in whole CNS tissues (pooled brain and spinal cord per mouse) in PD and CD steady state mice. Data are shown as means ± SD, n=7; *p<0.05, **p<0.005, ***p<0.0005.

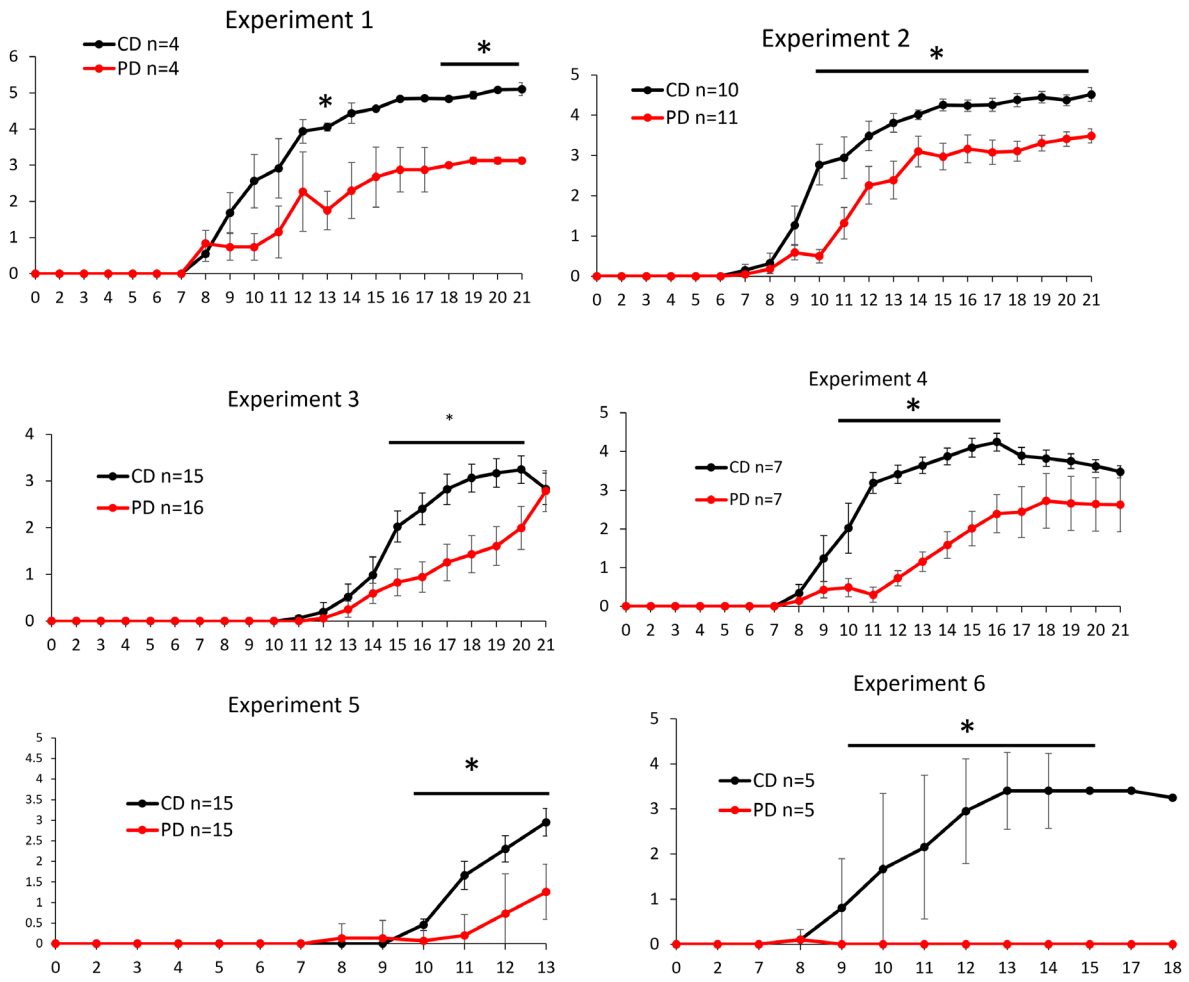

Additional file 2: Clinical EAE course of individual experiments.

Mice were placed in CD or PD diets seven days before EAE induction and maintained in their respective diets up to the end of the experiment. Mice were scored daily for neurological deficits. All experiments except experiment 6 were averaged to generate the clinical score graph in Figure 3.

Data are shown as means ±SEM, n values are displayed within each chart; *p<0.05.

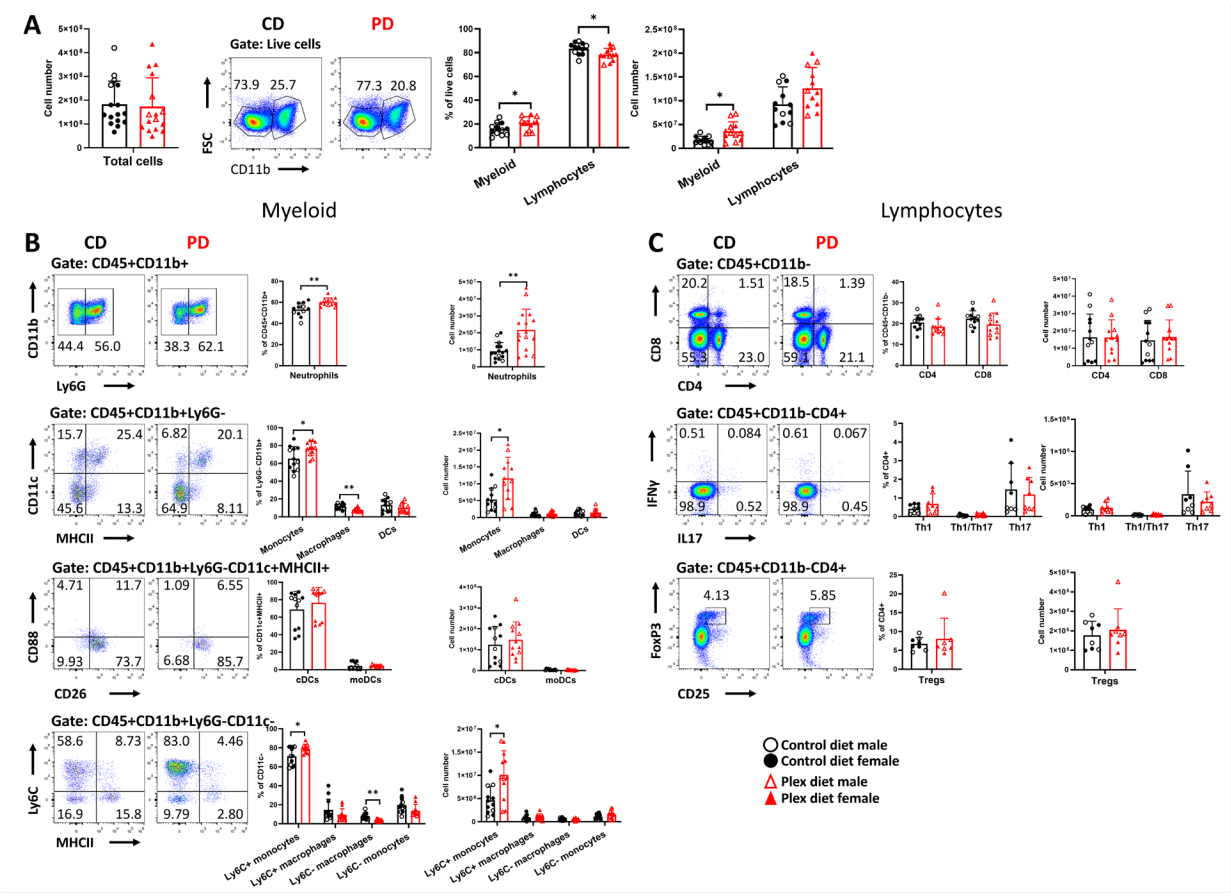

Additional file 3: Increased neutrophils and inflammatory monocytes persist in the SLOs of PD mice during acute EAE.

A-C Single cell suspensions of pooled spleen and draining lymph nodes were analyzed for myeloid (B) or lymphocytic populations (C) during acute EAE. Both frequencies and numbers of neutrophils and Ly6C+ monocytes were elevated in the SLOs of PD compared to CD mice. No other differences were detected. Data are shown as means ±SD, n=12; *p<0.05, **p<0.005.

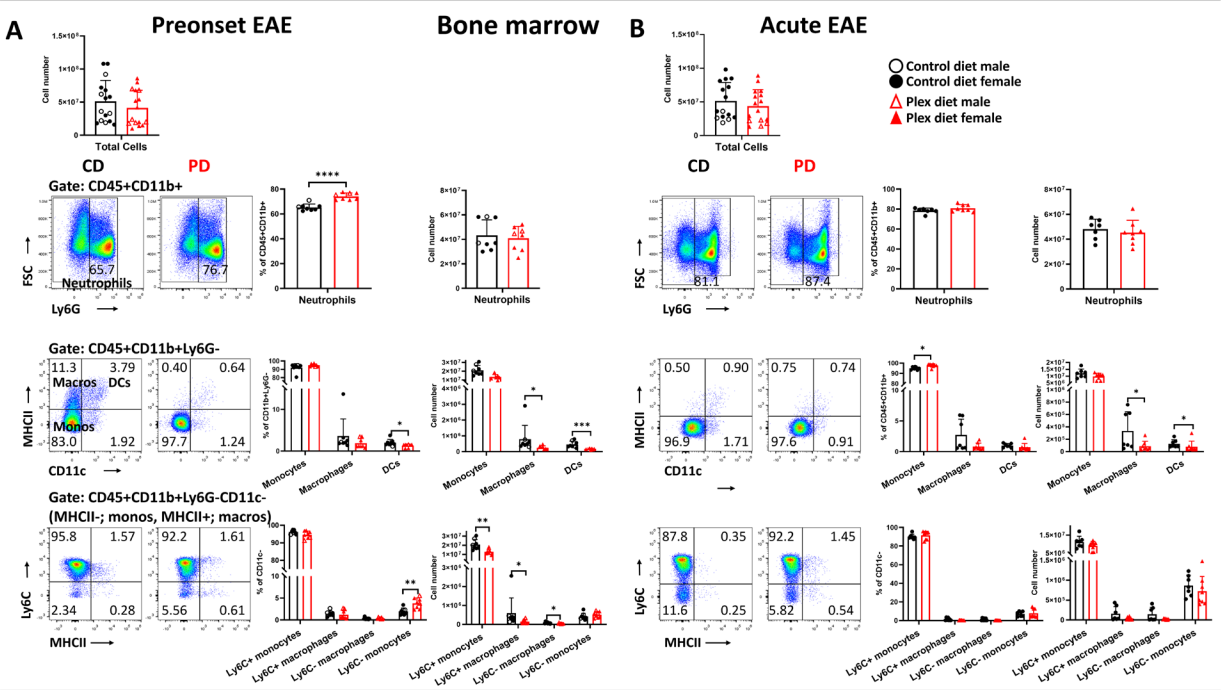

Additional file 4: CSF1R antagonism affects cellular composition in the bone marrow during EAE.

Flow cytometric analysis of the bone marrow myeloid cell subsets in PD and CD mice before clinical symptoms (A) and during acute EAE (B).

Data are shown as means ±SD, n=8; *p<0.05, **p<0.005, ***p<0.0005, ****p<0.00005.

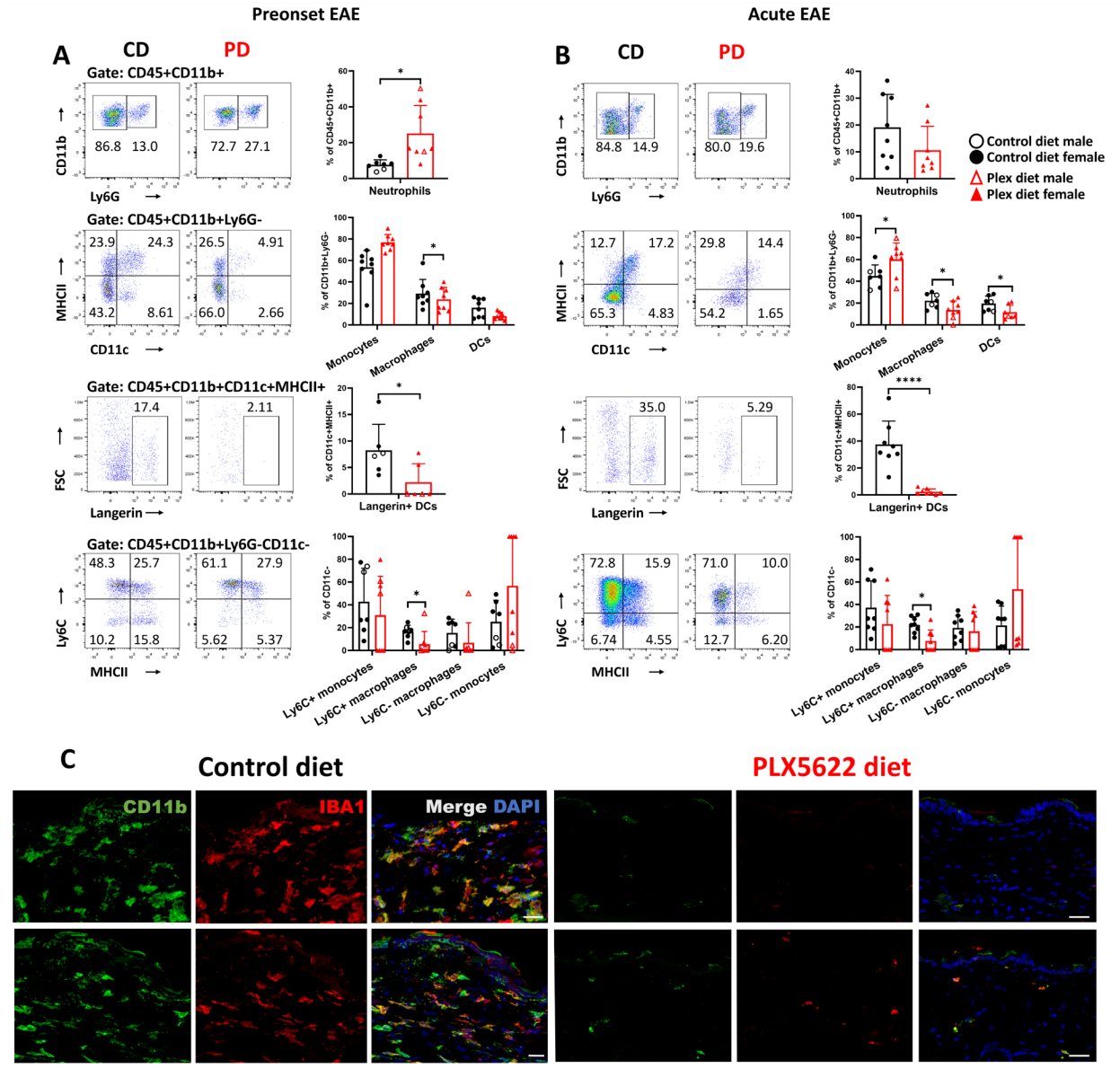

Additional file 5: CSF1R antagonism depletes antigen presenting cells and other myeloid subsets in the skin during EAE.

A Flow cytometric analysis of skin myeloid cell subsets in PD and CD mice before clinical symptoms (preonset) and **B** during acute EAE show that langerin+ DCs are dramatically reduced in PD mice. **C** Immunohistological analysis showed that CD11b+ cells and IBA1+ cells, which are all myeloid cells and macrophages, respectively, are reduced in the skin of PD compared to CD mice.

Scale bars denote 25µm. Data are shown as means ±SD, n=8, *p<0.05, ****p<0.00005

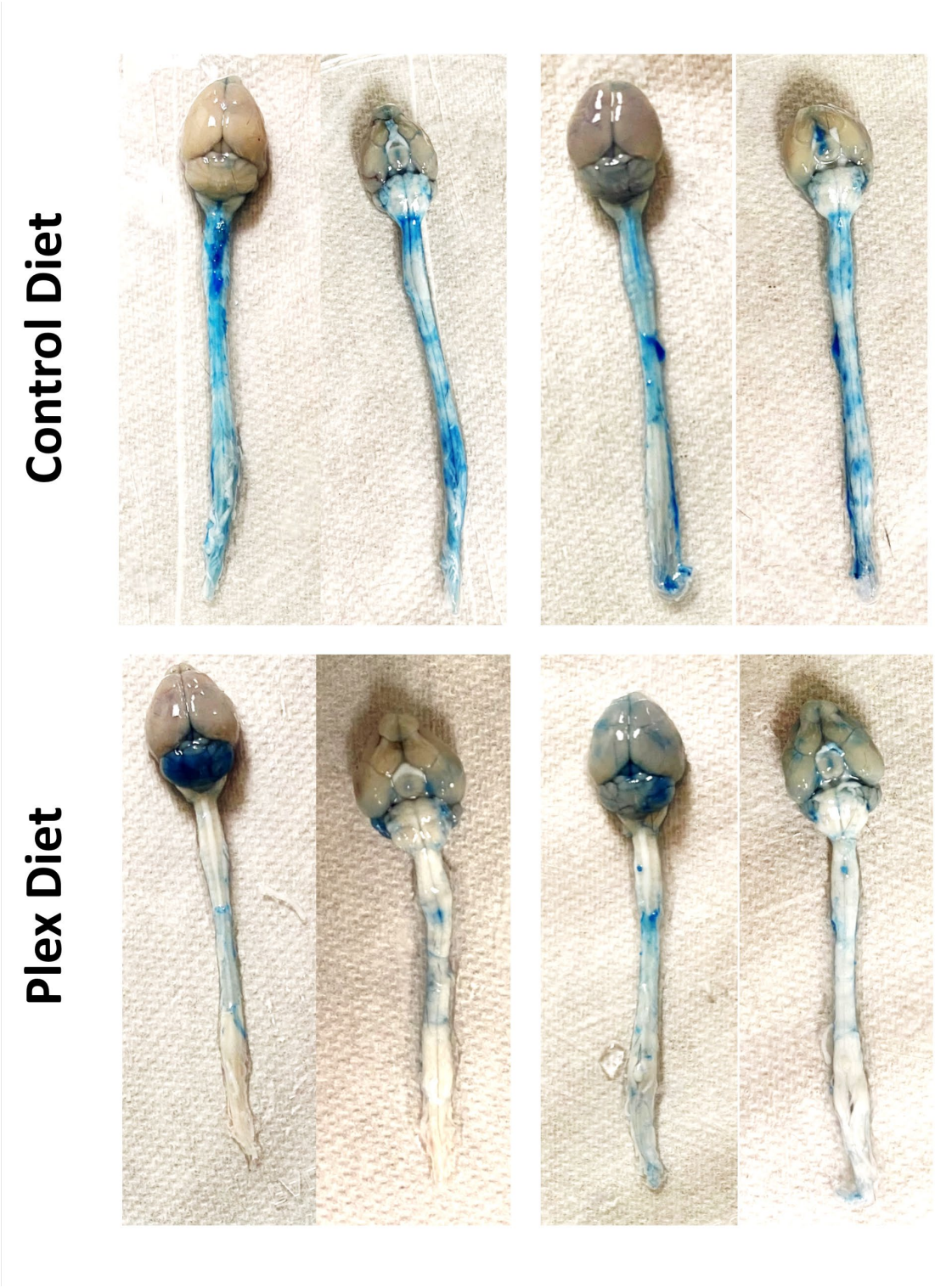

Additional file 6. Mapping areas of CNS infiltration using Evans blue dye.

Evans blue dye was injected intravenously into CD and PD mice with EAE**.** Ninety minutes later, mice were euthanized, and tissue was isolated. Dorsal and ventral images were acquired on day 13 EAE (onset) in CD and PD mice.

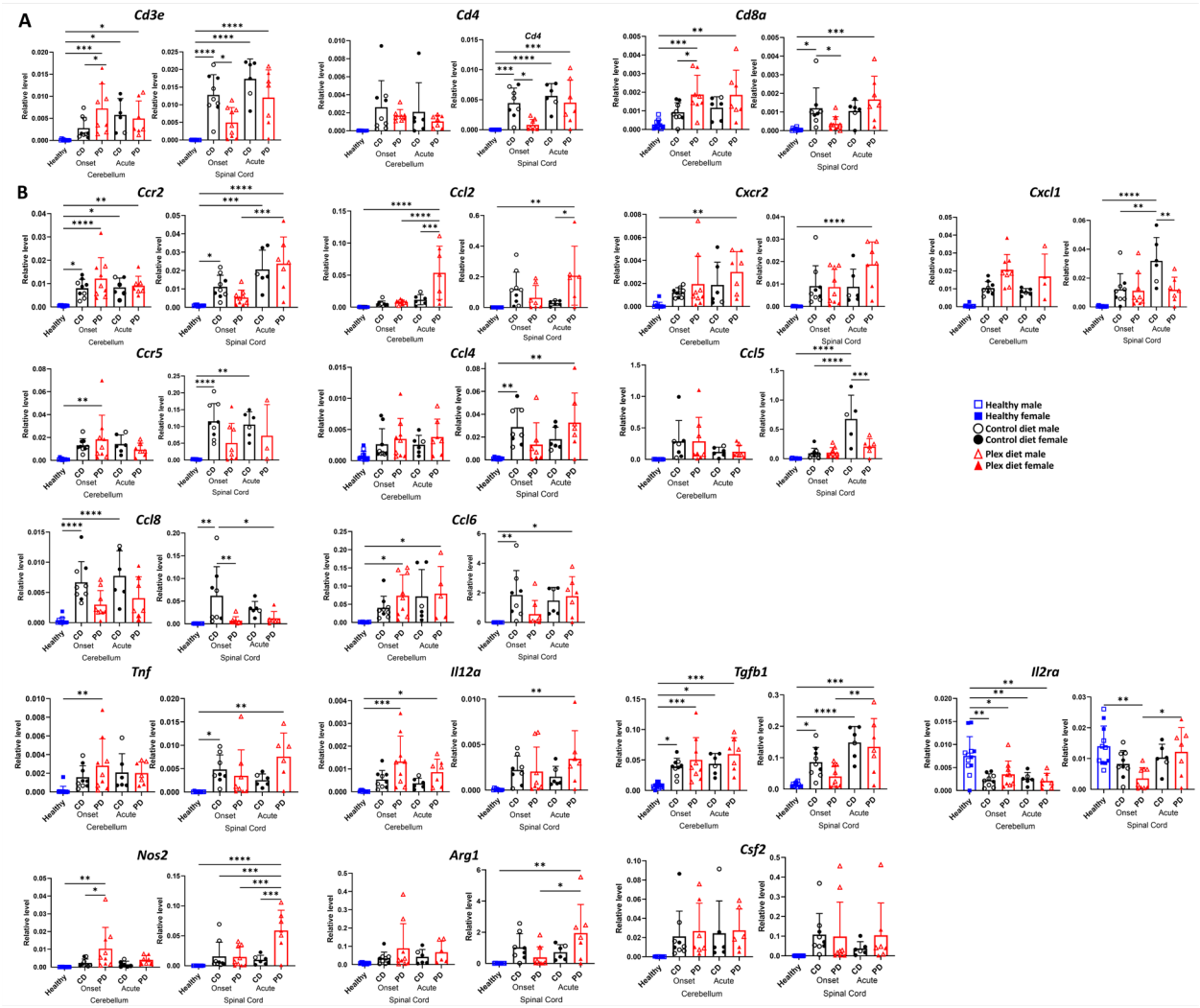

Additional file 7: RNA transcript levels in the CNS compartments of CD and PD mice during EAE.

Cerebella and spinal cords were isolated from CD and PD mice during steady state, and clinical onset and acute EAE. RNA transcripts were measured using qPCR analysis.

Data are shown as means ±SD, n= 6-12; *p<0.05, **p<0.005, ***p<0.0005, ****p<0.00005.

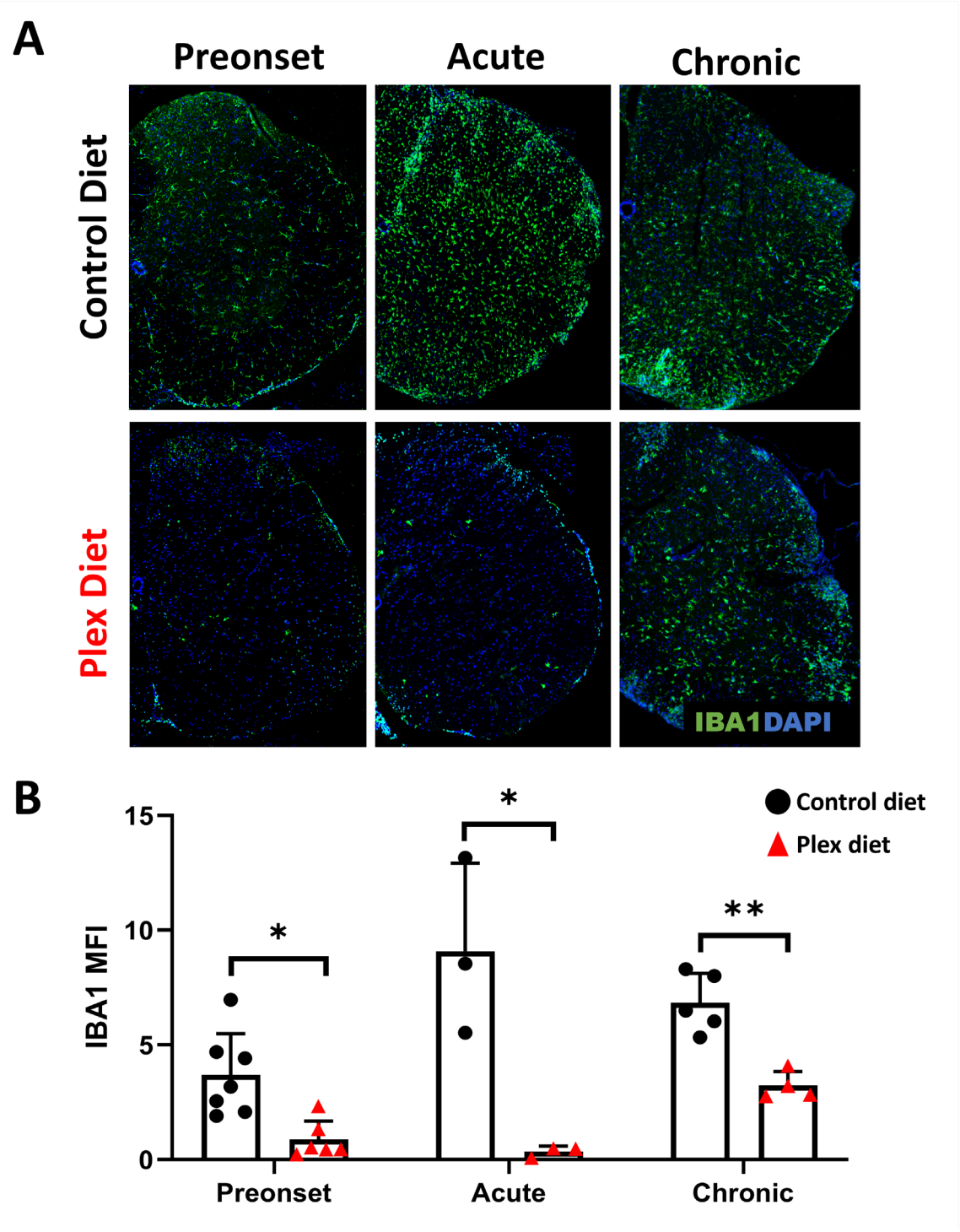

Additional file 8. Repopulation of lumbar spinal cords of PD mice by microglia during chronic EAE.

A Spinal cord of CD and PD mice were isolated during different stages of EAE and immunostained with IBA1**. B** quantification of **(A)** shows IBA1 MFI increases over time in the PD spinal cord. These mice were still maintained in PLX5622 diet. It is unclear whether these are cells that originate from a local progenitor or an infiltrating monocytic cell.

Table 1: Antibodies used for flow cytometric analysis.

Target	Clone	Manufacturer	Cat. number
CD4	RM4-5	BD	558107
CD8	53-6.7	BD	553031
CD11b	M1/70	Biolegend	191241
CD11b	M1/70	Invitrogen	48-0112-82
CD11b	M1/70	BD	552850
CD11c	HL3	Biolegend	550261
CD11c	HL3	BD	561241
CD11c	N418	Biolegend	117305
CD25	PC61.5	Invitrogen	17-0251-82
CD26	DPP-4	Biolegend	137803
CD45	RA3-6B2	Invitrogen	11-0452-82
CD45	30-F11	Biolegend	103130
CD88	20/70	Biolegend	135807
CD115	AFS98	Biolegend	135513
CD115	T38-320	BD	565249
FoxP3	FJK-15s	Invitrogen	12-5773-82
IFNγ	XMG1.2	BD	554413

IL17	TC11-18H10	BD	559502
Langerin	4C7	Biolegend	144206
Ly6C	HK1.4	Biolegend	128033
Ly6G	1A8	BD	551460
Ly6G	1A8	BD	560601
MHCII	M5/114.15.2	Biolegend	107652

Table 2: List of primers used in the study.

Gene name	NCBI Gene ID	Cat. number/ primer sequence (Fwd:Rev)	
Hsp90	NM_015516	QT01039864	
Csf1r	NM_007779	QT01055810	
Csf2	NM_009969	QT00251286	
Csf3	NM_009971	QT00105140	
Il34	NM_029646	QT00198142	
Csf1	NM_007778	QT01164324	
Il1beta	NM_008361	QT01048355	
Ifng	NM_008337	QT01038821	
Il17a	NM_010552	QT00103278	
Tnf	NM_013693	QT00104006	
Il2ra	NM_008367	QT00101108	
Il12a	NM_008351	QT01048334	
Tgfb1	NM_011577	QT00145250	
Nos2	NM_010927	CAGCTGGGCTGTACAAACCTT	CATTGGAAGTGAAGCGTTTCG

Arg1	NM_007482	QT00134288	
Foxp3	NM_054039	AGGAGCCGCAAGCTAAAAGC	TGCCTTCGTGCCCACTGT
Rorgc	NM_011281	CCGCTGAGAGGGCTTCAC	TGCAGGAGTAGGCCACATTACA
Ccr2	NM_009915	ATCCACGGCATACTATCAACATC	CAAGGCTCACCATCATCGTAG
Ccr5	NM_009917	GTCAGAACGGTCAACTTTGGG	GCCCAGAGTGATACAGATGTCAA
Ccr6	NM_009835	TCGTCCAGGCAACCAAATCCT	TCAGAGAACTTCCAGGTGAAGA
Cd3e	NM_007648.5	TGCCTCAGAAGCATGATAAGC	AAATGGACGCCGAACTTGGT
Cd4	NM_013488.3	TCCTAGCTGTCACTCAAGGGA	GTGTGGAAAATGAGGACTGCAT
Cd8a	NM_001081110.2	CCACGTTATCTTGTTGTGGGATG	GGGCTTGAGATGATGATGGAGA
Cxcr2	NM_009909	ATGCCCTCTATTCTGCCAGAT	GTGCTCCGGTTGTATAAGATGAC
Cxcr3	NM_009910	TATGGGGAAAACGAGAGCGAC	GCGCTGACTCAGTAGCACAG
Ccl2	NM_011333	QT00167832	
Ccl4	NM_013652	TTCCTGCTGTTTCTCTTACACCT	CTGTCTGCCTCTTTTGGTCAG
Ccl6	NM_009139	GCTGGCCTCATACAAGAAATGG	GCTTAGGCACCTCTGAACTCTC
Ccl8	NM_021443	TCTACGCAGTGCTTCTTTGCC	AAGGGGGATCTTCAGCTTTAGTA
Ccl20	NM_016960	QT02326394	
Cxcl1	NM_008176	CTGGGATTCACCTCAAGAACATC	CAGGGTCAAGGCAAGCCTC
Cxcl9	NM_008599	TCCTTTTGGGCATCATCTTCC	TTTGTAGTGGATCGTGCCTCG
Cxcl10	NM_021274	QT00093436	
Cxcl11	NM_011330	GAATCACCAACAACAGATGCAC	ATCCTGGACCCACTTCTTCTT
Vcam1	NM_011693	QT00128793	
Itga4	NM_010576	QT00121044	
Icam1	NM_010493	QT00155078	

Itgal	NM_001253874	QT01744085	

Chapter 3:

Microglia promotes oligodendrocyte differentiation through 5-Lipoxygenase

Marilyn Wang, Athena Soulika (other authors/author order TBD)

To be submitted to *Glia*

3.1 Introduction

Microglia promotes oligodendrocyte differentiation through 5-Lipoxygenase

5 lipoxygenase (5LO) is the rate limiting enzyme in the synthesis of leukotrienes (LT), which consists of LTB4, and the cysteinyl leukotrienes, or the cysLTs LTC4, LTD4, and LTE4 (See Figure 1A) [1]. Leukotrienes are mostly considered as pro-inflammatory mediators during inflammatory conditions [1]. In homeostasis, 5LO is the highest expressed in the respiratory system, bone marrow, and the skin, compartments in which the mucosal immune system is active [2]. 5LO function in the respiratory system is well studied [3], but its role in other organs is relatively unknown.

In the intact CNS, 5LO is also expressed in detectable levels [2]. However, the cellular source of 5LO is unknown. Previous studies report that 5LO appears to be expressed in neurons by Lammers at al. in mRNA [4], in microglia by Uhlen et al in the Human Protein Atlas [2] and by Zhang et al in the Brain RNAseq database [5]. Furthermore, leukotrienes signal through various receptors. The cysLTs signal through cysLT receptor 1 and 2, and LTB4 via BLT1 receptor [6]. From the Brain RNAseq single cell database from Zhang et al, cysLT receptor 1 has been detected on microglia and oligodendrocyte progenitor cells (OPCs), cysLT receptor 2 reported on endothelial cells, and BLT1 on microglia [5]. Although still controversial, LTD4 has also been shown to signal through GPR17 [7, 8], which is detected on oligodendrocytes [9].

Oligodendrocytes are the myelin-producing and trophically-supporting glia of the CNS. They proliferate as oligodendrocyte progenitor cells (OPCs), and then differentiate into immature (IM), mature, and then mature myelinating oligodendrocytes (MO) [10]. OLC differentiation begins during the late embryonic stages, and peaks during developmental myelination at postnatal day 14-28 in the corpus callosum [10]. Following this, differentiation continues but at slower rates at 8 months postnatally in mice [10]. Although adult mice and humans are 99% myelinated, oligodendrocyte differentiation still persists in adulthood [10]. This has been proposed to be either to replace dying OLCs, or to myelinate new axon

segments [11]. Hence, OLCs are the most dynamic glia in the intact CNS, and the many mechanisms that regulate OLC differentiation remain unknown.

OLCs engage in cross-talk with microglia as well; OLCs can downregulate microglial activity through immune inhibitory molecules [12]. Conversely, CSF1R knockout mice, which have essentially no microglia, display a ~50% decrease in mature oligodendrocytes in the cortex at p21 [13]. Importantly, microglia have been shown to be instrumental in regulating OLC differentiation through secreted factors. Although some factors have been suggested to play a role, such as IGF-1 [14] and CX3CL1 [15], much work still remains to identify these factors which promote OLC differentiation. Minocycline-mediated inhibition of microglial activation decreased oligodendrocyte differentiation in the SVZ during early postnatal development [16], and when OLCs are co-cultured with microglia [17] or cultured in microglia conditioned media [18], OLCs differentiate at a greater rate.

In this study, we characterize the expression and activity of 5LO and the expression of 5LO pathway components in the homeostatic CNS. We show a new mechanism in which cysLTs regulate OL differentiation, and propose that this mechanism is predominately mediated by microglia.

3.2 Materials and Methods

Animals

C57BL/6 mice were obtained from Jackson Laboratory, and *Alox5*$^{-/-}$ and *Alox5*$^{+/+}$ littermate control mice were made by the Soulika Laboratory. CX3CR1-CreERT2 mice were obtained from Jackson Laboratory, and bred to *Alox5* fl/fl mice made by the Soulika Laboratory. All mice were maintained by the Mouse Biology Program at University of California, Davis. Animal procedures were approved by the Institutional Animal Care and Use Committee of UC Davis. Animals were age- and sex-matched for each experiment.

Isolation of primary murine OPCs

Anesthetized P1-P6 rat pups were euthanized by decapitation, and cortexes were isolated. Tissue was minced, dissociated using papain (Worthington) at 37°C, and passed through a 100 µm filter. Mixed glia was plated in N1 media (5 µg/ml insulin, 50 µg/ml transferrin, 100 µM Putrescine, 30 nM sodium selenite, 20 nM P4 in DMEM high glucose media) on poly-D-lysine-coated T75 flasks (2-3 pups per plate). Supernatant was changed every 2 days.

After 100% confluency is reached, T flasks were secured on a shaking platform, and shaken at 200rpm. After 2 hours, the supernatant was discarded and the flask bottom was washed with HBSS (+) (Gibco). Fresh N1 media is placed back onto the cells, and shaking is resumed. Shaking continues for 16 hours, and then supernatant is collected, counted, and plated at 30% confluency in poly-D-lysine-coated T75 flasks.

Leukotriene differentiation assay

OPCs are proliferated in complete growth media (10 ng/mL biotin, 30% B104 conditioned media, 1% penicillin streptomycin, 5 ng/mL FGF2, 5 µM Forskolin, 1% Glutamax in N1 media) in 24 well culture plates with poly-d-lysine coated circular cover slips until they are ~70% confluent, and then the supernatant is changed to differentiation media (12.5 µg/ml insulin, 50 µg/ml Transferrin, 100 µM Putrescine, 24 nM sodium selenite, 10 nM progesterone, 10 ng/mL biotin, 30 ng/mL 3',5-Triiodo-L-thyronine sodium salt, 40 ng/ml L-Thyroxine sodium salt pentahydrate, 1% Glutamax, 1% penicillin streptomycin, in DMEM/F12 media) with vehicle, LTB4, LTC4, LTD4, or LTE4 (Cayman Chemical).

Coverslips were stained with primary antibodies against surface antigen O4 (Miltenyi Biotec) in 150 µl of their culture media in their culture wells, and incubated at 37°C for 30 minutes. Media was moved, and washed in their wells with HBSS(+) (Gibco). HBSS(+) was removed, and cover slips were incubated with 4% PFA in their culture wells for 15 minutes at room temperature. Following fixation, cells were permeabilized with 250 µl of pre-chilled 100% methanol at -20°C for 15 minutes. Coverslips were then collected with forceps and washed in PBS three times. CC1 (Cal BioChem) and Sox10 (Abcam) antibodies

in 10% Donkey serum was added directly onto coverslips, and incubated for 30 minutes at room temperature. Following three PBS washes, secondary antibodies at 1:100 in 10% Donkey serum was incubated on coverslips for 30 minutes at room temperature. Following three PBS washes, DAPI (Cell Signaling Technologies) was counterstained, coverslips were washed, and coverslips were mounted using Fluoromount-G (Electron Microscopy Services) onto slides. Images were taken with Nikon C2 confocal microscope.

Fate mapping studies using BrdU

5-Bromo-2'-deoxyuridine was injected intraperitoneally once daily on 5 consecutive days at 50 µg/g body weight. At the time of tissue collection, mice were anesthetized using ketamine/xylazine, exsanguinated using ice-cold PBS, and brain and spinal cord tissues were isolated. After 4% PFA overnight post-fix, tissues were desiccated in 30% sucrose for 3 days, frozen in OCT, and 10 µm cryosections were collected. Cryosections were immunostained with CC1 (CalBiochem), BrdU (Abcam), Sox10 (Abcam), counterstained with DAPI. Cells were enumerated using Imaris version 9.2.0 (Oxford Instruments).

Microglial 5LO depletion

To deplete microglia, 1200 mg/kg PLX5622 (Plexxikon, Inc) was formulated into AIN-76A diet by Research Diets, Inc. PLX5622 diet and AIN76A control diet were fed to mice ad libitum.

To induce CX3CR1-Cre-ERT2 activity, 10 mg/ml tamoxifen formulated in sunflower seed oil was injected at 0.075mg/g body weight IP once daily for 5 consecutive days.

Fluorescence-activated cell sorting (FACS)

Ketamine/xylazine-anesthetized mice were exsanguinated using ice-cold PBS, and brain and spinal cord tissues were isolated, and a small piece of spinal cord tissue was collected for qPCR analysis. The rest of the CNS tissue was minced, enzymatically dissociated using papain (Worthington) at 37°C, and passed

through a 100 µm filter. After myelin removal using a 37% Percoll (GE Healthcare) gradient, single cell suspensions were immunolabeled using CD11b (Biolegend) and CD45 (Biolegend) antibodies. Following washes, cells were pushed through filter-top FACS tubes. Cells were sorted on a FACS Aria (BD Biosciences), pelleted, and lysed using RLT buffer (Qiagen). Lysis was stored at -80°C until ready for RNA purification.

RNA purification, and Quantitative Polymerase Chain Reaction (qPCR)

Ketamine/xylazine-anesthetized mice were exsanguinated using ice-cold PBS. Whole CNS or microdissected brain and spinal cord tissues were stored in RNA later (ThermoFisher Scientific). Tissue was homogenized in Qiazol (Qiagen), and RNA was extracted using phenol chloroform extraction. RNA was purified using the RNeasy mini kit (Qiagen) according to manufacturer's instructions. FACS-sorted cell lysates were homogenized using a QiaShredder spin column (Qiagen) and RNA was purified using the RNeasy mini kit (Qiagen) according to manufacturer's instructions. cDNA was synthesized using the Quantitect Reverse Transcription Kit (Qiagen). cDNA was combined with primers and SYBR Green Master Mix (Qiagen), and analyzed using the AriaMX real-time PCR system (Agilent).

Statistical analysis

Comparisons between means of two groups were analyzed using student's T test. Comparisons between means of more than two were analyzed using ANOVA. Data were significant if $p>0.05$. When appropriate, data were log-transformed.

3.3 Results

5 Lipoxygenase (5LO) and the 5LO pathway are expressed and active in development and adulthood

5 Lipoxygenase (5LO) is involved in the synthesis of short-lived lipid mediators, eicosanoids, all of which originate from the breakdown of nuclear membrane phospholipids by cyclic phospholipase 2 (cPLA2). Of these pathways, 5LO is most crucial for the synthesis of leukotrienes (within black box; Figure 1A). 5LO

(gene *Alox5*) and important mediators in the leukotriene pathway, 5LO-activating protein (FLAP; gene *Alox5ap*) and cytosolic phospholipase A2 (cPLA2; gene *Pla2ga2*), are detected both in the spinal cord (Figure 1B) and brain (Figure 1C), many of them peaking during developmental myelination. Leukotrienes are detected at p14, and many are increased in adulthood (Figure 1D).

To determine if 5LO, and LTAH and LTC4S (enzymes which synthesize LTB4 and the cysLTs, respectively) and LT receptors are specifically expressed in any compartment of the CNS during healthy conditions, WT mouse CNS was microdissected into cortex (Ctx), corpus callosum (CC), cerebellum (Cb), and spinal cord (SC). 5LO (encoded by *Alox5*) transcript was highest in the spinal cord (Figure 1E). Interestingly, statistically significantly higher *Alox5* transcript was detected in females compared to males in the spinal cord (Figure 1F). LTAH (*Lta4h*) and LTC4S (*Ltc4s*) were both detected in the CNS (Figure 1G). LTB4 receptor BLT1 (*Ltb4r1*) transcript was detected at very low levels in the CNS, and there were no differences between CNS compartments in expression (Figure 1H), while BLT2 was not detected in the CNS (data not shown). CysLT receptors cysLTR1 (*Cyslt1*) transcript was highest in the cortex, while cysLTR2 (*Cysltr2)* was expressed at lower levels but ubiquitously throughout all compartments (Figure 1I), and GPR17 was expressed highest in the CC (Figure 1J).

Increased BrdU+ cells in 5LO knockout mice are oligodendrocytes

As 5LO has been shown to promote proliferation and differentiation of many cell types in the periphery [19-24], we employed *in vivo* BrdU fate mapping studies to determine if 5LO promotes proliferation and/or differentiation in the CNS as well. We combine fate mapping studies and our in-house made 5LO global knockout, *Alox5*$^{-/-}$. First, *Alox5* was indeed knocked out in *Alox5*$^{-/-}$ mice (Figure 3A). To follow CNS cells over time, BrdU was injected IP daily on 5 consecutive days beginning from the initiation of developmental myelination at postnatal day 14 (p14) into *Alox5*$^{-/-}$ mice and WT littermate controls. CNS regions were analyzed in 16 week old mice (schema in Figure 3B), when we detected that a majority of

BrdU+ cells co-localized with Sox10. Due to the high concentrations of white matter and oligodendrocytes in the corpus callosa (CC), we analyzed for BrdU, Sox10, and CC1 immunolabeling primarily in the CC (Figure 3C). Images in Figure 3C are quantified in Figure 3D; in *Alox5*$^{-/-}$ mice, BrdU, Sox10+BrdU+, and Sox10+CC1+BrdU+ populations were increased. This trend was significant in males and in all mice, approaching significance in females, and significant when sexes were combined (Figure 3D).

CysLTs promote OL differentiation

Due to the differences in labeled mature oligodendrocytes identified in the *Alox5*$^{-/-}$ mouse, we assessed the direct effect of LTs on oligodendrocyte development. In our *in vitro* model for oligodendrocyte differentiation, we isolated mixed glia from neonatal rat pups, purified OPCs from these cultures, proliferated them in growth media (GM), and differentiated them in differentiation media (DM). In our model, after two days in DM, OLCs are predominately IM (identified by markers Sox10 and O4). Following this, O4 levels decrease, while MBP levels increase as OLCs become more mature [25].

Incubation of OPCs with individual LTs added to differentiation media was initiated on day 0 (Schema in Figure 2A). On day 2, vehicle and cultures with LTs added were analyzed for Sox10, MBP, and O4 immunocytochemically; representative images for vehicle and the LTD4 condition are shown (Figure 2B; zoomed in images on the bottom). O4+MBP- (IM), O4+MBP+ (late IM), O4-MBP+ (MO) cells were quantified as a percentage of Sox10+ cells. None of the LTs affected the frequencies of the O4+MBP- (IM) population. Addition of all cysLTs increased frequencies of O4+MBP+ cells, but only addition of LTD4 increased the frequency of the most mature OL subset, O4-MBP+ cells (Figure 2C), on day 2. Interestingly, we detected no differences in populations when LTB4 was added (Figure 2C).

Individual LTs were again added to DM, which is placed on OPCs on day 0, and on day 4 (Schema in Figure 2A), cultures were immunocytochemically analyzed for Sox10, O4, and MBP (Figure 2D; representative images for vehicle and LTD4 with zoomed in images on the bottom are shown). On day 4 in DM, increased frequencies of O4-MBP+ cells were detected when LTD4 was added. No other differences were detected (Figure 2E).

All of these suggest that cysteinyl leukotrienes, but not LTB4, directly promote OLC differentiation.

Microglia are the predominant expressors of 5LO in the intact CNS

To determine the cellular source of 5LO and leukotrienes, we first fed WT mice a CSF1R antagonist, PLX5622, formulated into rodent chow (PLX5622 diet; PD), and analyzed these mice compared to mice that have received AIN56A (control diet; CD) (Schema in Figure 5A). We determined that microglia (IBA1+ cells) were indeed depleted in CNS tissue in PD mice (Figure 5B), as well as their transcripts (*Cd11b* expression) (Figure 5C) in PD mice. We measured *Alox5* transcripts in whole spinal cord tissue, and determined that when microglia are depleted, total *Alox5* is depleted (Figure 5D).

Expression of CSF1R has been detected in many non-microglial cells such as neurons [26]. Due to the lack of specificity of CSF1R to microglia, we also adopted a genetic method to deplete microglial 5LO. CX3CR1$^{creER/wt}$x *Alox5* fl/fl (microglia icKO) mice and *Alox5* fl/fl (WT fl control) mice were injected with tamoxifen daily for 5 consecutive days to induce Cre recombinase expression in CX3CR1-expressing cells. CX3CR1 is expressed in both macrophages and microglia [27]; although macrophages in CX3CR1$^{creER/wt}$x *Alox5* fl/fl mice initially lack 5LO, after 4 weeks, these macrophages are replaced with wildtype progenitors. Conversely, microglia are long lived and remain depleted of *Alox5.* A portion each CNS tissue from microglia icKO and WT fl control mice is collected for transcript analyses, and the rest of the tissue is FACS sorted for CD11b+CD45lo (microglia) and CD11b-CD45- (all else; mostly astrocytes and

OLCs) (schema in Figure 5E). *Cre* transcripts are determined to indeed be specific in the microglia icKO in sorted microglia, and not detected in WT fl controls (Figure 5F). *Alox5* is indeed detected to be ablated in sorted microglia from microglia icKO mice but not in microglia from WT fl controls (Figure 5G). When whole spinal cord tissue is analyzed for *Alox5* expression, it was determined that total tissue *Alox5* was depleted when microglial *Alox5* was depleted in microglia icKO mice.

This suggests that microglia are the predominant expressors of 5LO in the healthy CNS.

Working model

Our working model is shown in Figure 5, depicting that microglia control OL differentiation through cysLTs, synthesized by 5LO at every timepoint. At p14, more OLCs have differentiated in *Alox5*$^{+/+}$ mice, so fewer OLCs are labeled at this initial timepoint then in *Alox5*$^{-/-}$ mice. These OPCs proliferate within 3 days [28], then at an intermediate timepoint of developmental myelination, the population is more mature, but still, there are fewer BrdU+ cells than in *Alox5*$^{-/-}$ mice. By the time of our analysis at p112, the majority of OLCs have matured, reaching the endpoint of their differentiation. Of these, *Alox5*$^{+/+}$ mice have fewer Sox10+CC1+BrdU+ cells, which were OPCs at the time of BrdU injection (Figure 5). Future directions include analyzing other timepoints to validate our working model.

3.4 Discussion

Our novel study establishes microglia's role in promoting oligodendrocyte differentiation through 5LO and cysteinyl leukotrienes, and expands current understanding of 5LO activity in the intact CNS. This work follows from previous studies that have proposed a link between cysLTs and oligodendrocyte differentiation via GPR17 signaling [9, 29]. However, GPR17 is a more recently deorphanized receptor in which it is both controversial whether it does [29] or does not [8] signal through cysLTs, and whether GPR17 signaling promotes [30, 31] or impairs [7, 9, 32] OLC differentiation.

As 5LO has been reported to control cell proliferation [19, 21, 24] and differentiation [20, 22, 23], we employed the BrdU fate mapping method to label CNS cells, and determine their fate over time. We employed an *in vivo* model, with our lab-bred *Alox5* global knockout mouse. We injected BrdU into *Alox5*$^{-/-}$ vs WT controls for 5 consecutive days at p14. During this developmental timepoint, there are high levels of cell proliferation in the CNS, thus maximizing labeling for fate mapping studies. From our data at 16 weeks, we see that a majority of these cells co-localized with Sox10+ cells (oligodendrocytes), specifically CC1+ mature oligodendrocytes. From this 16 week data, we have extrapolated a working model. In our working model, fewer OPCs are available to be labeled in WT mice than *Alox5*$^{-/-}$ due to earlier differentiation of WT OLCs; then OPCs divide at p17 [28]; then at an intermediate timepoint of development, the OLCs in WT mice are more differentiated but fewer OLCs are labeled than in the Alox5$^{-/-}$ mice. Lastly, at the timepoint of analysis, p112 (16 weeks), in which most OLCs have reached their mature endpoint of differentiation, there are more labeled CC1+ OLCs. We propose that 5LO/leukotrienes promoted OLC differentiation. Interestingly, we did not detect large differences between males and females in these experiments as expected. Other groups have shown that androgens impair 5LO-FLAP assembly and thus decrease the efficiently of 5LO activity in male mice [33]. It is possible that the differences in LT production are not sufficient to cause downstream effects in OLC differentiation.

Our *in vivo* results suggest that 5LO may affect OL differentiation. To determine if this is the case, we employ an *in vitro* model, and add the products of 5LO, leukotrienes, onto differentiating primary OLCs and demonstrated that cysLTs but not LTB4 directly promoted oligodendrocyte differentiation. We determined that addition of cysLTs increased numbers of late IM and MO on day 2 in DM. On day 4 only LTD4 increased MOs. Interestingly, cysLT signaling only affects OLC differentiation during the early stages. In agreement with Ciana et al, cysLT (but not LTB4) signaling promotes OLC differentiation [29]. These experiments demonstrated the direct effect of LTs on OLC differentiation, but siRNA studies to inhibit

GPR17 are necessary to separate the effect of GPR17 and cysLTR1, which are both detected on OLCs [6, 29] and signal through cysLTs [6, 29].

Studies showing the effects of GPR17 inhibition are seemingly contradictory; these differences may be because GPR17 and cysLT1R have similar affinities for cysLTs [29] and antagonists [34]. In fact, montelukast and pranlukast are primarily known as cysLT1R antagonists, but bind to GPR17 as well [34]. Additionally, studies have shown that GPR17 may negatively regulate cysLT1R [35], but the effect of cysLT1R on GPR17 is unknown. Thus, opposing phenotypes may arise from GPR17 vs CysLT1R signaling. Although GPR17 silencing studies must be conducted in the future to isolate the effect of cysLT1R-cysLT signaling from GPR17-cysLT signaling, our current *in vitro* model more accurately recapitulates an *in vivo* model.

Lastly, GPR17 is expectedly highest in the corpus callosum in the CNS due to the corpus callosum containing the highest concentration of white matter and of OLCs [36], which express GPR17 [9]. Similarly to our *in vitro* experiments, both CysLTR1 and GPR17 are present on OLCs in the corpus callosum, and a GPR17 OLC conditional knockout is needed to assess whether LTs promote OLC developmental differentiation via cysLTR1 or GPR17.

Next, we aimed to isolate regional differences in the 5LO pathway in the CNS. Interestingly, *Alox5* was expressed the highest level of transcripts in the spinal cord, and within the spinal cord, there are higher levels of in females than males.

5LO expression has been reported in neurons [4] in the past, but more recent expression databases suggest that glia [2, 5] are the main expressors of 5LO. Due to microglia's manifold regulatory functions with other cell types, we tested the contribution of microglial 5LO to total 5LO in the healthy CNS. We first pharmacologically depleted microglia using the PLX5622 diet (PD). Although PD effectively depletes microglia, CSF1R antagonism-mediated effects are not limited to microglial depletion, as shown in several studies [37-39]. To minimize off-target effects, we employed the CX3CR1-CreERT2 tamoxifen-

inducible Cre mouse model. However, this model relies on Cre recombinase efficiency, which as an inducible enzyme model, is never at 100% [40]. In fact, our PD-mediated deletion of microglia is slightly more effective in ablating total 5LO in the tissue. Although neither model accounts for the long-lived tissue resident macrophages that contribute to LT production that may be depleted or become functionally impaired by either model, these populations are negligible in size compared to microglial populations. In agreement with previous RNAseq [5] and immunohistochemical staining [2] databases, we determined that 5LO is mainly expressed in microglia in the healthy CNS.

As previously mentioned, microglial-OLC crosstalk has been well established [12, 14-16, 18], but the mechanisms and molecules which facilitate these mechanisms have been poorly defined. In our study, our results newly suggest that microglia mediate developmental OLC differentiation through the LT pathway. Our results can be applied to solve the unmet therapeutic needs of neurodevelopmental disorders, which arise from impairments in developmental myelination [41].

3.5 References

1. Hedi, H. and G. Norbert, *5-Lipoxygenase Pathway, Dendritic Cells, and Adaptive Immunity.* J Biomed Biotechnol, 2004. **2004**(2): p. 99-105.
2. Uhlen, M., et al., *Proteomics. Tissue-based map of the human proteome.* Science, 2015. **347**(6220): p. 1260419.
3. Jo-Watanabe, A., T. Okuno, and T. Yokomizo, *The Role of Leukotrienes as Potential Therapeutic Targets in Allergic Disorders.* Int J Mol Sci, 2019. **20**(14).
4. Lammers, C.H., et al., *Arachidonate 5-lipoxygenase and its activating protein: prominent hippocampal expression and role in somatostatin signaling.* J Neurochem, 1996. **66**(1): p. 147-52.
5. Zhang, Y., et al., *An RNA-sequencing transcriptome and splicing database of glia, neurons, and vascular cells of the cerebral cortex.* J Neurosci, 2014. **34**(36): p. 11929-47.
6. Ghosh, A., et al., *Cysteinyl Leukotrienes and Their Receptors: Emerging Therapeutic Targets in Central Nervous System Disorders.* CNS Neurosci Ther, 2016. **22**(12): p. 943-951.
7. Merten, N., et al., *Repurposing HAMI3379 to Block GPR17 and Promote Rodent and Human Oligodendrocyte Differentiation.* Cell Chem Biol, 2018. **25**(6): p. 775-786 e5.
8. Qi, A.D., T.K. Harden, and R.A. Nicholas, *Is GPR17 a P2Y/leukotriene receptor? examination of uracil nucleotides, nucleotide sugars, and cysteinyl leukotrienes as agonists of GPR17.* J Pharmacol Exp Ther, 2013. **347**(1): p. 38-46.
9. Chen, Y., et al., *The oligodendrocyte-specific G protein-coupled receptor GPR17 is a cell-intrinsic timer of myelination.* Nat Neurosci, 2009. **12**(11): p. 1398-406.
10. Bergles, D.E. and W.D. Richardson, *Oligodendrocyte Development and Plasticity.* Cold Spring Harb Perspect Biol, 2015. **8**(2): p. a020453.
11. Chapman, T.W. and R.A. Hill, *Myelin plasticity in adulthood and aging.* Neurosci Lett, 2020. **715**: p. 134645.
12. Koning, N., et al., *Distribution of the immune inhibitory molecules CD200 and CD200R in the normal central nervous system and multiple sclerosis lesions suggests neuron-glia and glia-glia interactions.* J Neuropathol Exp Neurol, 2009. **68**(2): p. 159-67.
13. Erblich, B., et al., *Absence of colony stimulation factor-1 receptor results in loss of microglia, disrupted brain development and olfactory deficits.* PLoS One, 2011. **6**(10): p. e26317.
14. D'Ercole, A.J., P. Ye, and J.R. O'Kusky, *Mutant mouse models of insulin-like growth factor actions in the central nervous system.* Neuropeptides, 2002. **36**(2-3): p. 209-20.
15. Hoshiko, M., et al., *Deficiency of the microglial receptor CX3CR1 impairs postnatal functional development of thalamocortical synapses in the barrel cortex.* J Neurosci, 2012. **32**(43): p. 15106-11.
16. Shigemoto-Mogami, Y., et al., *Microglia enhance neurogenesis and oligodendrogenesis in the early postnatal subventricular zone.* J Neurosci, 2014. **34**(6): p. 2231-43.
17. Hamilton, S.P. and L.H. Rome, *Stimulation of in vitro myelin synthesis by microglia.* Glia, 1994. **11**(4): p. 326-35.
18. Pang, Y., et al., *Differential roles of astrocyte and microglia in supporting oligodendrocyte development and myelination in vitro.* Brain Behav, 2013. **3**(5): p. 503-14.
19. Chung, J.W., et al., *Leukotriene B4 pathway regulates the fate of the hematopoietic stem cells.* Exp Mol Med, 2005. **37**(1): p. 45-50.
20. Coffey, M.J., M. Gyetko, and M. Peters-Golden, *1,25-Dihydroxyvitamin D3 upregulates 5-lipoxygenase metabolism and 5-lipoxygenase activating protein in peripheral blood monocytes as they differentiate into mature macrophages.* J Lipid Mediat, 1993. **6**(1-3): p. 43-51.

21. Dholia, N. and U.C.S. Yadav, *Lipid mediator Leukotriene D(4)-induces airway epithelial cells proliferation through EGFR/ERK1/2 pathway.* Prostaglandins Other Lipid Mediat, 2018. **136**: p. 55-63.
22. Fujita, H., et al., *Cysteinyl leukotriene receptor 1 is dispensable for osteoclast differentiation and bone resorption.* PLoS One, 2022. **17**(11): p. e0277307.
23. Hirata, K., et al., *Critical role of leukotriene B4 receptor signaling in mouse 3T3-L1 preadipocyte differentiation.* Lipids Health Dis, 2013. **12**: p. 122.
24. Tian, W., et al., *Leukotrienes in Tumor-Associated Inflammation.* Front Pharmacol, 2020. **11**: p. 1289.
25. Kuhn, S., et al., *Oligodendrocytes in Development, Myelin Generation and Beyond.* Cells, 2019. **8**(11).
26. Bo, L. and X. Bo, *Colony stimulating factor 1: friend or foe of neurons?* Neural Regen Res, 2022. **17**(4): p. 773-774.
27. Lee, M., et al., *Tissue-specific Role of CX(3)CR1 Expressing Immune Cells and Their Relationships with Human Disease.* Immune Netw, 2018. **18**(1): p. e5.
28. Psachoulia, K., et al., *Cell cycle dynamics of NG2 cells in the postnatal and ageing brain.* Neuron Glia Biol, 2009. **5**(3-4): p. 57-67.
29. Ciana, P., et al., *The orphan receptor GPR17 identified as a new dual uracil nucleotides/cysteinyl-leukotrienes receptor.* EMBO J, 2006. **25**(19): p. 4615-27.
30. Fumagalli, M., et al., *Phenotypic changes, signaling pathway, and functional correlates of GPR17-expressing neural precursor cells during oligodendrocyte differentiation.* J Biol Chem, 2011. **286**(12): p. 10593-604.
31. Eriksson, Y., et al., *The anti-asthmatic drug, montelukast, modifies the neurogenic potential in the young healthy and irradiated brain.* Cell Death Dis, 2018. **9**(7): p. 775.
32. Simon, K., et al., *The Orphan G Protein-coupled Receptor GPR17 Negatively Regulates Oligodendrocyte Differentiation via Galphai/o and Its Downstream Effector Molecules.* J Biol Chem, 2016. **291**(2): p. 705-18.
33. Pace, S., et al., *Androgen-mediated sex bias impairs efficiency of leukotriene biosynthesis inhibitors in males.* J Clin Invest, 2017. **127**(8): p. 3167-3176.
34. Marucci, G., et al., *The G Protein-Coupled Receptor GPR17: Overview and Update.* ChemMedChem, 2016. **11**(23): p. 2567-2574.
35. Maekawa, A., et al., *GPR17 is a negative regulator of the cysteinyl leukotriene 1 receptor response to leukotriene D4.* Proc Natl Acad Sci U S A, 2009. **106**(28): p. 11685-90.
36. Ohtomo, R., A. Iwata, and K. Arai, *Molecular Mechanisms of Oligodendrocyte Regeneration in White Matter-Related Diseases.* Int J Mol Sci, 2018. **19**(6).
37. Lei, F., et al., *CSF1R inhibition by a small-molecule inhibitor is not microglia specific; affecting hematopoiesis and the function of macrophages.* Proc Natl Acad Sci U S A, 2020. **117**(38): p. 23336-23338.
38. Hwang, D., et al., *CSF-1 maintains pathogenic but not homeostatic myeloid cells in the central nervous system during autoimmune neuroinflammation.* Proc Natl Acad Sci U S A, 2022. **119**(14): p. e2111804119.
39. Wang, M., et al., *CSF1R antagonism results in increased supraspinal infiltration in EAE.* J Neuroinflammation, 2024. **21**(1): p. 103.
40. Tian, X. and B. Zhou, *Strategies for site-specific recombination with high efficiency and precise spatiotemporal resolution.* J Biol Chem, 2021. **296**: p. 100509.
41. Rokach, M., et al., *Tackling myelin deficits in neurodevelopmental disorders using drug delivery systems.* Adv Drug Deliv Rev, 2024. **207**: p. 115218.

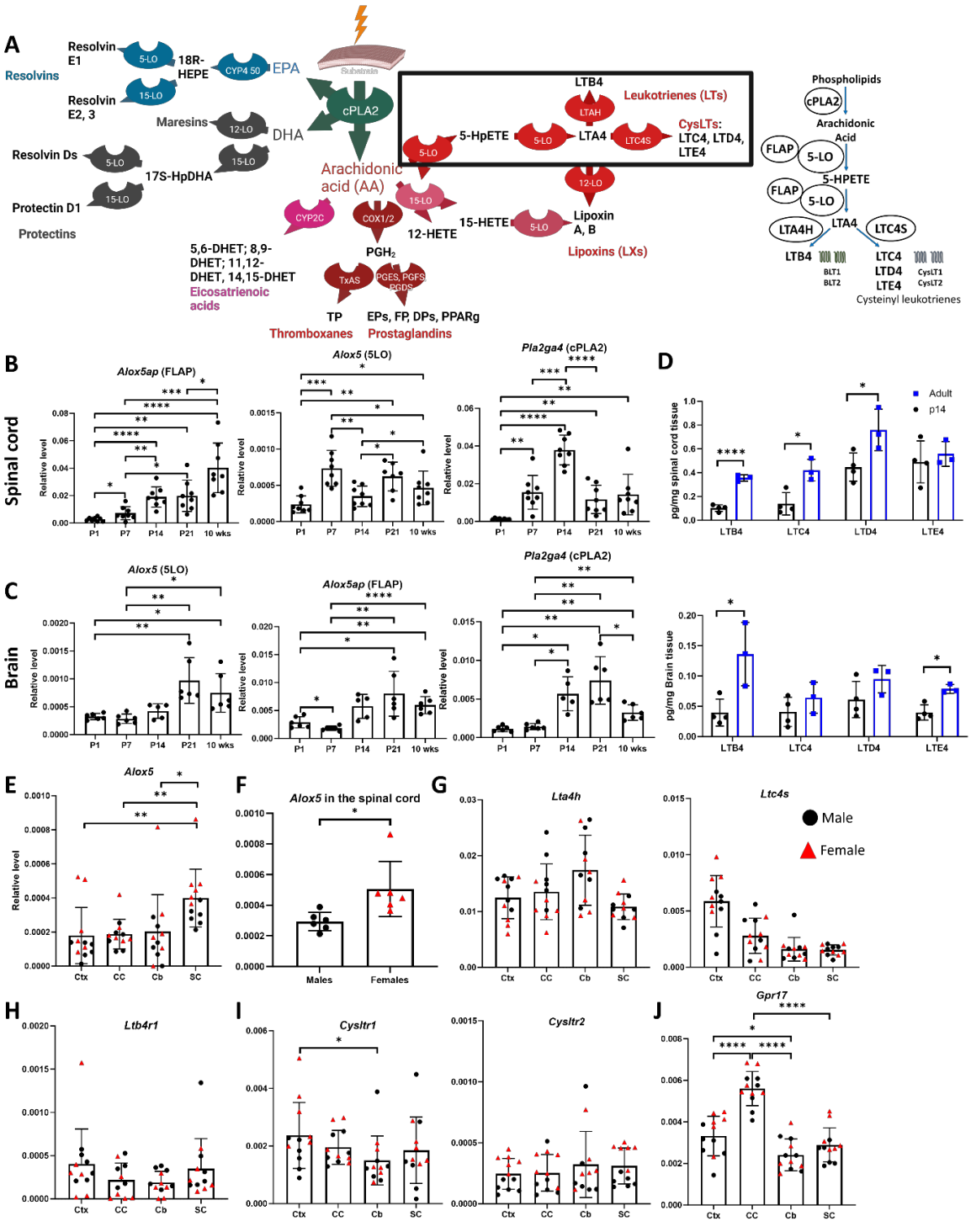
A
Resolvins
Resolvin E1
Resolvin E2, 3
Resolvin Ds
Protectin D1
Protectins
5-LO
15-LO
12-LO
18R-HEPE
17S-HpDHA
CYP4 50
EPA
DHA
Maresins
cPLA2
Arachidonic acid (AA)
CYP2C
COX1/2
PGH2
TxAS
PGES, PGFS, PGDS
TP
EPs, FP, DPs, PPARg
Thromboxanes
Prostaglandins
5,6-DHET; 8,9-DHET; 11,12-DHET, 14,15-DHET
Eicosatrienoic acids
12-HETE
15-HETE
5-HpETE
LTA4
LTAH
LTC4S
LTB4
Leukotrienes (LTs)
CysLTs: LTC4, LTD4, LTE4
Lipoxin A, B
Lipoxins (LXs)
Phospholipids
Arachidonic Acid
FLAP
5-HPETE
LTA4H
BLT1
BLT2
CysLT1
CysLT2
Cysteinyl leukotrienes
B
Spinal cord
Alox5ap (FLAP)
Alox5 (5LO)
Pla2ga4 (cPLA2)
Relative level
P1
P7
P14
P21
10 wks
D
Adult
p14
pg/mg spinal cord tissue
LTB4
LTC4
LTD4
LTE4
C
Brain
pg/mg Brain tissue
E
Alox5
Ctx
CC
Cb
SC
F
Alox5 in the spinal cord
Males
Females
G
Lta4h
Ltc4s
Male
Female
H
Ltb4r1
I
Cysltr1
Cysltr2
J
Gpr17

Figure 1 5LO and its pathway components are detected and active during development and adulthood. A) Leukotrienes are one of many products of lipid membrane metabolism by cytosolic phospholipase, and belong to a family of lipid mediators with both pro-inflammatory and anti-inflammatory functions known as eicosanoids. The 5LO-leukotriene pathway (cut-out on right) is the most readily detected 5LO pathway, but not the only one. **B,C)** 5LO pathway component transcripts *Alox5ap, Alox5, and Pla2ga4* peak during developmental stages, but area expressed during all stages of development and adulthood in the spinal cord (B) and the brain (C) **D)** Leukotrienes production is detected during p14, and increased in adulthood in the spinal cord and the brain. **E-J)** *Alox5* (E and F) *Lta4h and Ltc4s* (G), *Ltb4r1* (H)*, Cysltr1 and Cysltr2* (I) *and Gpr17* (J) are expressed in the Ctx (cortex), CC (corpus callosum), Cb (cerebellum) and SC (spinal cord) in WT

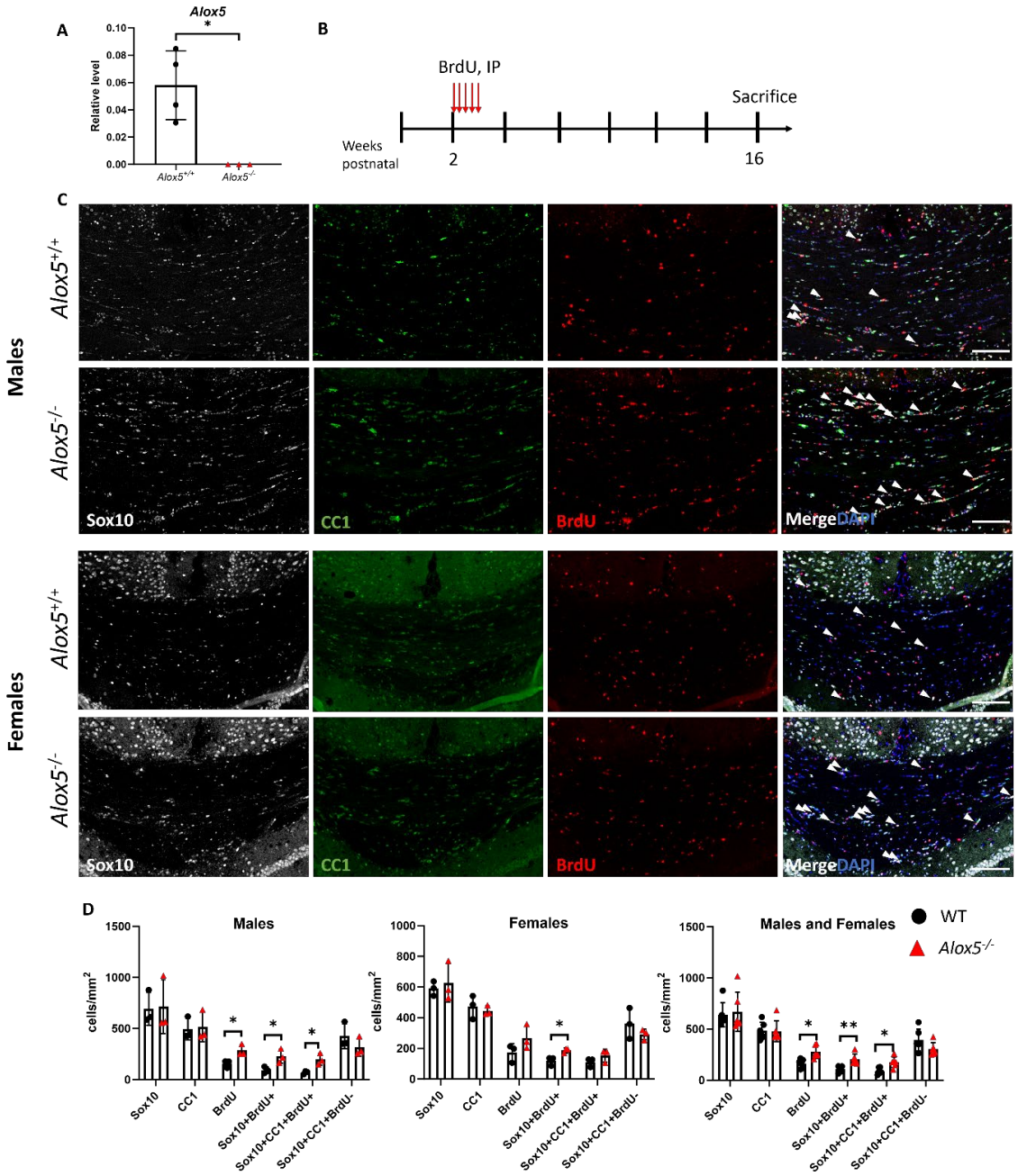
A
Alox5
*
Relative level
0.10
0.08
0.06
0.04
0.02
0.00
Alox5+/+
Alox5-/-
B
BrdU, IP
Sacrifice
Weeks postnatal
2
16
C
Males
Females
Alox5+/+
Alox5-/-
Sox10
CC1
BrdU
Merge DAPI
D
Males
Females
Males and Females
WT
Alox5-/-
cells/mm2
Sox10
CC1
BrdU
Sox10+BrdU+
Sox10+CC1+BrdU+
Sox10+CC1+BrdU-

Figure 2 5 lipoxygenase promotes OL differentiation *in vivo*. A) Our *in vivo* model employs an *Alox5* global knockout, *Alox5*$^{-/-}$ that was made by our lab. We validate that 5LO transcripts were indeed ablated in our *Alox5*$^{-/-}$ mouse compared to wildtype littermate controls (*Alox5*$^{+/+}$) **B)** Experimental schema depicting that mice received daily IP injections of BrdU for 5 consecutive days at postnatal week 2. Mice were analyzed at 16 weeks. **C)** Representative images of middle sections of *Alox5*$^{-/-}$ (bottom) and *Alox5*$^{+/+}$ (top) corpus callosa labeled with Sox10 (all OLCs), CC1 (mature OLCs), and BrdU (fate mapped OLCs) **D)** Quantification of (C) in males, females, and males and females together

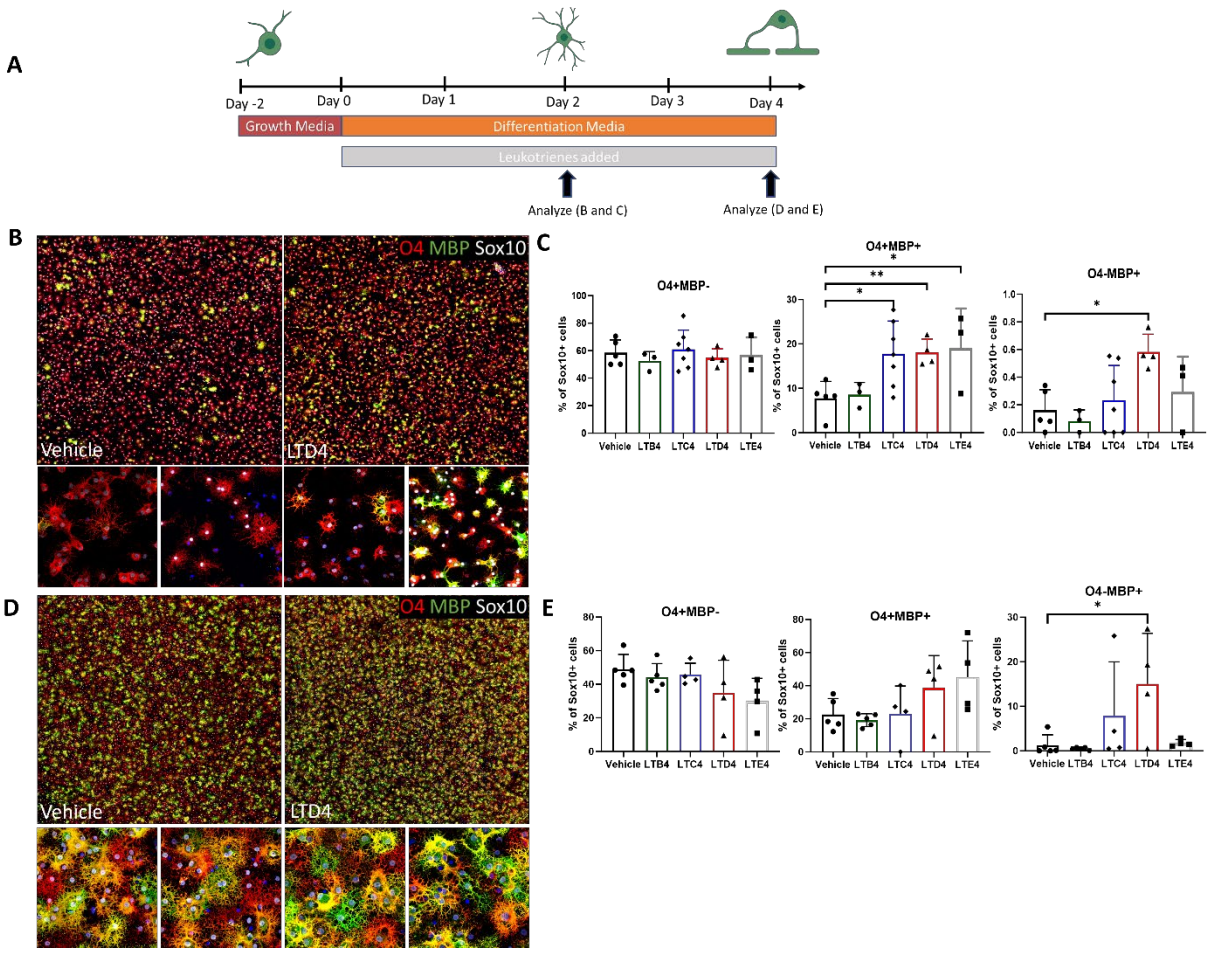

Figure 3 Cysteinyl leukotrienes promote oligodendrocyte differentiation. A) Experimental schema depicting our *in vitro* model of oligodendrocyte differentiation in which OPCs are proliferated in growth media, and then differentiated in differentiation media into predominately immature OLCs on day 2, and more mature OLCs on day 4. We add individual leukotrienes into the differentiation media on the day of initiation of differentiation and analyze on day 2 (B, C) and day 4 (D, E). **B, D)** Representative large images (top) and zoomed in cutouts (bottom) of immunocytochemical analysis of O4 (less mature), MBP (more mature) and Sox10 (all OLCs) in vehicle and LTD4 conditions on day 2 (B) and day 4 (D). **C, E)** Quantification of immunocytochemistry in B and D for day 2 (C) and day 4 (E)

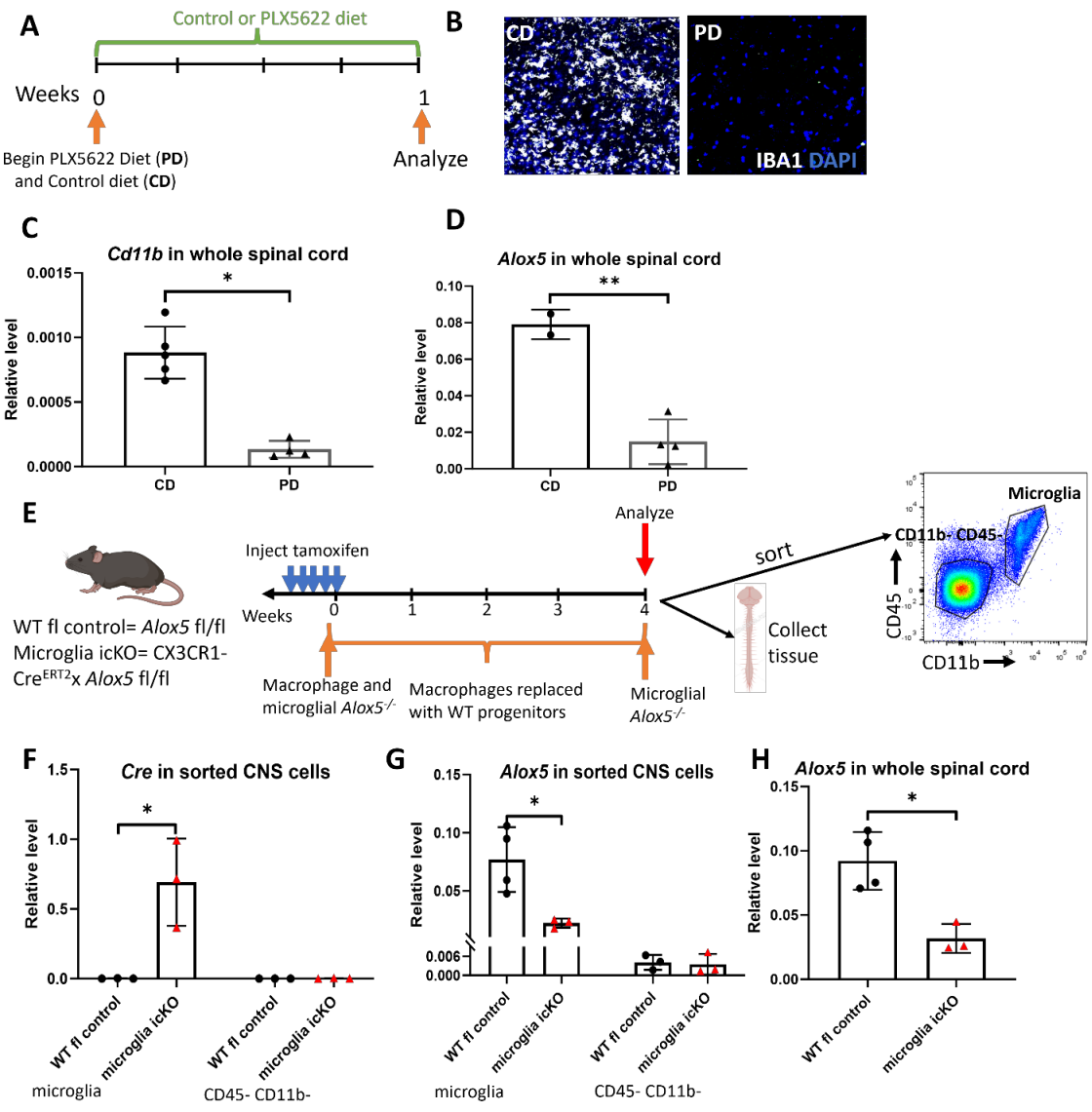
A
Control or PLX5622 diet
Weeks 0
1
Begin PLX5622 Diet (PD) and Control diet (CD)
Analyze
B
CD
PD
IBA1 DAPI
C
Cd11b in whole spinal cord
Relative level
0.0015
0.0010
0.0005
0.0000
*
CD
PD
D
Alox5 in whole spinal cord
Relative level
0.10
0.08
0.06
0.04
0.02
0.00
**
CD
PD
E
WT fl control= Alox5 fl/fl
Microglia icKO= CX3CR1-Cre^ERT2 x Alox5 fl/fl
Inject tamoxifen
Weeks 0 1 2 3 4
Analyze
Macrophage and microglial Alox5-/-
Macrophages replaced with WT progenitors
Microglial Alox5-/-
sort
Collect tissue
Microglia
CD11b- CD45-
CD45
CD11b
F
Cre in sorted CNS cells
Relative level
1.5
1.0
0.5
0.0
*
WT fl control
microglia icKO
WT fl control
microglia icKO
microglia
CD45- CD11b-
G
Alox5 in sorted CNS cells
Relative level
0.15
0.10
0.05
0.006
0.000
*
WT fl control
microglia icKO
WT fl control
microglia icKO
microglia
CD45- CD11b-
H
Alox5 in whole spinal cord
Relative level
0.15
0.10
0.05
0.00
*
WT fl control
microglia icKO

Figure 4 Microglia are the predominant expressors of 5LO in the intact CNS A) Experimental schema depicting that wildtype mice were placed on control diet (CD) or PLX5622 diet (PD) for one week, and then analyzed **B)** CD and PD mice were immunostained with IBA1 for detect microglia to determine that microglia were indeed depleted in PD mice **C)** Whole spinal cord tissue was measured for Cd11b transcripts to confirm microglial depletion. **D)** Total *Alox5* expression was ablated when microglia were depleted using PD in spinal cord tissue **E)** *Alox5* fl/fl (WT fl control mice) and CX3CR1-Cre^{ERT2}x *Alox5* fl/fl (microglia icKO mice) were injected with tamoxifen IP daily for 5 consecutive days to deplete *Alox5* from all CX3CR1 expressing cells. After 4 weeks, WT macrophages from the bone marrow have replaced *Alox5*$^{-/-}$ macrophages, leaving only *Alox5*$^{-/-}$ microglia in microglia icKO mice. WT fl control mice and microglia icKO mice are then analyzed- a portion of each CNS is collected for qPCR analysis, and a portion is FACS sorted into CD11b+CD45+ cells (microglia) and CD11b-CD45- cells (all else; includes predominately oligodendrocytes and astrocytes) **F)** *Cre* is specific to sorted microglia from microglia icKO mice only **G)** *Alox5* is detected at significantly lower levels in sorted microglia from microglia icKO compared to sorted microglia from WT fl controls. **H)** *Alox5* transcript is ablated in whole spinal cord tissue when microglial *Alox5* is ablated

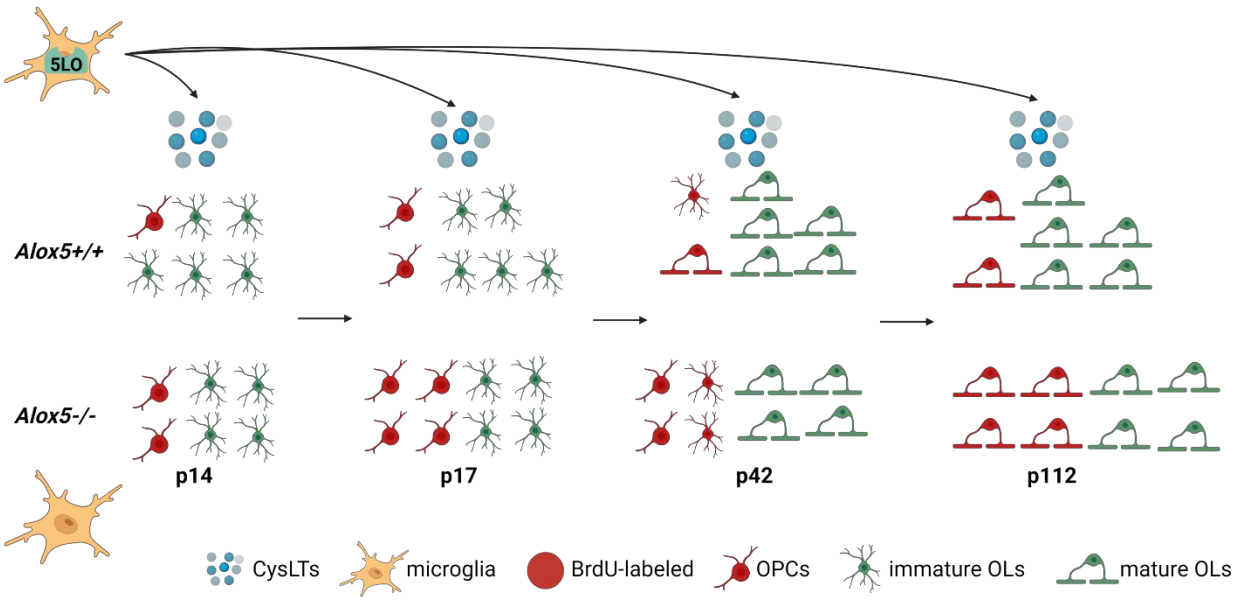

Figure 5 Working model. Microglia make cysteinyl leukotrienes (cysLTs) through 5LO. At P14, *Alox5* delays oligodendrocyte differentiation, so more OPCs are still proliferating and are labeled. At p17, OPCs have proliferated. At p42, OLs are differentiating, and by p112, a majority of OLs have differentiated into mature OLs.

Chapter 4: Conclusions and future directions

My dissertation work unites two areas focus in neuroimmunology: the mechanisms controlling EAE disease, as well as controlling myelination by providing evidence of myeloid cells as major players in both. To establish a foundation for Chapters 2 and 3, in Chapter 1, I review current literature to establish the indispensable role of myeloid cells in multiple sclerosis and review current myeloid-cell targeting therapeutics commercially available to treat MS.

I follow with evidence that a receptor expressed on almost all myeloid cells involved in EAE, CSF1R, is involved in dictating the localization of inflammatory lesions. Although it was previously reported that depleting microglia using PLX5622 diet is the source of the amelioration of EAE clinical symptoms, I challenge that microglial depletion is not the only culprit. I show that when CSF1R is antagonized, numerous other myeloid subsets are affected, and downstream of that, T cell polarization; downstream of that still, I report that this causes cells to infiltrate primarily into the cerebellum. Thus, inflammatory damage manifests less in motor deficits, and perhaps more in behavioral, psychological and other neurological impairments, which evade detection using our conventional, motor-deficit-centric methods of measuring EAE.

This study could benefit from future investigation. First, although I analyzed brain and spinal cord together in my flow cytometric experiments, it would have been beneficial to show differences in numbers and relative frequencies between the cerebellum and spinal cords in control diet vs PLX5622 mice. This will

aid in our efforts to demonstrate the mechanism behind this. Also, a battery of behavioral tests are needed to evaluate changes in cognitive and psychological function from cerebellar infiltration.

Furthermore, another particular area of interest in neuroimmunology is the control of OLC differentiation and myelination. Some factors controlling differentiation have been identified, but more remain to be discovered. Although another dogma of immunology is that leukotrienes from 5LO are inflammatory lipid mediators involved in propagating allergy and asthma, in my work, I show that in the healthy CNS, 5LO is involved in promoting OLC differentiation. Next, due to the previously documented role of primary microglia conditioned media in promoting OLC differentiation, we investigate the effects of 5LO the myeloid cell in the intact CNS, microglia. We conclude that microglial 5LO is controlling oligodendrocyte differentiation.

Future studies could involve co-culturing primary microglia from *Alox5*$^{-/-}$ and WT mice with primary oligodendrocytes from WT mice to show the direct effect of microglial 5LO on OLC differentiation *in vitro*. We will establish a baseline of autocrine regulation of differentiation via OLC 5LO by co culturing primary microglia from WT mice with primary OLCs from *Alox5*$^{-/-}$ and WT mice. It will also be necessary to conduct siRNA studies to determine the receptor that LTs signal through to control OLC differentiation.

In conclusion, by challenging two dogmas in immunology, the role of CSF1R in EAE and the function(s) of leukotrienes, my work has elucidated some previously unknown mechanisms for EAE and myelination. This information may be translatable in the areas of neuroinflammation and developmental myelination for therapeutic discovery.